



TECHNISCHE UNIVERSITÄT MÜNCHEN

Fakultät Chemie

Lehrstuhl für Organische Chemie II

**Target identification and validation of natural products or
synthetic compounds by activity-based protein profiling**

Kyu Myung Lee

Vollständiger Abdruck der von der Fakultät für Chemie der Technischen
Universität München zur Erlangung des akademischen Grades eines

DOKTORS DER NATURWISSENSCHAFTEN (Dr. rer. nat)
genehmigten Dissertation.

Vorsitzende: Prof. Dr. Michael Groll
Prüfer der Dissertation: 1. Prof. Dr. Stephan Sieber
2. Prof. Dr. Kathrin Lang

Die Dissertation wurde am 23.12.2019 bei der Technischen Universität München
eingereicht und durch die Fakultät für Chemie am 26.02.2020 angenommen.



TECHNISCHE UNIVERSITÄT MÜNCHEN

FAKULTÄT CHEMIE

LEHRSTUHL FÜR ORGANISCHE CHEMIE II



Target identification and validation of natural products or
synthetic compounds by activity-based protein profiling

DISSERTATION ZUR ERLANGUNG DES AKADEMISCHEN GRADES EINES
DOKTORS DER NATURWISSENSCHAFTEN VON

Kyu Myung Lee

MÜNCHEN 2019

FÜR MICH

Table of Contents

Acknowledgements	1
Introductory remark	3
Abstract	4
Kurzfassung	5
I. Introduction	6
1. Natural Product and Drug Discovery	7
2. Activity-Based Protein Profiling	9
II. Exploring a Natural Product, Smenothiazole A and B	12
1. Introduction	13
2. Result and discussion	17
2.1. Synthetic route I	17
2.2. Synthetic route II	20
2.3. Synthetic route III	22
2.4. Synthetic route IV	25
3. Conclusion	30
III. Degrasyn exhibits antibiotic activity against multi-resistant Staphylococcus aureus by modifying several essential cysteines	32
1. Introduction	33
1.1. Advantages of drug repurposing	33

1.2. Potential of degrasyn in drug repurposing	34
2. Result and Discussion	36
2.1. Biological validation of degrasyn by MIC assay	36
2.2 Structure activity relationship of degrasyn	37
2.3. Gel-free activity-based protein profiling	40
2.4. Competitive isoDTB-ABPP.....	42
2.5. Global proteomics analysis	45
3. Summary and outlook.....	48
IV. LK1602 as a potent inhibitor against gram positive and negative bacteria	49
1. Introduction	50
1.1. The crisis caused by multidrug resistant microbes	50
1.2. Discovery of hybrids of indolin-2-one and nitroimidazole	50
2. Result and Discussion	52
2.1. Synthesis and biological validation of LK1602	52
2.2. Synthesis of alkyne probe of LK1602	52
2.2.1. Nitrogen of amide	53
2.2.2. Phenyl ring of indolin-2-one	54
2.2.3. 1-position of imidazole	56
2.3. Biological validation of alkyne probes of LK1602 by MIC assay	56
2.4. Gel-based ABPP for active and inactive probes	58
3. Summary and outlook.....	60
V. Experimental section	61

1. Chemistry	62
1.1. General remarks	62
1.2. Synthesis of Smenothiazole A and Phoroprobe of Smenothiazole B	63
1.3. Degrasyn exhibits antibiotic activity in multi-resistant Staphylococcus aureus through modification of several essential cysteines	71
1.4. LK1602 as a potent inhibitor against gram positive and negative bacteria	86
2. Microbiology	96
2.1. Bacterial strains and media	96
2.2. Cultivation methods	97
3. Proteomics	99
3.1. Activity-based protein profiling experiments	99
3.1.1 Analytical gel-based ABPP	99
3.1.2. Gel-free quantitative ABPP	100
3.1.3. Competition ABPP experiment	103
3.1.4. Competitive isoDTB-ABPP	103
3.2. Global proteomics analysis	108
VI. NMR spectra	110
Bibliography	135

Acknowledgements

This is one of the greatest moments of my life and it was not possible without all the loving and caring people around me.

First and foremost I would like to express my gratitude to Prof. Dr. Stephan A. Sieber who accepted me to work in his fantastic group as a PhD student and guided my research with a lot of effort. It was my great pleasure to work on challenging and multidisciplinary projects as well as develop my competence as a researcher under his supervision. He is a person who has a strong thirst for knowledge, so his creativity and enthusiasm have been always big supports and driving fuels to me during my research. He instructed me so many valuable virtues to become a real scientist; how to look at nature, how to criticize science but with fair eyes, how to develop and approach our own and significant research areas. He also allowed me to be independent in the project which sometimes went to nowhere, however he never forgot to straighten it up by hitting the bull's eye and encouraging me to grab tight. I truly feel grateful for having him as an advisor.

I would also like to thank to Dr. Stephan M. Hacker for providing his great methodology, isoDTB-ABPP, in my degrassyn project.

I really would like to say how deeply I appreciate great people with whom I spent most of time during my PhD life. Talents and kindness of our aksieber research group members were helpful not only in science to make me a better scientist but also in my life in foreign country. Thanks to all very first members when I came here who made me feel welcome. Especially, Dr. Franziska Mandl, Dr. Mathias Hackl, Dr. Weining Zhao, Dr. Markus Lakemeyer, Dr. Barbara Eyermann, Dr. Anja Fux, and Volker Kirsch, they cared for me and helped me find a flat when I was living out of a suitcase in München where is a hard city to do house-hunting. Thanks to former upstairs members Dr. Christian Fetzer, and Dr. Vadim Korotkov, we were in the same camp for two years far away from coffee corner the most important place. Thanks to Dóra Balogh who fed me at Mensa until I got my student card. Thanks to Thomas Gronauer, Jonas Drechsel, and Ines Hübner, they joined aksieber at about the same time and took care of me both when I was up and downstairs. Thanks to Martin Pfanzelt, a big fan of Kimbab as well as my neighbor in Garching, he kindly conferred a favor on me whenever I needed help. Caroline Gleißner, next seat to me, I received a lot of help from her when I prepared my first paper. Thanks to Patrick Allihn, Patrick Zanon, and Till

Reinhardt, they were the best sports partners. Thanks to Theresa Rauh, and Jonas Drechsel again, they always kindly answered my stupid questions. Thanks to Angela Weigert Muñoz, and Josef Braun, I learned a lot through their sincere style on the research. Thanks to Jan-Niklas Dienemann, and Konstantin Eckel, new aksieber members, if we met earlier, we would've more fun time. Anyway, you are good guys for me. Last, I was able to start and complete degrasyn project thank to Dr. Philipp Le when I had been stuck in smenothiazole project. Subsequently, he taught me practical work in biology experiment to be a biochemist.

This thesis was funded by Korea Research Institute of Chemical Technology (KRICT), and I was able to get this great opportunity thank to Dr. Prof. Jin-Hee Ahn. I would like to extend my thanks to Dr. Prof. Won Koo Lee who had me take the first step into the field of organic chemistry.

Finally, I must thank my parents, younger brother and parents in law who have always supported and encouraged me to keep up with my studies. And I know they have always been praying for me. And my wife, Sung Hee Park, whom I had a beautiful time with throughout the days in München. I wouldn't be where I am today without you. You've been a great wife at home and perfect travel partner on vacation. I've been truly blessed by her unfailing love and support. And I look forward to all of the adventures that lie ahead of us. I love you with all of my heart, and I thank you for ensuring that I actually finished this dissertation.

Thank you, city of München, it was the only city where a bunch of exciting and various experiences could happen.

Introductory remarks

This dissertation was accomplished from April 2016 to December 2019 under the supervision of Prof. Dr. Stephan A. Sieber at the Chair of Organic Chemistry II at the Department of Chemistry, Technische Universität München.

Parts of this thesis will be published in:

Kyu Myung Lee, Philipp Le, Stephan A. Sieber*, and Stephan M. Hacker*: Degrasyn exhibits antibiotic activity against multi-resistant *Staphylococcus aureus* by modifying several essential cysteines, *Chem. Commun.* accepted.

*contributed equally

Publication not highlighted in this thesis:

Christian Fetzer, Vadim S. Korotkov, Robert Thänert, Kyu Myung Lee, Martin Neuenschwander, Jens Peter von Kries, Eva Medina, and Stephan A. Sieber: A chemical disruptor of the ClpX chaperone complex attenuates the virulence of multidrug-resistant *Staphylococcus aureus*, *Angew. Chem. Int. Ed.* **2017**, 56, 15746-15750.

Abstract

Natural products have played an important role in the history of modern drug discovery, since penicillin was discovered by Scottish scientist Alexander Fleming in 1927. Afterwards, scientists concentrated on the isolation or extraction of the bioactive substrates from natural products. From 1950s, a number of scientists started not only to isolate or extract something, but also to analyze the chemical structure of it with the advent of NMR spectroscopy to date. With the development of it, researchers have been able to synthesize natural products or synthetic compounds in the lab, which could be leads or candidates for drug development.

Activity-based protein profiling (ABPP) is a very powerful tool of chemical proteomics. And the ABP probe is derived from its original bioactive-compound by introducing cell permeable moieties such as a terminal alkyne or an azide, thereby being tagged to a reporter group which enables isolation of probe-labeled protein(s).

This thesis describes the entire process of early part of drug discovery, from discovery and synthesis of natural products, artificial compounds, and their ABP probes to target identification and validation by the ABPP experiment and other biological assays.

The first part of the thesis covers synthetic approaches towards the total synthesis of smenothiazole A, B and their probes. Next, degrasyn originally developed as the human deubiquitination enzyme (DUB) inhibitor was repurposed as an antimicrobial compound, and its activity against gram positive bacteria, *Staphylococcus aureus* (*S. aureus*) and its methicillin-resistant strains was confirmed. Subsequently, a polypharmacological mode-of-action was corroborated by the ABPP experiments, competitive isoDTB-ABPP, and global proteome analysis. Last, a hybrid of the indolin-2-one and the nitroimidazole compound, LK1602, exhibited excellent activity against both gram positive and negative bacteria, and its ABP probes preserves the bioactivities against *S. aureus*. Therefore, target protein(s) of it will be identified by ABPP experiments.

Kurzfassung

Seit der Entdeckung des Penicillins 1927 durch Alexander Fleming ist die enorme Bedeutung von Naturstoffen in der Medikamentenentwicklung bekannt. Die Isolation und Extraktion solcher aktiven Substanzen steht seither im Mittelpunkt vieler Wissenschaftler. Durch moderne Methoden wie der NMR-Spektroskopie konnten die Strukturen auch aufgeklärt werden. Damit sind sie synthetisch zugänglich und potentielle Kandidaten für die Medikamentenentwicklung.

Aktivitäts-basiertes Protein (ABPP) ist eine leistungsfähige Methode für chemische Proteomik. Dazu wird eine aktivitäts-basierte Sonde (ABP) von der bioaktiven Ursprungsstruktur abgeleitet, welche zellpermeabel ist und eine Alkin- oder Azid-Funktionalität besitzt, um die gebundenen Zielproteine später durch Affinitätschromatographie isolieren zu können.

Diese Arbeit befasst sich mit dem kompletten Prozess der frühen Medikamentenentwicklung, von der Entdeckung und Synthese von Naturstoffen sowie anderen aktiven Molekülen und deren ABP's, um damit die Zielproteine identifizieren und validieren zu können.

Der erste Teil handelt von synthetischen Ansätzen, die Naturstoffe Smenoithiazol A, B und deren ABP's herzustellen. Danach wurde die Aktivität des ursprünglich als Inhibitor des humanen deubiquitylierungs-Enzyms (DUB) geltende Degrasyn gegenüber gram-positive Staphylococcus aureus und dessen Methicillin-resistente Stämme auf antimikrobielle Eigenschaften getestet. Weiterhin wurde ein polypharmakologischer Wirkungsmechanismus durch konventionelle ABPP- sowie kompetitive isoDTB-ABPP-Experimente und globale Proteomanalysen bestätigt. Zuletzt wird die hervorragende Aktivität der Verbindung LK1602, ein Indolin-2-on Derivat mit einer Nitroimizalol-Einheit, gegen gram-positive als auch gram-negative Bakterien beschrieben. Für die Entschlüsselung der Zielproteine dieser Verbindung wurden abermals ABP's synthetisiert, wovon zwei Sonden die Aktivität bewahrten und somit in weiteren ABPP-Experimenten zum Einsatz kommen werden.



I. Introduction

1. Natural product and drug discovery

Natural products, produced by living organism, have been the most fruitful ingredients of medicines.^{1,2,3} Before the era of the total synthesis of natural products, they were extracted or isolated from plants or animals. Penicillin was discovered by Scottish scientist Alexander Fleming who found that mold on staphylococci culture plates inhibited bacterial growth as a serendipitous accident, and concluded the mold released a certain substance preventing bacteria from growing and promoting lysis of bacteria.⁴ And it has been known as a first natural product drug and still used as the first medication for several bacterial infections caused by *streptococci* even though many bacteria have developed resistance against it. Afterwards, natural products have been not only extracted or isolated, but also synthesized in the lab as the field of organic chemistry progressed with the analysis of their structures by the advent of NMR spectroscopy. Therefore, of 1,562 new approved drugs from 1981 to 2014, 67% are natural products, their derivatives or derived from pharmacophores of them.⁵ (Figure 1a)

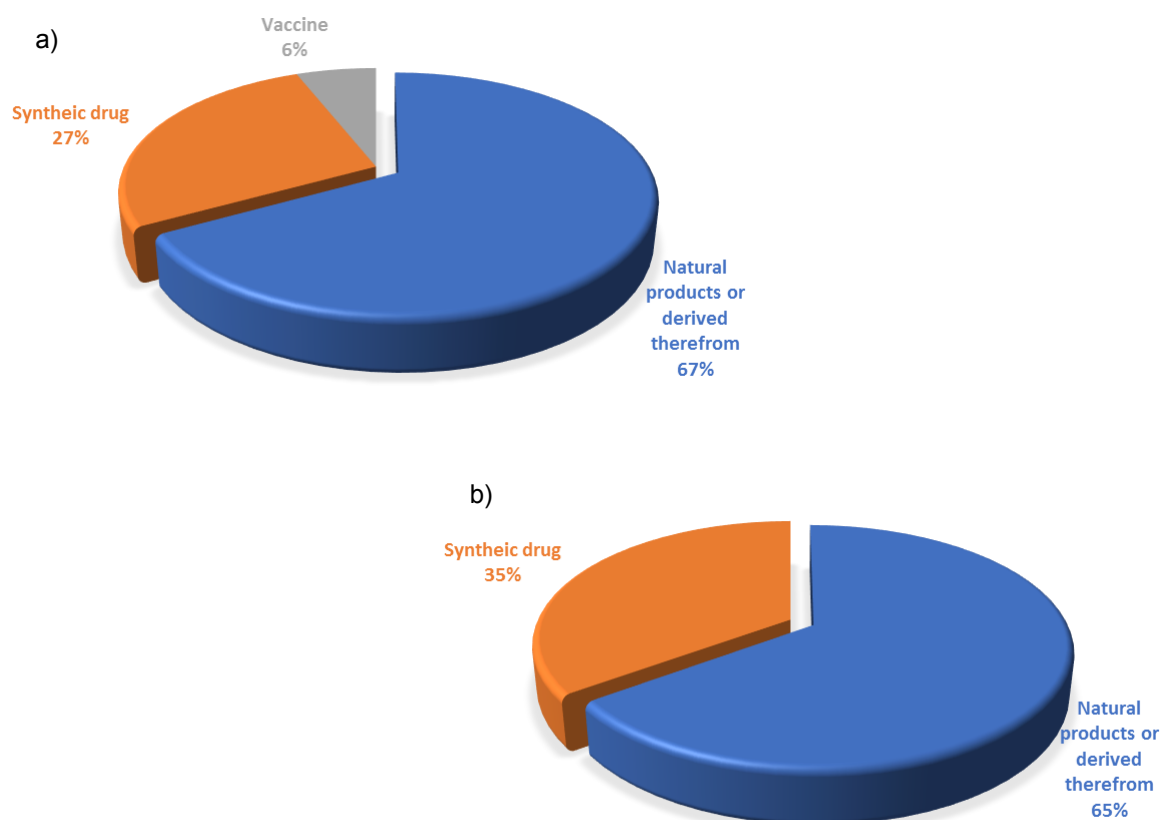


Figure 1. a) All new approved drugs, and b) all small-molecule approved drugs 1981-2014.⁵

However, synthesizing natural product is challenging due to the low yield and complexity of structure has turned researchers' attention to small molecules. For example, from 1940s to 2014 in the area of cancer, 131 out of 175 small molecules anticancer drugs are either natural products or -based/inspired.^{4,6} In other areas, aspirin⁷ and hypericin⁸ are medicine based on natural product, but also tamiflu (or oseltamivir)⁹ famous for the medicine against influenza A virus subtype H1N1 was synthesized from star anise, an evergreen tree native to northeast Vietnam and southwest China. In total, of 1,211 small molecule approved drugs from 1981 to 2014, 65% are natural products, their derivatives or derived from pharmacophore of them.⁴ (Figure 1b) And natural product library with high-throughput screening based on natural product scaffold is arguably still the center of drug discovery after the advent of the post-genomic era.^{10,11,12}

2. Activity-based protein profiling

After the genome project was completed successfully in 2003, the focus of pharmaceutical field has shifted towards proteins which enable us to precisely understand complicated pathological and physiological process, since they are main subjects that carry out functional activities.¹³ Meanwhile, the field of proteomics has sought to develop methods and strategies for the global analysis of protein expression and function.¹⁴ Until the early 2000s, two dimensional gel electrophoresis (2DE) was a major tool for proteome analysis,^{13,15,16} but it is difficult to analyze membrane associated and low abundance proteins due to the inherent lack of resolving power.^{14,17,18} Moreover, since 2DE tends to follow changes of protein abundance, it might miss important post-translational events.^{20,19} Therefore, more quantitative analysis of enzyme or protein activities is required for a deeper appreciation of cell and organismal biology.

Activity-based protein profiling (ABPP) established by the research group of *Cravatt*^{20,21,22,23} and *Bogyo*^{24,25,26} is one of the mature strategies for chemical proteomics. Using ABPP probe based on a variety of chemical scaffolds including mechanism-based inhibitors,²⁷ protein reactive natural products,²⁸ and general electrophilic chemotypes²⁹ and thereby it can profile the functional state of enzymes in complex proteomes.³⁰ For the integrity of enzyme active sites in complex proteome, the probe consists of three group; 1) a reacting or binding group, which covalently modify the active sites of a given enzyme, 2) a linker part, so called spacer, which connects reacting group and reporter group (tag) and also able to adjust the entire character of the probe, such as hydrophobicity or solubility, 3) reporter group (tags), like biotin or fluorophore, that enables isolation of probe-labeled enzymes or detection. (Figure 3)

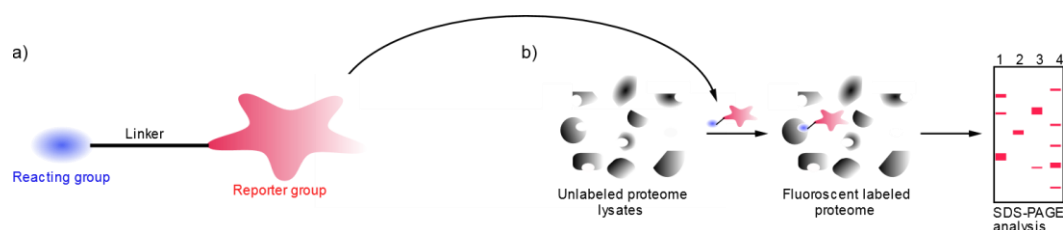


Figure 3. a) Structure of ABPP probe consists of reacting group, linker and reporter group. The reporter group often introduces poor cell permeability. b) Basic concept of activity-based protein profiling. Target protein in the complex proteome is labeled and separated through SDS-PAGE analysis.

The largest disadvantage of this kind of tagged probes is poor permeability into living cell which implies they are not available with *in vivo* application. Since most enzyme activities are dependent on factors in its intracellular microenvironment, labeling of cell lysates can't depict precise information on protein activity in living cells. To overcome this challenge, tag-free probes were developed based on click chemistry,²⁶ established by Sharpless and coworkers,³¹ which is copper-catalyzed azide alkyne cycloaddition (CuAAC) and later developed more for activity-based proteomics.^{32,33} In this approach, intact living cells can be labeled with cell-permeable terminal alkyne (or azide) attached to probes instead of bulky reporter group such as biotin. After labeling, the cells are lysed, labeled proteins are tagged to reporter group, which has complementary azide (or alkyne) functional group, by click chemistry.^{34,35,36} Depending on which tag is linked with the functional group, fluorescent dye or avidin affinity tag, tagged proteins can then be visualized by fluorescence-scanning or enriched and identified by MS. (Figure 4)

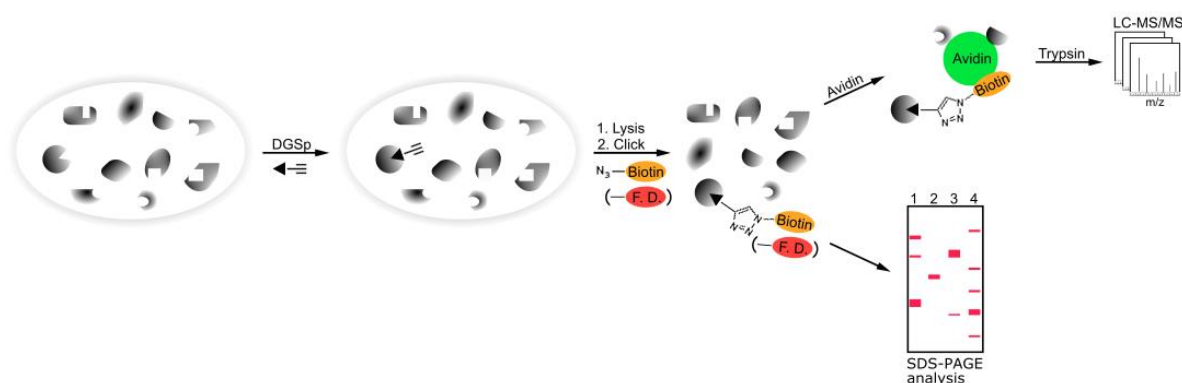


Figure 4. Basic concept of activity-based protein profiling with tag-free probe. After the click chemistry, target protein can be either enriched and analyzed by MS (Biotin case) or separated and visualized by fluorescence-scanning (F. D.-fluorescent dye case).

The additional advantage of tag-free probes is that the probes structurally resemble their corresponding parent molecule. Furthermore, they can be used tools for affinity-based protein profiling (AfBPP) after equipped with a photocrosslinker which mediates irreversible linkages between ligands and proteins upon UV irradiation. Amongst three major photo-reactive groups, benzophenone, aryl azide and diazirine, which differ in their size, efficacy, and possible side products, the diazirine group is the most frequently used one due to their small size and high crosslinking efficiency.^{37,38} (Figure 5) Therefore, ABPP or AfBPP

with tag-free probes is highly regarded as an excellent technique in drug discovery process.



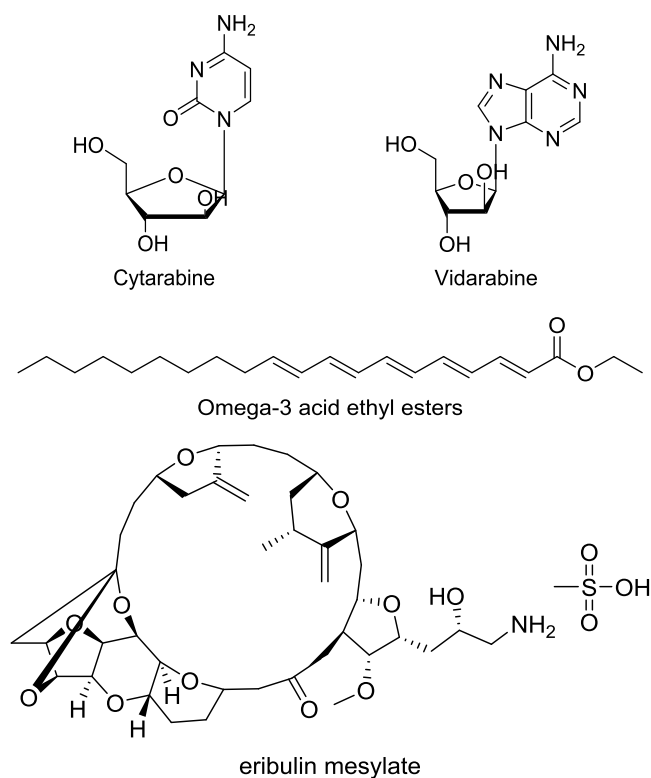
Figure 5. Structures of three major photoreactive groups aryl azide, benzophenone, and diazirine in order.

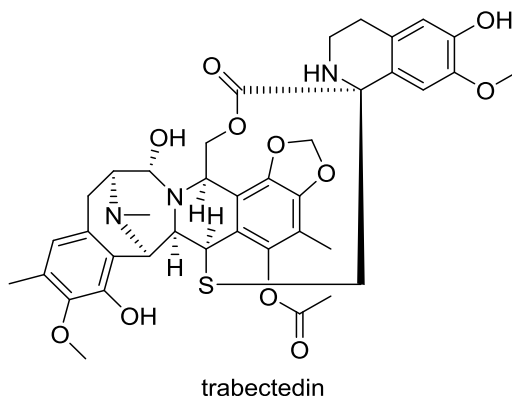
As mentioned above, natural products have been the most productive source in drug discovery, and they attract attention again in the era of antibiotic crisis caused by drug resistance. But their target proteins and inhibitory mechanisms are still unknown in most cases. And it is needed to investigate mode of action of natural products and thereby enabling further target-directed inhibitor development by fine-tuning their structures.

II. Exploring a natural product, smenothiazole A and B

1. Introduction

As mentioned in chapter I, natural products have been productive source of therapeutic reagents. Above all, marine natural products, genetically distinct from terrestrial ones, have huge potential, since about 80% of the organisms on Earth inhabit the ocean and most of them have not yet been studied or identified.³⁹ Therefore, many scientific groups are exploring marine environment and identifying compounds with active pharmacological properties.^{40,41,42,43} Some of the drugs of marine origin were approved from U.S. Food and Drug Administration (FDA) or European Union (EU), (Figure 6) and several compounds are now in preclinical or clinical stage.⁴⁴





Compound name	Marine organism	Chemical class	Disease area
Cytarabine	Sponge	Nucleoside	Cancer, leukemia
Vidarabine	Sponge	Nucleoside	Anti-viral
Omega-3 acid ethyl esters	Fish	Omega-3 fatty acid	Hypertriglyceridemia
eribulin mesylate	Sponge	Macrolide	Breast cancer
trabectedin	Tunicate	Alkaloid	Cancer

Figure 6. Examples of marine drugs.

Smenothiazole A and B were coincidentally isolated from the Caribbean sponge, *Smenospongia aurea* (*S. aurea*), and analyzed by *G. Esposito et al.* in 2015.⁴⁵ (Figure 7) The authors struggled with isolation of the previously known smenamides due to the difficulties of separation, so they improved the isolation procedure which revealed presence of two other compounds, smenothiazole A and B. Subsequently, their *in vitro* biological activities were investigated by MTT (3-(4,5-dimethylthiazol-2-yl)-2,5-diphenyltetrazolium bromide) assay⁴⁹ (Figure 8). It is a simple way to measure cell viability and is the first step for testing the cytotoxic effect of a compound. Viable cells with active metabolism convert MTT into the corresponding purple-colored insoluble formazan, while dead cells cannot do it.

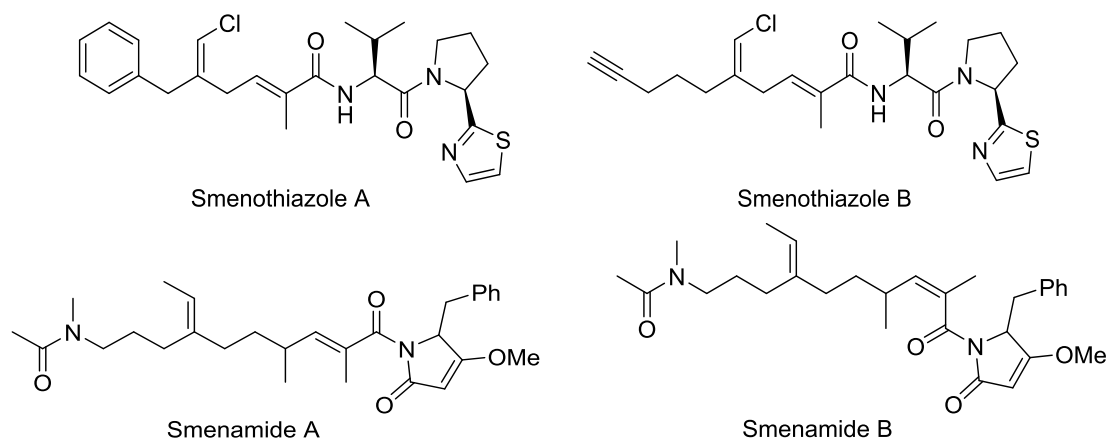


Figure 7. Structures of smenothiazole A and B and smenamamide A and B.

Smenothiazoles significantly reduced cell viability in the Calu-1 and LC31 lung-cancer cell lines and in the A2780 ovary cancer cell lines.⁴⁹ Some differences were observed between different cell lines, as well as between the two compounds, but no general trend could be observed. It is noteworthy, however, that smenothiazole A was significantly active on the A2780 ovarian cells at concentration as low as 10 nM. The activity on the breast-cancer MCF-7 cells was less remarkable, and cell viability was still in the range of 40%–50% of the control, even at the highest concentration tested.

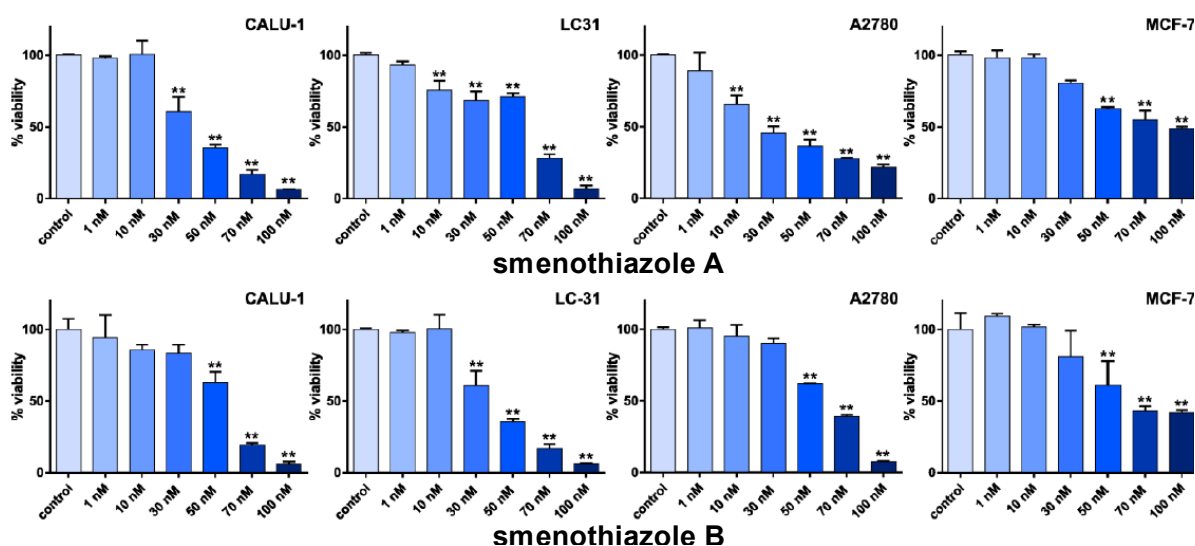


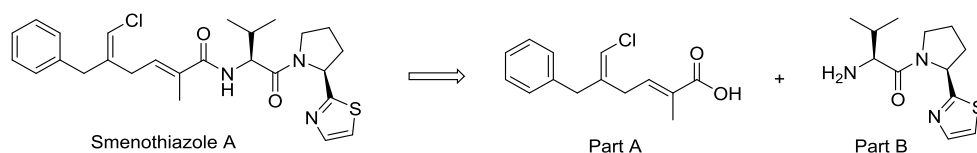
Figure 8. Evaluation by the MTT assay of viability of four cancer cell line after 48 h of treatment with smenothiazole A and smenothiazole B. ** $p < 0.0005$.⁴⁹

As a result, it was confirmed that smenothiazoles are selectively active against ovarian cancer cells at nanomolar level. However, only small amounts of compounds could be isolated and only the MTT assay could be performed to check bioactivity. A lot of further experiments still have to be done to investigate their target(s), mode of action, and toxicity. Therefore, synthesizing smenothiazoles as well as smenothiazole-derived probes equipped with photocrosslinker moieties, checking their antimicrobial activity, and figuring out target proteins and mode of action are the goals of this project.

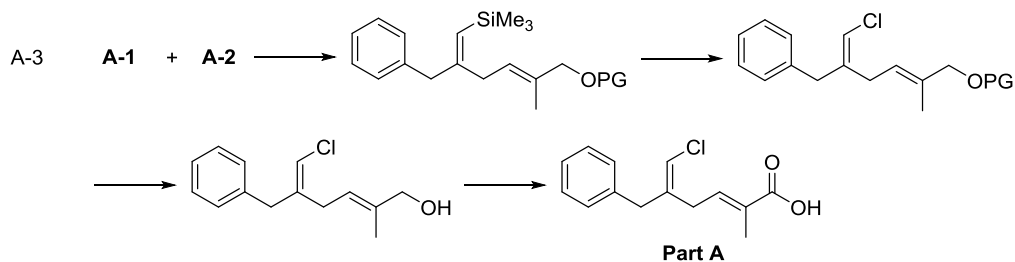
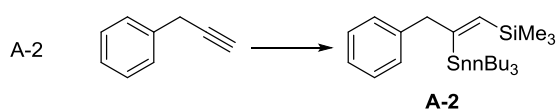
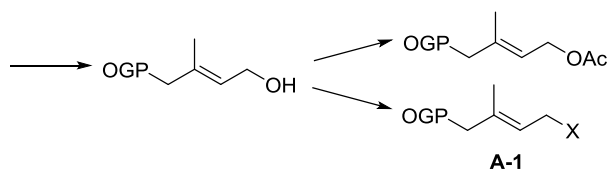
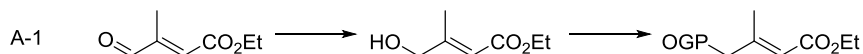
2. Result and Discussion

2.1. Synthetic route I

Retrosynthetic analysis of Smenothiazole A is based on the fact that this molecule contains two amide groups, and the first retrosynthetic disconnection gives two fragments A and B, which are expected to be easily coupled in the last step. (Figure 9) Additionally, there is already an efficient procedure for the part B published in 2011 by *E. Owusu-Ansah et al.*⁴⁶ Accordingly the synthesis efforts were focused on the part A. The total synthesis of this molecule was believed to be challenging since no methods of construction of such structures were known at the time.



[Part A]



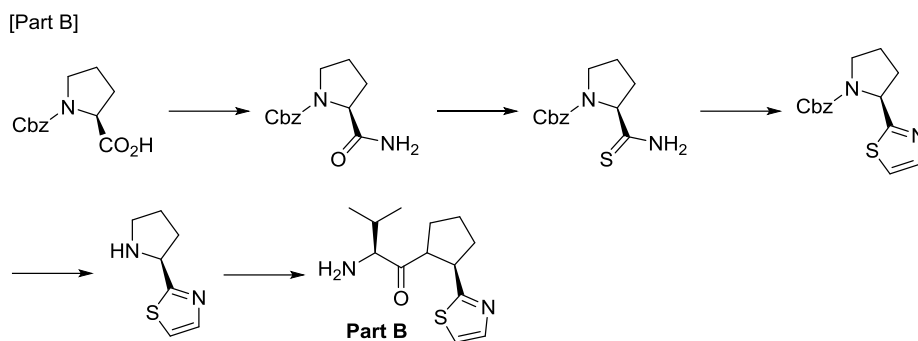
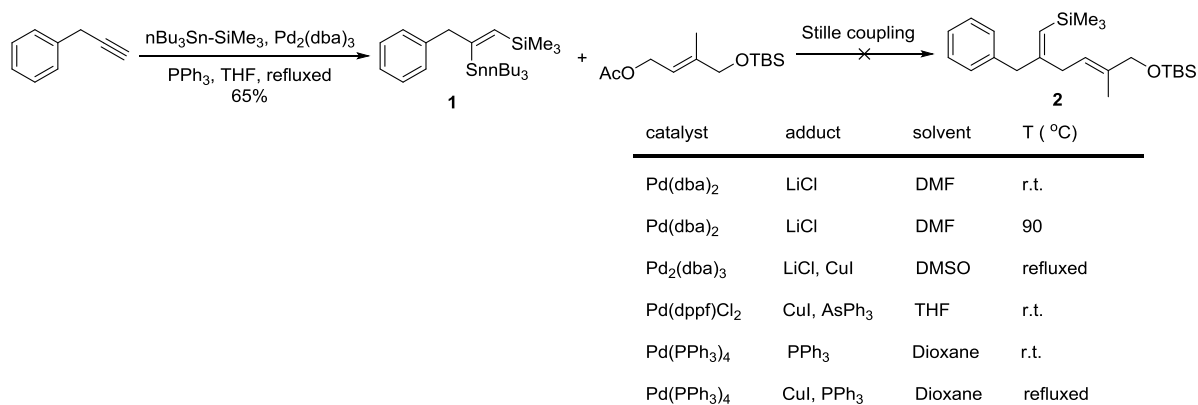


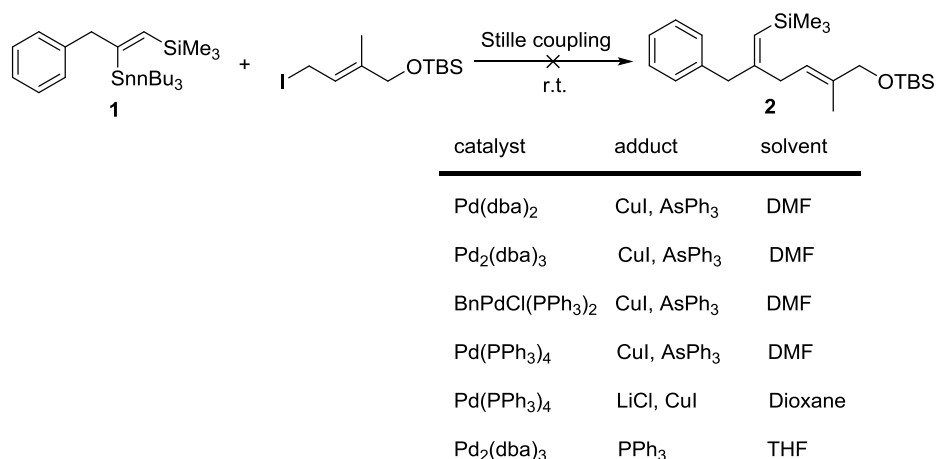
Figure 9. Retrosynthesis of smenothiazole A and a plausible synthetic route of part A and B.

In accordance with the discussed retrosynthetic scheme, the following synthetic steps were performed. The successful silastannylation of prop-2-yn-1-ylbenzene was followed by Stille coupling, which turned to be the crucial part of this synthetic pathway. (Scheme 1) The coupling reaction was conducted under several conditions, different kinds of palladium catalysts, adducts, solvents and temperatures were tried, but no traces of **2** could be observed.



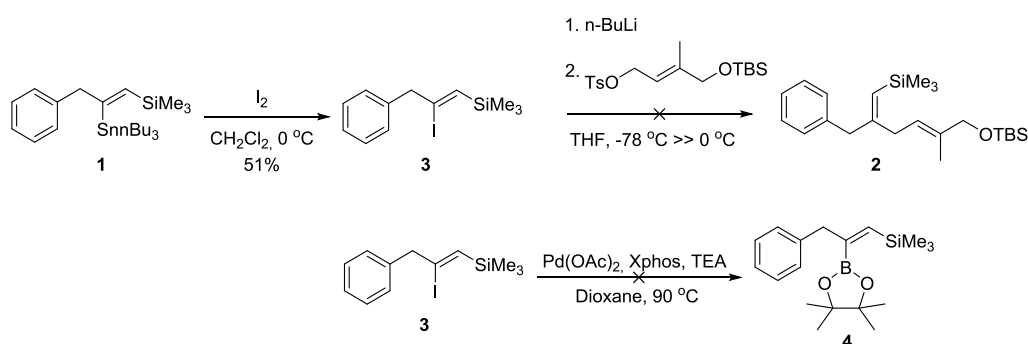
Scheme 1. Various Stille coupling conditions with allyl acetate.

The leaving group was then changed from acetate to iodide, which, unfortunately, did not alter the result in any way. (Scheme 2)



Scheme 2. Various Stille coupling conditions with allyl iodine.

Lithiation with following nucleophilic substitution and Suzuki coupling were chosen as alternative approaches for the coupling step. Substitution of tin to halogen was required as a first step for both of them. (Scheme 3) Treatment of **1** with iodine generated the iodide **3**. Following lithiation and reaction with the tosylate caused, unfortunately, many byproducts as seen on TLC. Next, the Suzuki coupling approach was tried. Since organoboron species are essential for Suzuki coupling, **3** had to be converted to **4** prior to coupling. However, the borylated intermediate was not obtained possibly due to steric hindrance of **3**. Therefore, an alternative synthetic route was needed to avoid the issue in the first scheme.



Scheme 3. Lithiation and borylation of intermediate **3**.

2.2. Synthetic route II

As mentioned above, difficulties with Stille coupling made it necessary to redesign the synthetic route without the need for metal coupling. In this case, Wittig olefination was used for the formation of a double bond. (Figure 10)

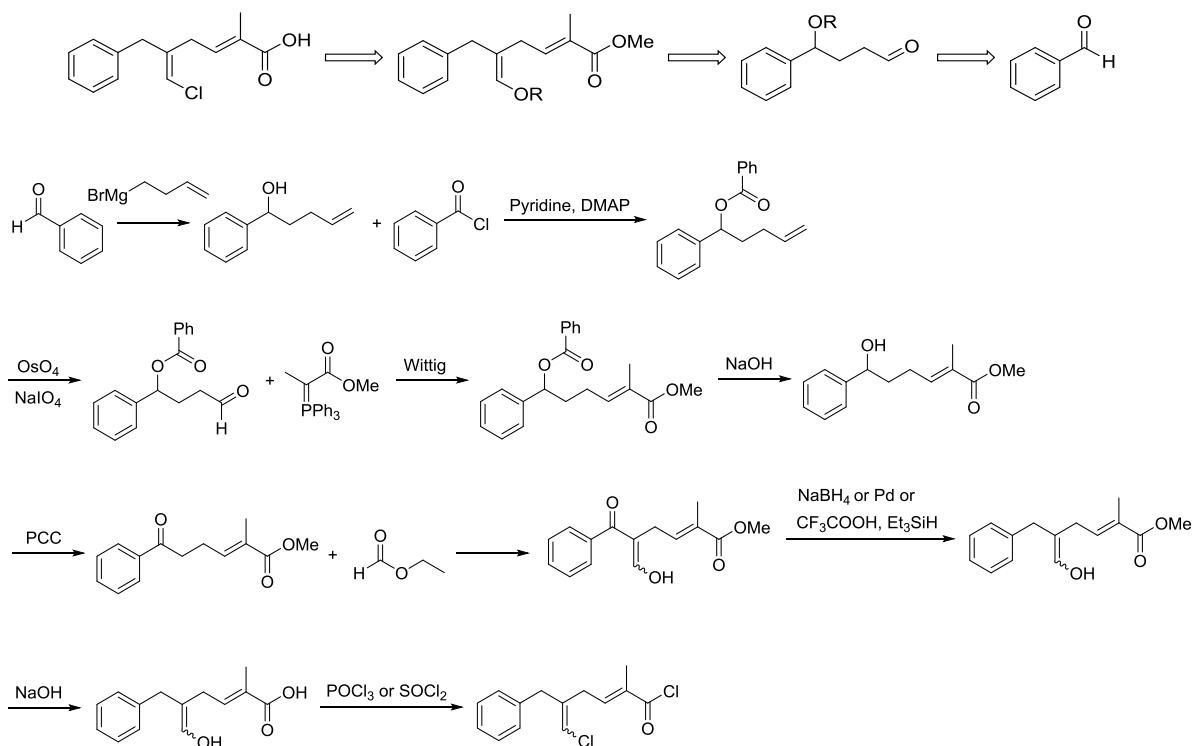
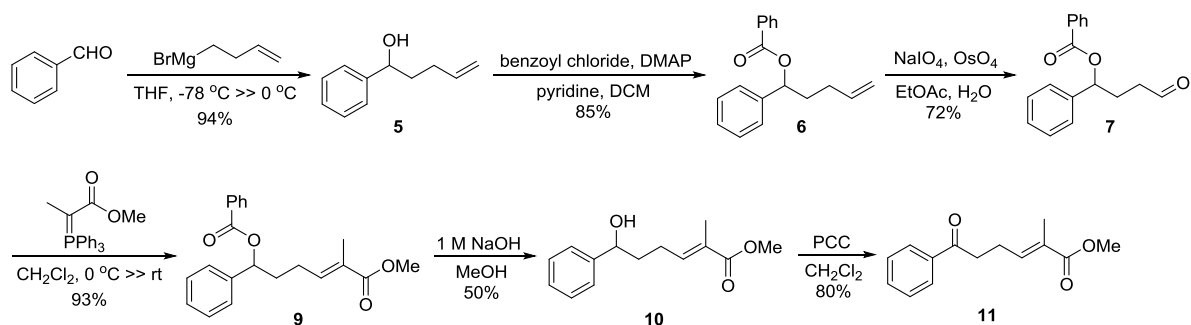
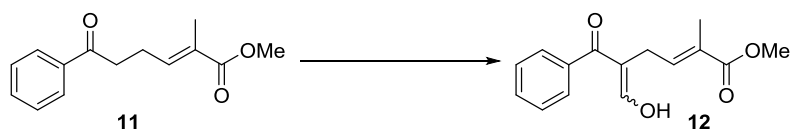


Figure 10. An alternative retrosynthesis of part A and a corresponding plausible synthetic route. Treatment of benzaldehyde with the Grignard reagent generated **5** in excellent yield. (Scheme 4) The alcohol was protected with benzoyl chloride and the olefin of **6** transformed to aldehyde, **7**, by oxidative cleavage using osmium tetroxide with sodium periodate as an oxidizing agent. Wittig reaction of aldehyde **7** with the triphenyl phosphonium ylide gave **9** in excellent yield. Deprotection of **9** followed by oxidation with PCC generated ketone **11**.



Scheme 4. Second route successfully proceeded to get intermediate **11**.

To introduce the chloromethylene moiety into α -position of the ketone, a hydroxyl-methylene group was needed first. Several methods were found and most of them were employed ethyl formate and several bases. (Scheme 5) First, the reaction was carried out with sodium methoxide as a base at three temperatures, however, no spot was detected under UV (254 nm) and product formation could not be detected by LCMS even though **11** was totally consumed.⁴⁷ Other bases, such as sodium ethoxide, potassium t-butoxide and sodium hydride, were used, but neither gave any promising results.^{48,49,50,51} Vilsmeier reaction was also conducted in two different solvents,^{52,53} however, without any success.



reagent	base	solvent	T (°C)
ethyl formate	NaOMe	toluene	0
ethyl formate	NaOMe	ether	0
ethyl formate	NaH	THF	0 >> r.t.
ethyl formate	NaH	benzene	0 >> r.t.
ethyl formate	t-BuOK	THF	r.t.
ethyl formate	LDA	THF	-78
POCl ₃ , DMF		THF	0 >> 40
POCl ₃ , DMF		DCM	0 >> refluxed

Scheme 5. Various conditions to introduce the hydroxymethylene group.

2.3. Synthetic route III

Due to the difficulties with the α -addition of the hydroxymethylene group, another retrosynthetic scheme based on β -aryl ketone moiety was designed. (Figure 11) Here, the chloromethylene group could be introduced by Wittig reaction of the corresponding ketone, making this synthetic pathway fundamentally different from the previous route.

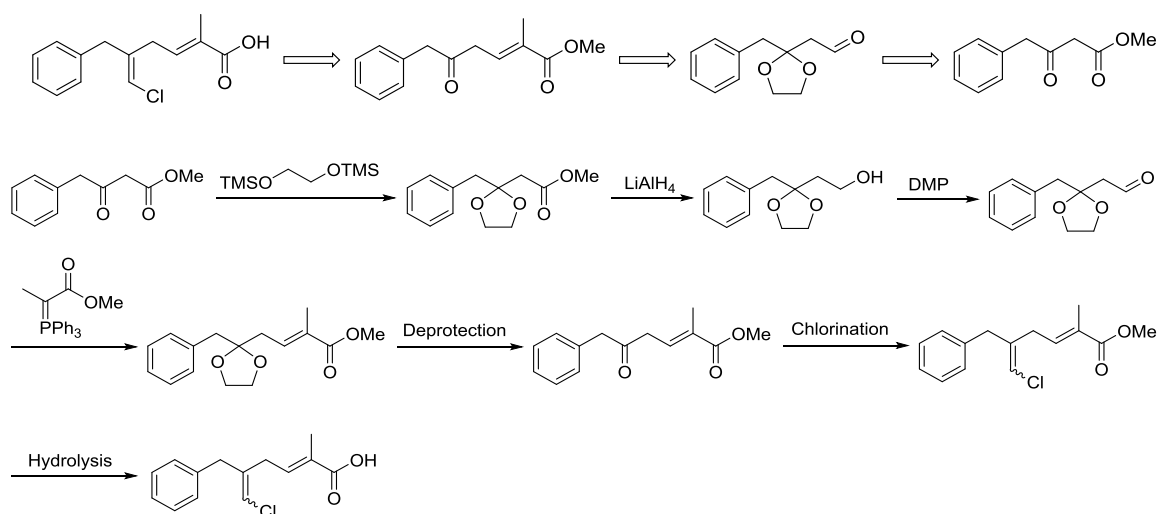
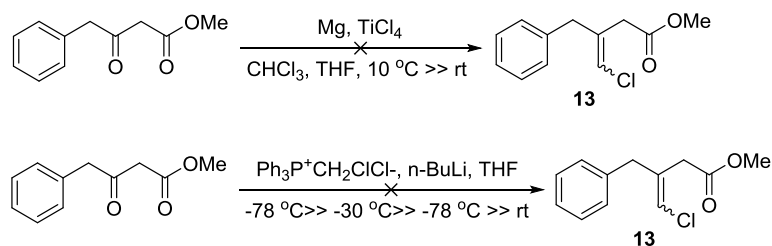


Figure 11. Third retrosynthesis of part A and a corresponding plausible synthetic route.

Because the introduction of the chloromethylene group might also be crucial in this scheme, it was tried first to confirm that this is possible in this system. (Scheme 6) It is known that direct oxidative addition of CHCl_3 to the Mg-TiCl_4 bimetallic species results in the generation of a highly nucleophilic and practically convenient chloromethylenetitanium complex, which efficiently promotes condensation with enolizable ketone,⁵⁴ but unfortunately, this chlorocarbenoid did not yield **13**. Next, Wittig olefination was conducted with $n\text{-BuLi}$ as a strong base, however, formation of **13** could not be observed, presumably due to steric hindrance caused by the phenyl and keto group in β -position.



Scheme 6. Two different way to introduce chloromethylene moiety onto ketone-C.

The scheme was modified to reduce steric hindrance and move the crucial step to the earlier part so that it could be determined fast whether this scheme was promising or not. (Figure 12)

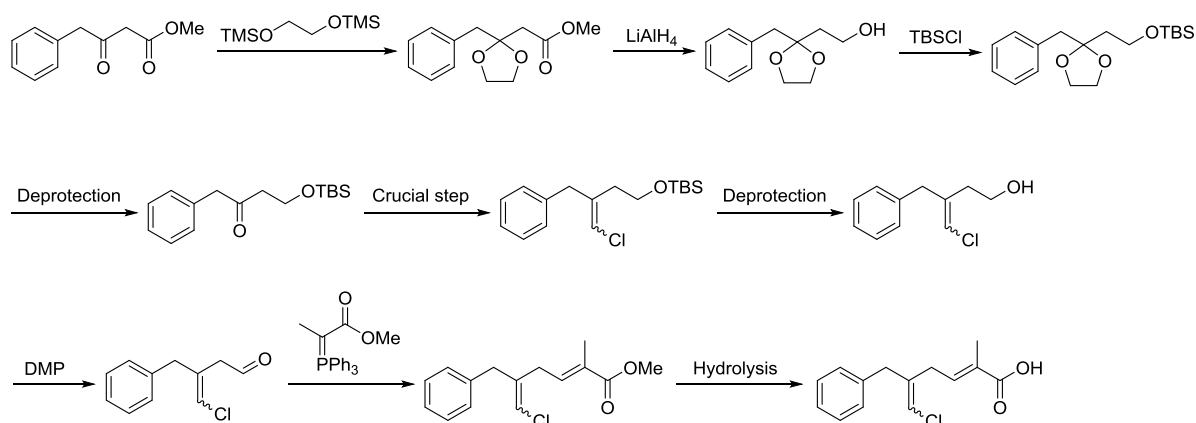
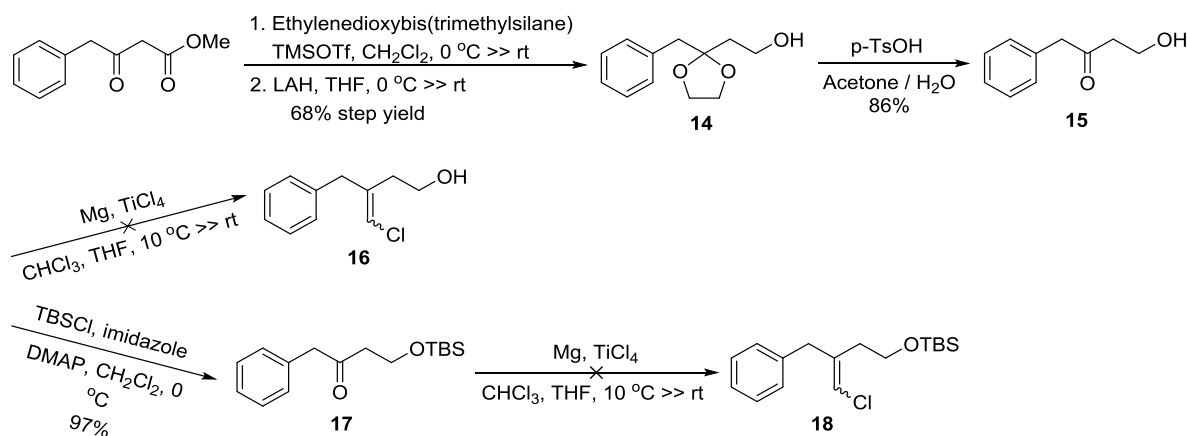


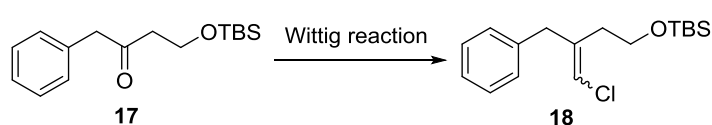
Figure 12. An adapted synthetic route for the previous scheme based on β -aryl ketone moiety

The starting material was converted into the ketone **15** in 3 steps. (Scheme 7) The chloromethylenetitanium complex did not yield **16**, probably due to the free alcohol group. Hence, the alcohol was protected first with TBS, and then the crucial step was conducted with the chloromethylenetitanium complex again, however, without success.



Scheme 7. Chloromethylenetitanium complex was used to introduce the chloromethylene group.

The remaining option was to use Wittig reaction, which was conducted with chloromethyltriphenylphosphonium chloride and different bases.^{55,56} (Scheme 8) However, all of these reactions resulted in the formation of many products as was confirmed by TLC.

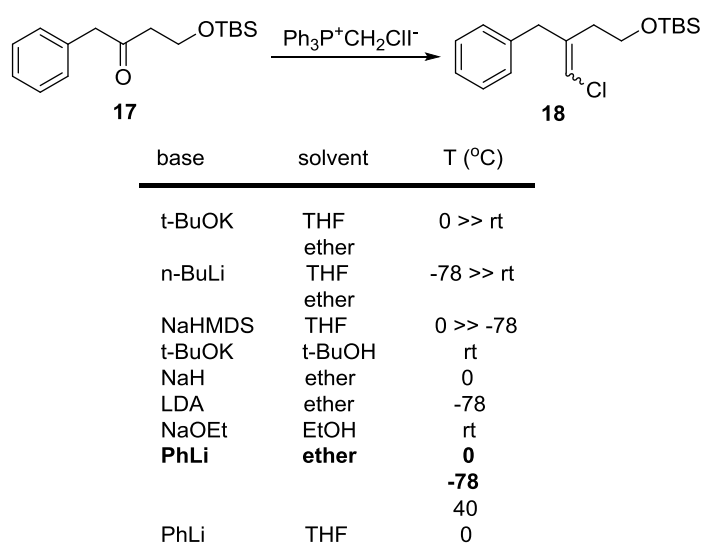


Reagent	Base	Solv.	T (°C)
Ph ₃ P ⁺ CH ₂ ClCl ⁻	n-BuLi	THF	-78 >> -30 >> -78 >> rt
	t-BuLi		0 >> rt
	t-BuOK		0 >> rt
Ph ₃ P ⁺ CH ₂ ClCl ⁻	PhLi	ether	0 >> rt
		THF	0 >> rt
Ph ₃ P ⁺ CH ₂ ClCl ⁻	NaHMDS	THF ether	0 >> -78 >> rt

Scheme 8. Wittig reaction with chloromethyltriphenylphosphonium chloride.

Amongst several papers regarding this kind of Wittig olefination, *A. Caso et al*⁵⁷ reported that chloromethyltriphenylphosphonium iodide yielded desired product in moderate yield. The olefination was conducted once more with it. (Scheme 9) The condition used in literature did not work on this moiety. Therefore, different bases, solvents, and reaction temperature were used. Intriguingly, only the reaction with phenyllithium in ether at -78

or 0 °C yielded the regioisomer mixture of the desired compound in 11% yield.



Scheme 9. Conditions for the Wittig reaction with chloromethyltriphenylphosphonium iodide.

Meanwhile, two other retrosynthesis were designed for part A. (Figure 13) They still included the crucial step as in Figure 12, however, different starting materials open the possibilities to overcome the low yield.

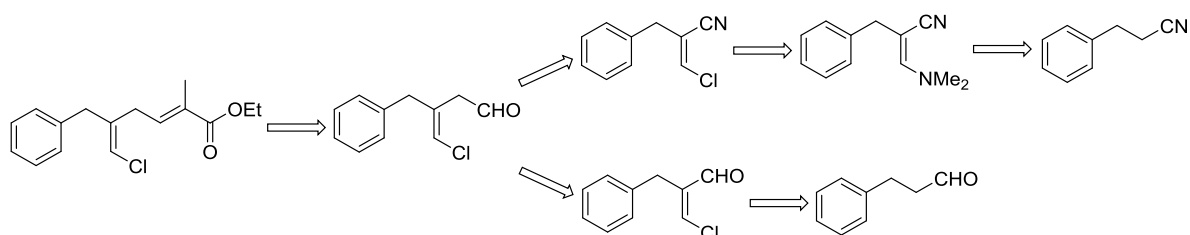


Figure 13. Two alternative retrosynthesis schemes of part A.

2.4. Synthetic route IV

In 2017, *X. Ma et al.*⁵⁸ published a paper addressing the total synthesis of smenothiazole A and B. However, they only reported the synthesis without any bioactivity data or target analysis. Therefore, it was decided to focus on synthesizing a photoprobe of smenothiazole

B and gather bioactivity data. Retrosynthesis of the probe was designed based on the published synthetic scheme. (Figure 14)

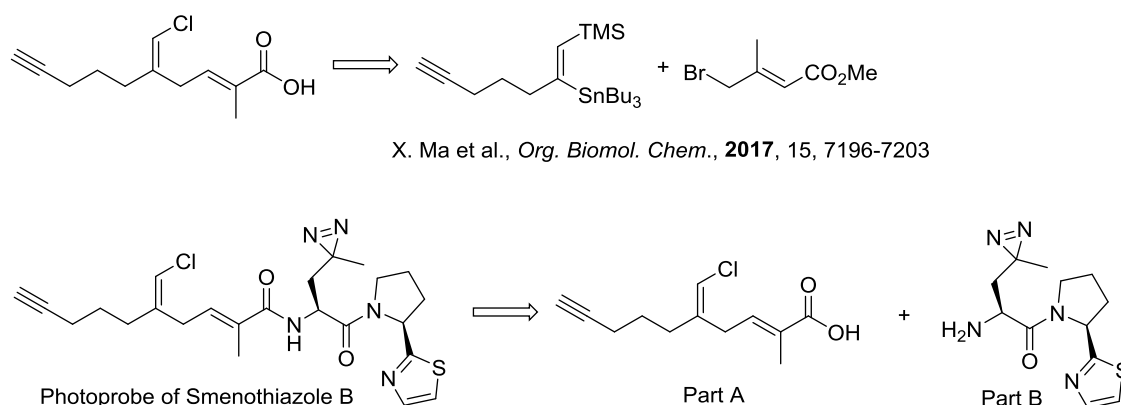


Figure 14. Published retrosynthesis of part A by X. Ma et al. and a plausible scheme for the synthesis of a photoprobe of smenothiazole B.

As mentioned in the introduction, a photocrosslinker containing probe has the advantage of irreversibly linking the compound of interest to its target protein upon irradiation with UV light. And part B might be appropriate place to introduce the diazine moiety since replacement of valine with photo-leucine seems to reduce the burden of the structural difference from the original compound, which is likely going to have the similar activity of it. (Figure 15) Additionally, synthesis of photo-leucine is well described by Y. Ikeda.⁵⁹

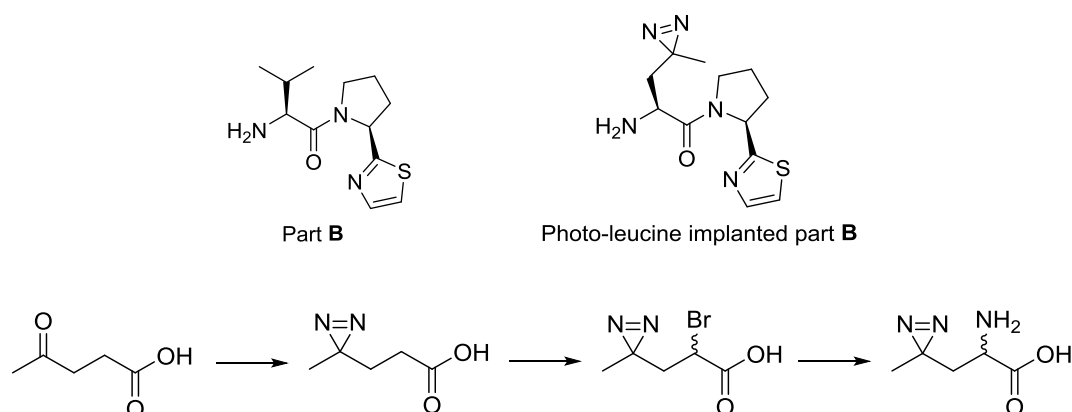
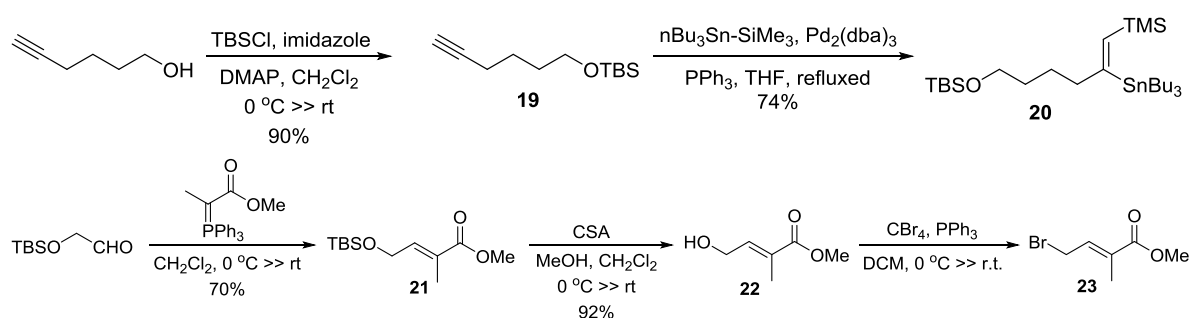


Figure 15. Structural similarity between original part B and diazine implanted one, and plausible synthetic route of photo-leucine.⁵⁹

For part A, protection of hex-5-yn-1-ol followed by silastannation generated **20** in good yield. (Scheme 10) Wittig olefination of 2-((*tert*-butyldimethylsilyl)oxy)acetaldehyde gave **21** followed by deprotection of the TBS group to convert the corresponding alcohol to bromine. After the following bromination, however, something that looked like a regioisomer mixture was obtained although starting material, **22**, was clearly one isomer in the NMR. (Figure 16) Those were not separable on TLC or by HPLC, and all attempts, such as changing solvent, bromine source, and reaction temperature, to resolve it failed.



Scheme 10. Synthetic strategy based on the reference.⁵⁸

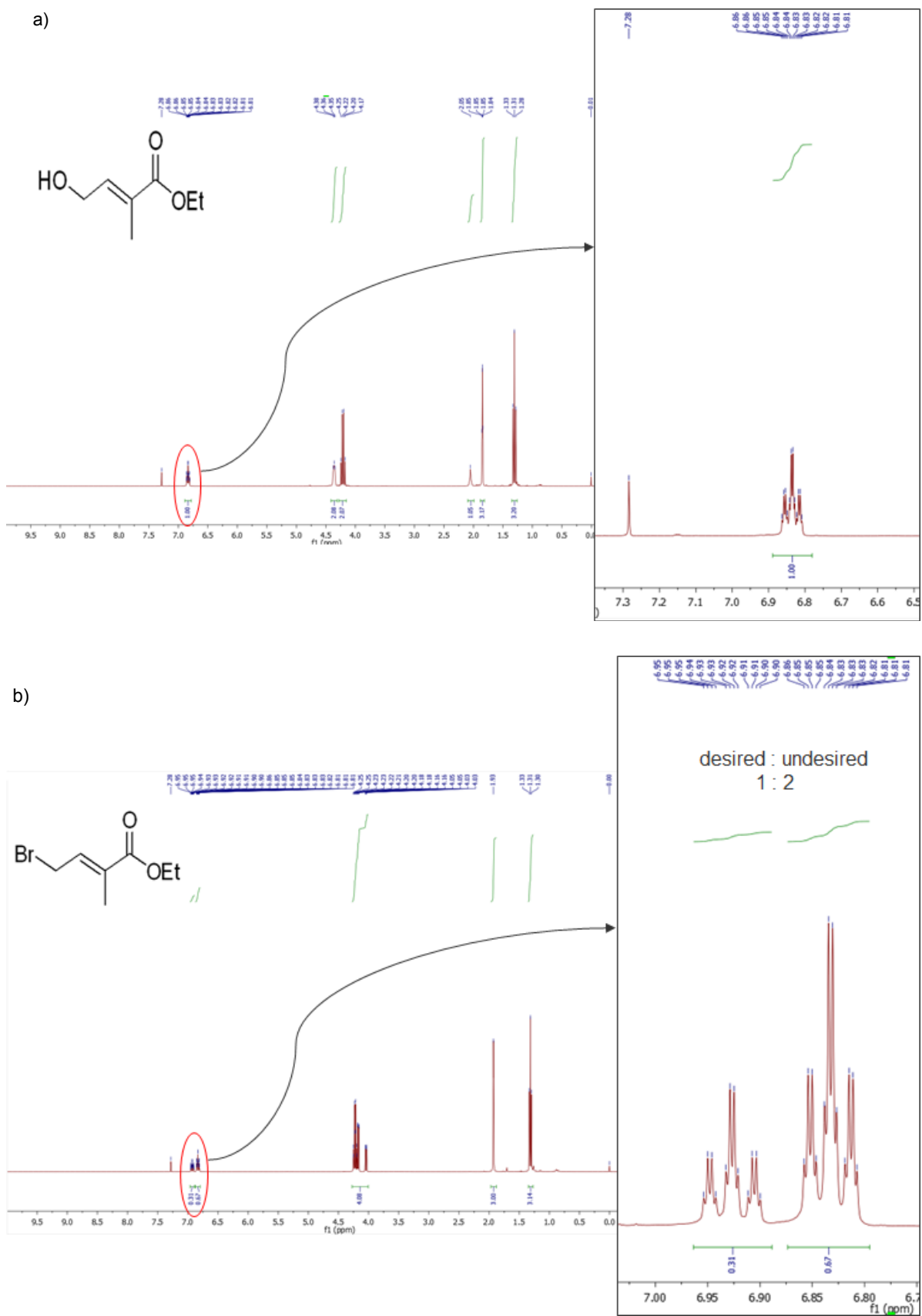


Figure 16. NMR spectra of a) 22, and b) 23.

Only lowering the temperature from 0 °C to -30 °C raised the ratio of the desired product, however, formation of the undesired isomer could not be completely prevented. (Figure 17) The other possibility was separate the isomers later in the synthesis. However, unfortunately, the purity of the intermediates in each step got worse presumably due to byproducts of each reaction and crude starting materials of each step.

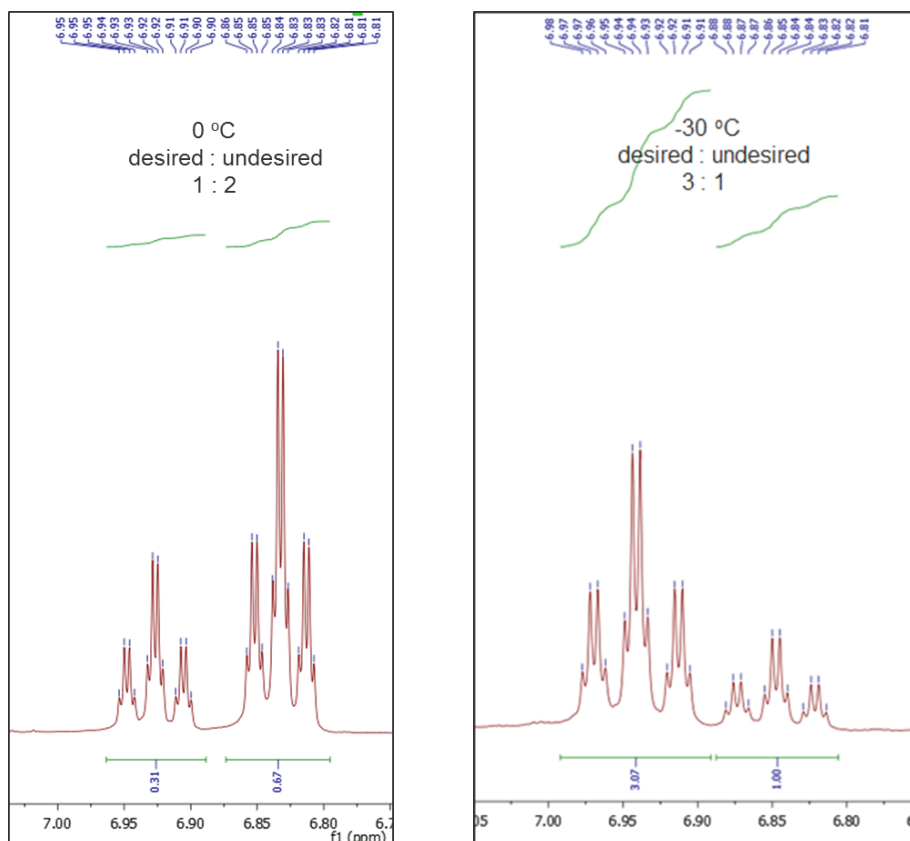


Figure 17. The ratio of regioisomer was changed as reaction temperature decreased.

3. Conclusion

Four strategies for synthesis of smenothiazole A and B or photoprobe of them were planned, but none was successful. The effort for the synthesis was concentrated on part A due to the existence of the known procedure³⁷ regarding part B (Figure 9). Stille coupling was challenging on synthesis of part A in the first strategy, and it was tried under several conditions, different palladium catalysts, adducts, solvents and reaction temperatures (Scheme 1 and 2), but all conditions did not yield the desired product. Furthermore, the borylation for Suzuki coupling and lithiation instead of Stille coupling did not work. (Scheme 3) To avoid coupling reactions catalyzed by metal complexes, Wittig-olefination was selected to extend the carbon chain in the second strategy (Figure 10), and it was successful until the oxidation of the benzylic alcohol. The following step, introducing hydroxymethylene group, turned out to be crucial, since it was necessary as a bridge towards chlorination. The chloride was regarded as one of the core structures for the activity of smenothiazoles as this part was well preserved in both structures. But all attempts winded up a number of faint spots on the TLC under UV (254 nm), which implied decomposition of the compound during the reaction. In the third strategy, introducing the chloromethylene group onto keto-carbon was adopted for the acquisition of chloride into the compound. (Figure 12) The chlorocarbenoid, a precursor of chloromethylene group, could be generated from chloromethyltriphenylphosphonium cation, and only the cation with iodide counter anion, not chloride, yielded the regioisomer mixture of desired compound in low yield. Meanwhile, a paper describing the total synthesis of smenothiazole A and B was published by *X. Ma et al.*⁵⁸, and the direction of our project shifted to synthesis of photoprobe of smenothiazole B using their procedure. (Figure 14) However, only a regioisomer mixture was obtained in the bromination step (Figure 16), and this crude generated the intermediates with inseparable byproducts.

The structural novelty and good activity against ovarian cancer cells of smenothiazole A and B make them appear promising and challenging, but there were severe difficulties in synthesizing the natural products and photoprobe of them. According to the paper, it takes 16 steps to synthesize smenothiazole B, which implies it will need even more steps to obtain the photoprobe. Furthermore, the synthetic scheme of the reference was not reproducible in our lab. So far, no other activity assay, target identification or pharmacokinetics of them has not been published, even though it has been four years

since they were isolated. One of the main reasons might be the difficulties of synthesis of the natural products. As mentioned above, natural products have great potential in drug discovery, however, it is also true that synthesis of them is challenging to accomplish.

III. Degrasyn exhibits antibiotic activity against multi-resistant *Staphylococcus aureus* by modifying several essential cysteines

The following chapters are based upon a manuscript which will be published in: Kyu Myung Lee, Philipp Le, Stephan A. Sieber*, and Stephan M. Hacker*: Degrasyn exhibits antibiotic activity against multi-resistant *Staphylococcus aureus* by modifying several essential cysteines, *Chem. Commun.* accepted.

*contributed equally

1. Introduction

1.1. Advantages of drug repurposing

One of the strategies to develop drugs is drug repurposing, also known as drug repositioning, which reuses marketed drugs for new medical indications.^{60,61,62} (Table 1) This strategy offers several advantages over developing a new drug for a given indication. First, and arguably, safety of existing drugs has already been verified by government authorities and patients, which means it's not likely going to fail due to safety issues in the end. Second, less effort and money are needed. The term, already verified, implies that there could be huge amount of savings in preclinical, phase I and phase II costs.⁶³ Third, time could be saved as well since bioavailability study, clinical evidence of effectiveness, and safety assessment have been completed. And finally, it could figure out new target(s) or mode of action in other species or organs.⁶⁰ Furthermore, this strategy can be also applied onto earlier stages of drug discovery with potent drug-like compounds instead of licensed drugs.

Drug name	Original indication	New indication	Date of approval	Comments on outcome of repurposing
Zidovudine	Cancer	HIV/AIDS	1987	Zidovudine was the first anti-HIV drug to be approved by the FDA
Minoxidil	Hypertension	Hair loss	1988	Global sales for minoxidil were US\$860 million in 2016
Sildenafil	Angina	Erectile dysfunction	1998	Marketed as Viagra, sildenafil became the leading product in the erectile dysfunction drug market, with global sales in 2012 of \$2.05 billion
Thalidomide	Morning sickness	Erythema nodosum leprosum and multiple myeloma	1998, 2006	Thalidomide derivatives have achieved substantial clinical and commercial success in multiple myeloma
Celecoxib	Pain and inflammation	Familial adenomatous polyps	2000	The total revenue from Celebrex (Pfizer) at the end of 2014 was \$2.69 billion
Atomoxetine	Parkinson disease	ADHD	2002	Strattera (Eli Lilly) recorded global sales of \$855 million in 2016
Duloxetine	Depression	SUI	2004	Approved by the EMA for SUI. The application was withdrawn in the US. Duloxetine is approved for the treatment of depression and chronic pain in the US

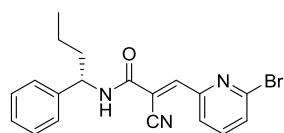
Rituximab	Various cancers	Rheumatoid arthritis	2006	Global sales of rituximab topped \$7 billion in 2015
Raloxifene	Osteoporosis	Breast cancer	2007	Approved by the FDA for invasive breast cancer. Worldwide sales of \$237 million in 2015
Fingolimod	Transplant rejection	MS	2010	First oral disease-modifying therapy to be approved for MS. Global sales for fingolimod (Gilenya) reached \$3.1 billion in 2017
Dapoxetine	Analgesia and depression	Premature ejaculation	2012	Approved in the UK and a number of European countries; still awaiting approval in the US. Peak sales are projected to reach \$750 million
Topiramate	Epilepsy	Obesity	2012	Qsymia (Vivus) contains topiramate in combination with phentermine
Ketoconazole	Fungal infections	Cushing syndrome	2014	Approved by the EMA for Cushing syndrome in adults and adolescents above the age of 12 years
Aspirin	Analgesia	Colorectal cancer	2015	US Preventive Services Task Force released draft recommendations in September 2015 regarding the use of aspirin to help prevent cardiovascular disease and colorectal cancer

Table 1. Selected successful drug repurposing examples.⁶⁰

1.2. Potential of degrasyn in drug repurposing

Rapid bacterial resistance development threatens human health. Thus, identifying new classes of antibiotics and bacterial target proteins for clinical intervention is a very urgent task. As mentioned above, one efficient strategy to address this is the repurposing of existing drugs originally developed to target human proteins.^{64,65} As illustrated by several recent examples,^{66,67,68,69} this strategy is very promising as bacterial and human cells share many homologous proteins with conserved structures that can serve as targets. In this way, established compounds targeting human proteins have the potential to coincidentally also address essential bacterial proteins. In a recent drug-repurposing screen, we investigated the antibiotic activity of a library mainly consisting of human kinase inhibitors and identified a derivative of sorafenib as a potent inhibitor of menaquinone biosynthesis and

an activator of signal peptidase.⁷⁰ Within this screen, another hit molecule, the human deubiquitination enzyme (DUB) inhibitor degrasyn (also called WP1130), was identified with a minimal inhibitory concentration (MIC) against the methicillin-sensitive *Staphylococcus aureus* (MSSA) strain NCTC8325 of 6.25 μM . (Figure 18) In human cells degrasyn down-regulates Mcl-1 and induces apoptosis of leukemia cells.^{71,72} Due to these promising properties the compound was further considered for clinical development. In addition, anti-infective effects of degrasyn, i.e. the reduction of intracellular replication of *Listeria monocytogenes* (*L. monocytogenes*) and viruses, were previously reported, but were so far mainly attributed to degrasyn inhibiting DUBs in macrophages and in this way increasing their anti-infective capacity.^{73,74,75,76,77} Direct antibiotic effects of degrasyn on isolated bacteria have to the best of our knowledge so far not been reported.



MIC : 6.25 μM against *S. aureus*

Figure 18. Structure and MIC of degrasyn (DGS).

2. Result and Discussion

2.1. Biological validation of degrasyn by MIC assay

As shown in Figure 18, degrasyn (**DGS**) is active against *S. aureus* NCTC8325 strain, and then was further exploited against other species. Several bacteria including gram negative as well as gram positive were selected for MIC assay. It turned out that **DGS** has potent activity against gram positive bacteria, *Staphylococcus aureus* (*S. aureus*) ACTT29213, and *L. monocytogenes* EGD-e, but no activity against gram negative bacteria, *Acinetobacter baumannii* (*A. baumannii*) DSM 30007, *Pseudomonas aeruginosa* (*P. aeruginosa*) DSM 19882, and *Salmonella Typhimurium* (*S. typhimurium*) LT2. (Figure 19) In spite of losing its activity over gram negative bacteria, it still shows potency against methicillin-resistant *S. aureus* (MRSA), USA300, which led to exploring activity against more MRSA strains. Satisfyingly, the activity of **DGS** largely retains over all MRSA on the list (Figure 20), and 10 out of 11 strains are clinical isolates⁷⁸ suggesting a different mode of action as compared to existing drugs.

Bacteria (gram positive)	<i>S. aureus</i> NCTC8325	<i>S. aureus</i> ACTT29213	<i>S. aureus</i> USA300*	<i>L. monocytogenes</i> EGD-e
MIC (μM)	6.25	12.5	25	6.25
Bacteria (gram negative)	<i>A. baumannii</i> DSM30007	<i>P. aeruginosa</i> DSM19882	<i>S. typhimurium</i> LT2	
MIC (μM)	> 100	> 100	> 100	

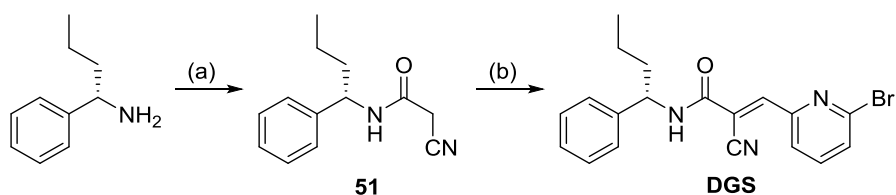
Figure 19. MIC of **DGS** against various species. *MRSA (methicillin-resistant *S. aureus*)

Strain	MIC (μM)	Strain	MIC (μM)
Mu50	12.5	VA417350*	12.5
VA402525*	12.5	IS050611*	12.5
VA409044*	12.5	IS050678*	12.5
VA402923*	6.25	BK097296*	6.25
VA412350*	12.5	BK095395*	6.25
VA418879*	6.25		

Figure 20. MIC of **DGS** against various MRSA strains.

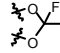
* clinical isolates.

2.2. Structure activity relationship of degrasyn



Scheme 12. Synthesis of **DGS**. (*R*)-**DGS** was synthesized using the same protocol starting from (*R*)-1-phenylbutan-1-amine. (a) 1-cyanoacetyl-3,5-dimethyl-1*H*-pyrazole, toluene, reflux, 75%; (b) 6-Bromo-2-pyridinecarboxaldehyde, piperidine, EtOH, reflux, 65%.

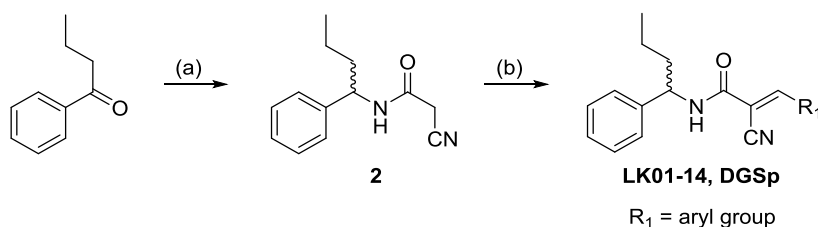
To elucidate the structure activity relationship of **DGS**, the scaffold was systematically altered by inverting the stereocenter, varying the substituents on the pyridine ring and fine-tuning of the reactive group. **DGS** and its enantiomer, (*R*)-**DGS**, were prepared according to established synthetic procedures. (Scheme 12) Acylation of (*S*)- or (*R*)-1-phenylbutan-1-amine with 1-cyanoacetyl-3,5-dimethyl-1*H*-pyrazole generated intermediate **51** or its enantiomer. The desired products were obtained by Knoevenagel condensation of **51** or its enantiomer with 6-bromopicolinaldehyde. A change of the stereocenter resulted in a drop of MIC from 6.25 μM of degrasyn to 12.5 μM for the derivative (*R*)-**DGS** suggesting only a minor role of the absolute configuration (Figure 21). Accordingly, a racemic mixture of (*R*)/(*S*)-**DGS** exhibited a comparable MIC value. The synthesis of pyridine variants followed a modular blueprint as outlined in Scheme 13. 2-cyano-*N*-(1-phenylbutyl)acetamide **52** was prepared from butyrophenone through oximation followed by hydrogenation and cyanoacetylation. **52** was then condensed with various aromatic aldehyde to afford degrasyn derivatives. (Figure 21) Due to the minor role of the stereocenter and for the ease of synthesis these reactions were carried out without stereocontrol and all products were obtained in racemic mixture.

Compd.	Configuration (*)	MIC (μM)	Compd.	R ₁	R ₂	R ₃	R ₄	MIC (μM)
DGS	S	6.25	LK05	H	H	Br	H	12.5
(R)-DGS	R	12.5	LK06	Br	H	H	H	12.5
(R,S)-DGS	R,S	6.25	LK07	H	H	Cl	H	12.5
			LK08	H	F	H	H	50
			LK09	H	I	H	H	> 100
			LK10	H	H	I	H	> 100
			LK11	H	OH	OH	H	> 100
			LK12	H	Br	OH	H	50
			LK13	H	Br	OH	OMe	50
			LK14	H			H	6.25
			DGSp	H	H	ethynyl	H	12.5

R ₁	R ₂	X	Y	MIC (μM)	
LK01	H	H	C	N	> 100
LK02	H	H	N	C	> 100
LK03	H	Br	C	N	25
LK04	Br	H	N	C	6.25

Compd.	MIC (μM)
DGS-re	> 100
DGS-CN	> 100

Figure 21. Substitution patterns and MIC values in *S. aureus* NCTC8325 for various degrasyn analogues synthesized in this study in order to investigate the structure activity relationships of DGS.

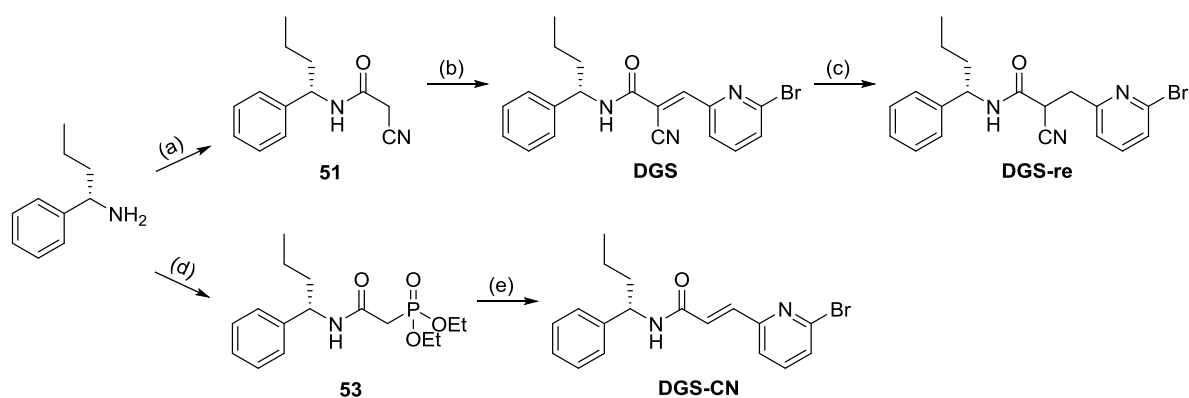


Scheme 13. Synthesis of derivatives (a) i) NH₂OH.HCl, NaOH, EtOH/H₂O, ii) H₂, Pd/C, MeOH, iii) 1-cyanoacetyl-3,5-dimethyl-1H-pyrazole, toluene, reflux, 69%; (b) aryl aldehyde, piperidine, EtOH, reflux, 33-75%

While unsubstituted pyridine rings led to a loss of antibiotic activity (**LK01**, **LK02**), varying the positions of bromine and the pyridine nitrogen atom were largely tolerated (**LK03**, **LK04**). In addition, bromine and chlorine substituted phenyl-rings were also sufficient to largely retain antibiotic effects (**LK05**, **LK06**, **LK07**). In contrast, fluoro- and iodo-substituted phenyl rings resulted in a loss of activity (**LK08**, **LK09**, **LK10**). While di- and tri-substitutions with electron-donating groups (e.g. -OH, -OMe, etc.) were largely not tolerated (**LK11**,

LK12, **LK13**), the introduction of a difluoroacetal moiety (**LK14**) retained full activity. Satisfyingly, substitution with an alkyne handle (**DGSp**) only slightly dropped the MIC, which is a prerequisite for subsequent target identification using conventional ABPP.

We next turned our synthetic efforts towards the reactive α -cyanoacrylamide moiety. Acrylamides are irreversible covalent inhibitors, which readily react with cysteine residues in.⁷⁹ Further fine-tuning with electron-withdrawing substituents such as nitriles yields reversibly covalent inhibitors, which have received great attention in drug development.^{80,81} by specifically modifying cysteine residues close to the active site and thereby prolonging the residence time. As degrasyn bears this signature moieties we investigated if the ability to act as a Michael acceptor and the fine-tuning as α -cyanoacrylamide are both relevant for the antibiotic effect. The synthesis of **DGS-red**, without the double bond of the *Michael* acceptor, was achieved by reduction of **DGS** using NaBH_4 (Scheme 14). The synthesis of **DGS-CN**, without the nitrile moiety, was performed using a *Horner-Wadsworth-Emmons* reaction (Scheme 14) starting from phosphonate ester **3** and 6-bromopicolinaldehyde. Interestingly, neither **DGS-red** nor **DGS-CN** showed any antibiotic activity highlighting that both the *Michael* acceptor as well as the electron-withdrawing substituent are mandatory (Figure 21).



Scheme 14. Synthesis of **DGS-re** and **DGS-CN** (a) 1-cyanoacetyl-3,5-dimethyl-1H-pyrazole, toluene, reflux, 75%; (b) 6-Bromo-2-pyridinecarboxaldehyde, piperidine, EtOH, reflux, 65%; (c) NaBH_4 , THF, 0 °C, 58%; (d) EDC.HCl, diethylphosphonoacetic acid, DMAP, DMF; (e) NaH, 6-Bromo-2-pyridinecarboxaldehyde, THF, 0 °C, 56%.

2.3. Gel-free activity-based protein profiling

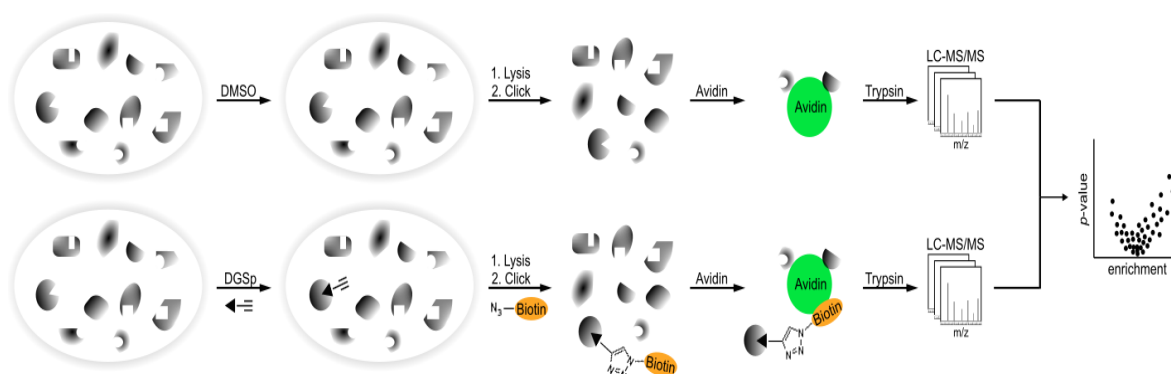


Figure 22. Workflow for conventional ABPP experiments. Enrichment is only seen, if the reversibly binding **DGSp** is attached to the protein throughout the entire workflow.

In order to better understand the mechanism of action of degrasyn, we set out to unravel its molecular targets in *S. aureus*. We first utilized the probe **DGSp** for ABPP studies. (Figure 22) Live bacterial cells were incubated with the probe, lysed, labeled proteins modified with biotin azide using copper-catalyzed azide alkyne cycloaddition (CuAAC)⁸² and subsequently analyzed via liquid chromatography coupled to tandem mass spectrometry (LC-MS/MS). The labeling was performed at three different concentrations (6.25 μ M, 12.5 μ M and 25 μ M) and data analysis was performed with label-free quantification (LFQ). However, no prominent enrichment of protein targets was observed. (Figure 23) In addition, competition studies with various concentrations of parent molecule degrasyn did not lead to an obvious target profile. (Figure 24) Thus, as expected from our SAR analysis, the reversibly covalent binding mechanism is not suitable for ABPP studies as the transient target binding is incompatible with the enrichment procedure for MS.

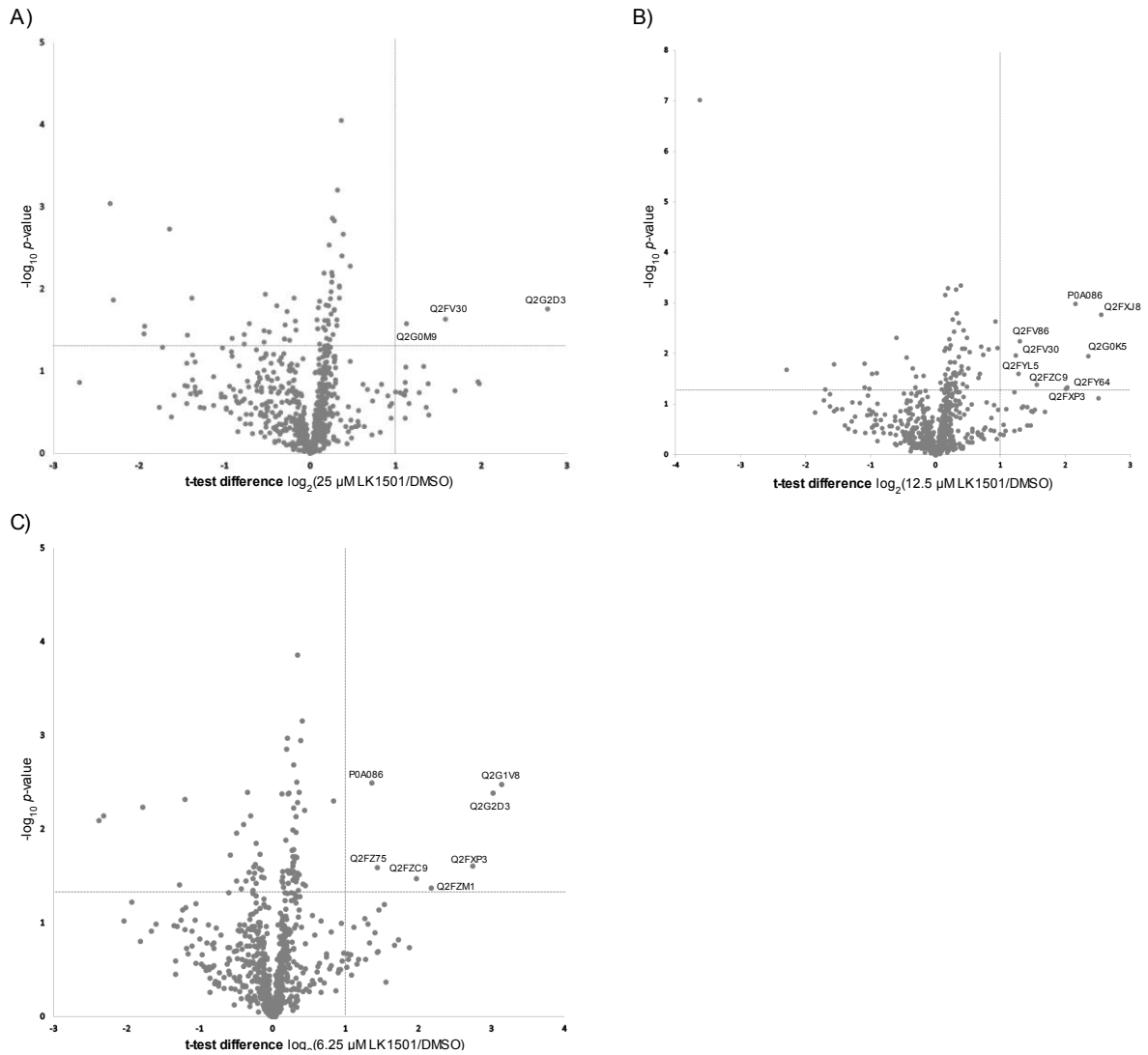


Figure 23. Results of the quantitative gel-free ABPP experiments using **DGSp** in *S. aureus* NCTC8325. Cells were treated with a) 25 μ M, b) 12.5 μ M and c) 6.25 μ M probe, respectively. The volcano plots display the statistical significance of protein enrichment levels as a function of protein enrichment ratios from probe treated to control cells, with a cut of at a $-\log_{10}(\text{p-value})$ of 1.3 and a t-test difference of 1.

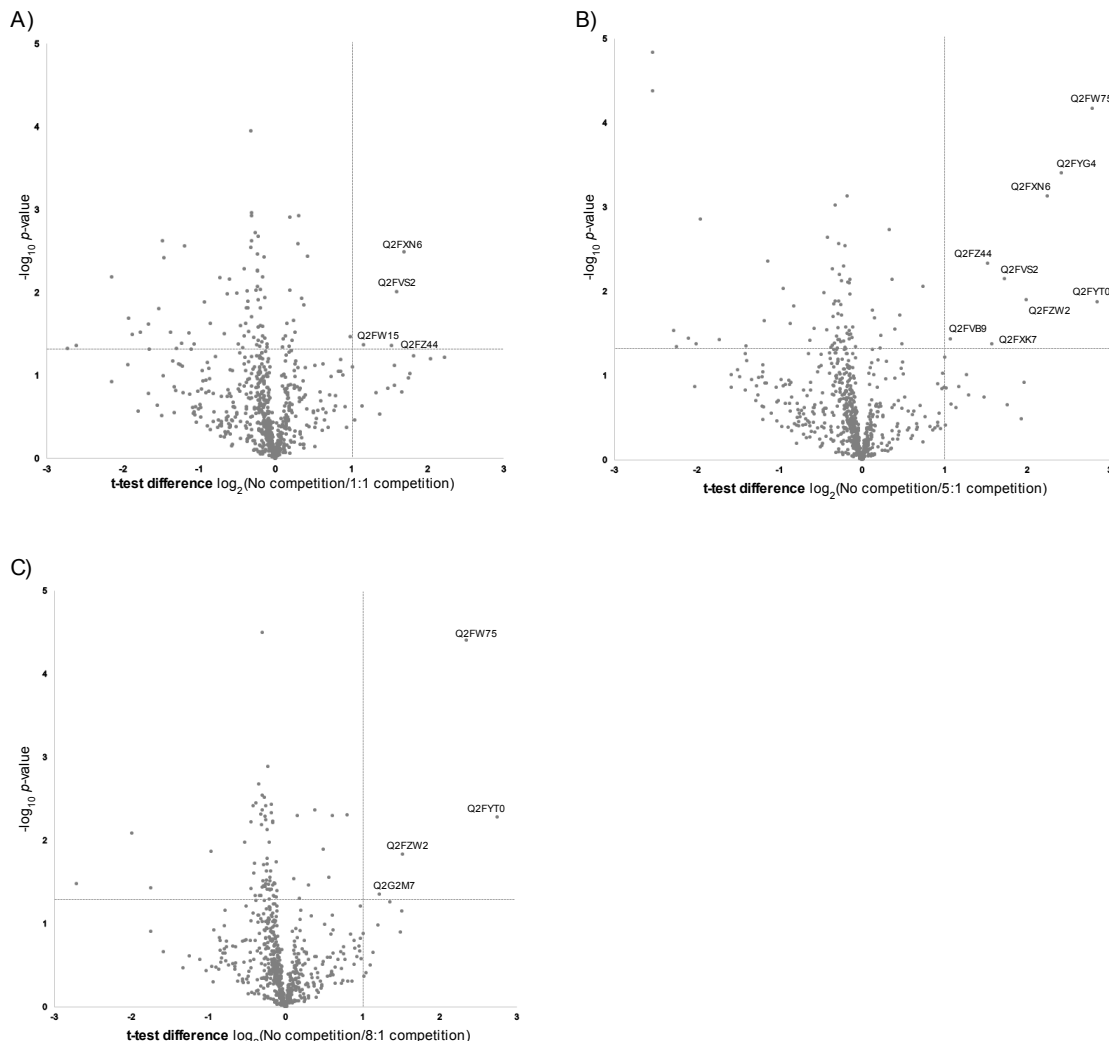


Figure 24. Results of the quantitative gel-free competition ABPP experiments using **DGS** and **DGS_p** in *S. aureus* NCTC8325. Cells were pretreated with a) 12.5 μ M, b) 62.5 μ M and c) 100 μ M **DGS** and treated with 12.5 μ M **DGS_p** in all experiments, respectively. The volcano plots display the statistical significance of protein enrichment levels as a function of protein enrichment ratios from no competed cells (pretreated with DMSO and treated 12.5 μ M **DGS_p**) to competed cells as a control, with a cut of at a $-\log_{10}(\text{p-value})$ of 1.3 and a t-test difference of 1.

2.4. Competitive isoDTB-ABPP

Since the α -cyanoacrylamide moiety, responsible for reversible binding mode to cysteines, is a hallmark of the antibiotic activity of degrasyn, we performed competitive residue-specific proteomics with degrasyn as an alternative strategy to standard affinity-based protein profiling (AfBPP).^{83,84} In this strategy, *S. aureus* cells are lysed and the lysate is split

into two samples. One sample is treated with degrasyn and the other one with DMSO as a control. (Figure 25) Afterwards, the samples are both treated with iodoacetamide-alkyne (IA-alkyne), which labels many cysteine residues in the proteome. Competitive cysteine binders such as degrasyn block this labeling at their specific binding sites in the proteome and thereby prevent alkylation at these residues. In order to read out these differences in alkylation, isotopically labeled desthiobiotin azide (isoDTB) tags⁸⁵ are appended using CuAAC. As the modified peptides from both samples are differentiated by the isotopically labeled tags, the samples are combined, enriched on streptavidin, digested with trypsin and the modified peptides eluted from the beads using 0.1% formic acid and 50% acetonitrile in water. The peptides are identified and quantified relative to each other using LC-MS/MS. The ratio R between the heavy-labeled (DMSO-treated) and light-labeled (degrasyn-treated) samples is a direct measure for the degree of modification of the specific cysteine with degrasyn.

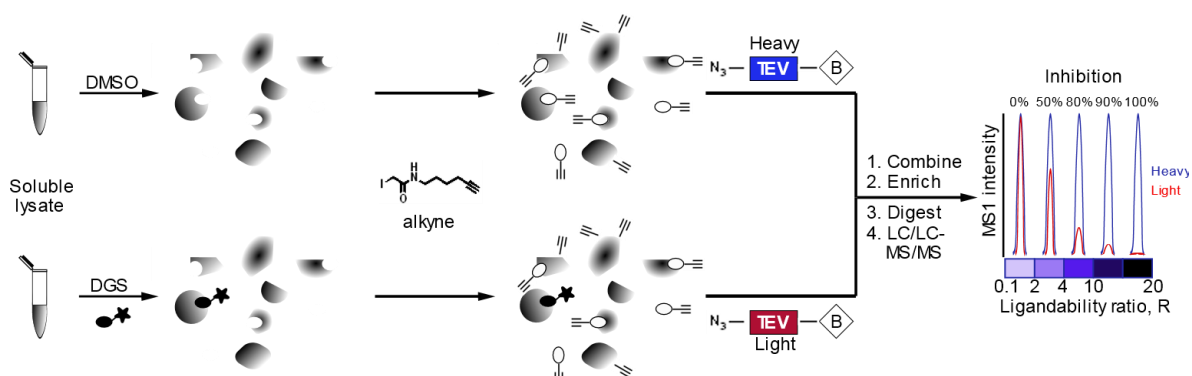


Figure 25. Workflow for competitive, residue-specific proteomics with the isoDTB-ABPP technology. Competition of IA-alkyne labeling by reversibly binding **DGS** is preserved throughout the workflow by the irreversibly binding probe. DTB: Desthiobiotin.

Besides the ability to obtain residue-specific information of binding with an unmodified covalent protein ligand, another important advantage of this approach is that also cysteines, which are reversibly engaged by degrasyn, are identified.⁸⁶ Satisfyingly, treatment of *S. aureus* lysate with various concentrations of degrasyn ranging from 100 μ M to 10 μ M led to the identification of 152 cysteines in 114 proteins targeted by degrasyn. (Figure 26)

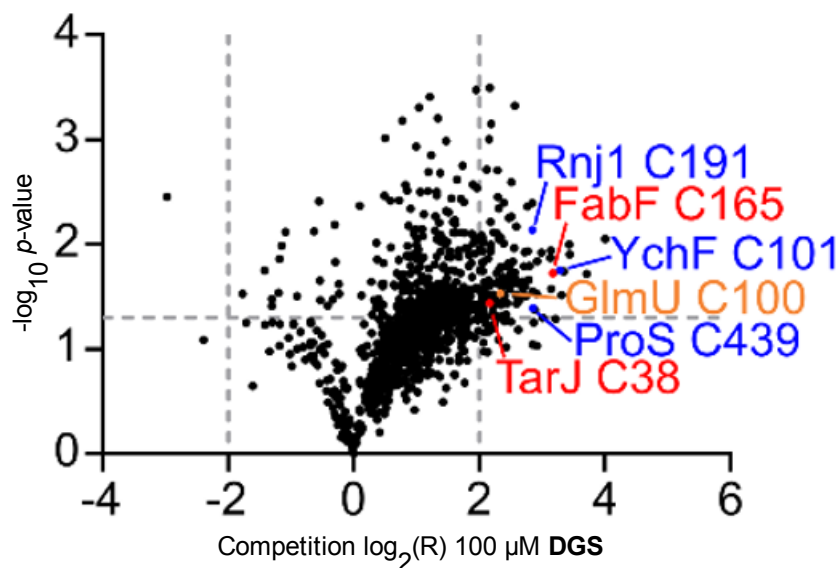


Figure 26. Volcano plot for the isoDTB-ABPP experiment with 100 μM **DGS** used as the competitor. Significantly competed cysteines that are discussed in the text are highlighted in red. Cysteines that are included in the concentration-dependent analysis (Figure. 27) are highlighted in blue. GlmU C100 that is included in both is highlighted in orange. The grey lines indicate cut-offs at $-\log_{10}(p) = 1.3$ and $\log_2(R) = \pm 2$ that were used as a criterion for hit selection.

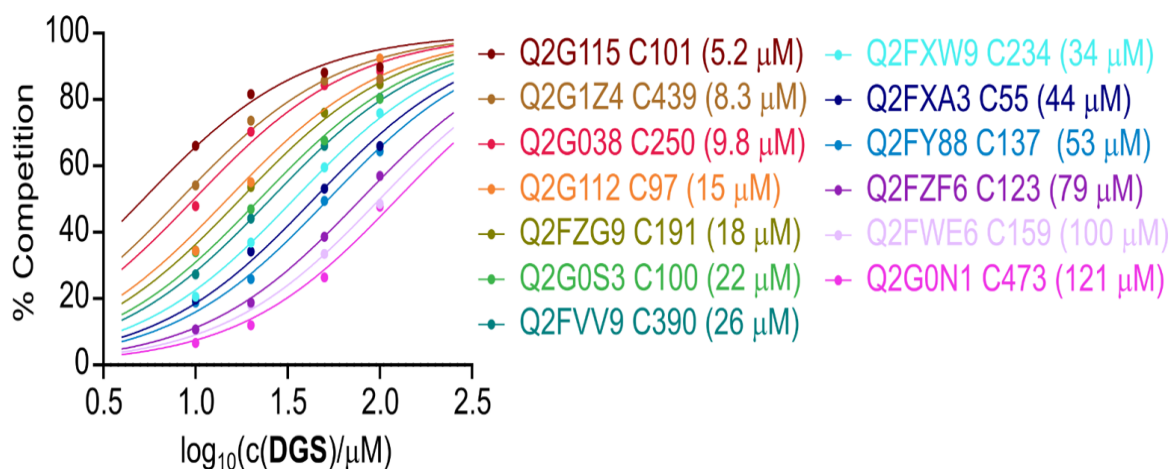


Figure 27. Dependence of the degree of competition in isoDTB-ABPP experiments on the **DGS** concentration. For each analyzed cysteine, the UniProt code of the respective protein and the residue number of the competed cysteine are given. The value in parentheses is the EC_{50} of the competition for the respective cysteine.

Interestingly, 96 of these cysteines were not liganded by any compound of 19 covalent α -chloroacetamides that were previously used to profile *S. aureus*.⁸¹ This indicates that the reversibly covalent α -cyanoacrylamide is able to interact with a unique set of cysteines.

Many cysteines respond to degrasyn treatment in a clearly concentration-dependent manner. (Figure 27) Of the 152 cysteines that are liganded by degrasyn, the data from the concentration-dependent experiments could be fitted with a dose-response curve with a median R^2 value of 0.92. This demonstrates that residue-specific proteomics with the isoDTB tags using a few different concentrations of a covalent protein ligand is able to deliver robust information on the binding affinity for many cysteines in parallel.

31 of the targeted cysteines belong to proteins with an essential function for the viability of *S. aureus*. **DGS** e.g. binds cysteine C100 of the bifunctional protein GlmU ($EC_{50} = 22.3 \mu\text{M}$, UniProt Code Q2G0S3), which is located close to the magnesium ion in the UDP-GlcNAc binding site of this protein.⁸⁷ GlmU is an essential protein in the synthesis of UDP-GlcNAc and therefore important in e.g. lipid A biosynthesis and lipopolysaccharide assembly.⁸⁸ **DGS** also binds cysteine C38 of the ribulose-5-phosphate reductase TarJ ($EC_{50} = 33.4 \mu\text{M}$, UniProt Code Q2G1B9), which is involved in the binding of the catalytic zinc ion.⁸⁹ TarJ is essential in the synthesis of poly (ribitol phosphate) teichoic acid, which are the main cell wall teichoic acids of *S. aureus*.⁹⁰ Furthermore, modification of the catalytic nucleophile C165 of the 3-oxoacyl-[acyl-carrier-protein] synthase FabF ($EC_{50} = 35.3 \mu\text{M}$, UniProt Code Q2FZR9), an enzyme essential for lipid biosynthesis, was detected.^{89,91} In this way, interaction of **DGS** with cysteine residues in functionally relevant binding sites of several essential proteins could be a major driver of its antibiotic activity.

2.5. Global proteomics analysis

To further complement these results, we performed a global analysis of cellular protein levels in response to degrasyn treatment. For this, cells were cultivated with $\frac{1}{2}$ MIC concentration of degrasyn (in order to prevent premature cell lysis), harvested and investigated by LC-MS/MS via LFQ. In line with the multiple targets observed via residue-specific proteomics, a large fraction of 33 proteins was significantly upregulated and only nine proteins were downregulated (Figure 28).

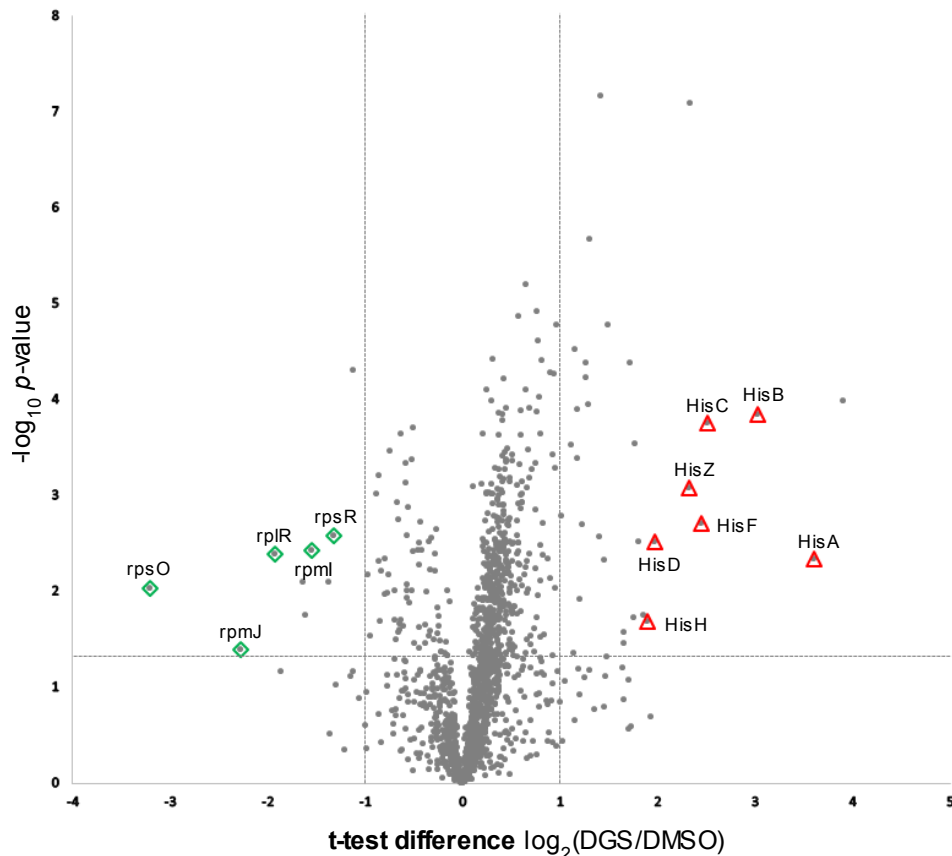


Figure 28. Volcano plot for a whole proteome analysis of protein expression comparing *S. aureus* NCTC8325 treated with $\frac{1}{2}$ MIC concentration of **DGS** to treatment with DMSO as a control. Upregulated proteins involved in the histidine biosynthetic process are highlighted in red and downregulated proteins involved in the ribosomal proteins are highlighted in green. The grey lines indicate cut-offs at $-\log_{10}(p) = 1.3$ and $\log_2(R) = \pm 1$ that were used as a criterion for selection of up- and down-regulated proteins.

Of the dysregulated proteins seven are essential for *S. aureus* survival, five of which were down-regulated ribosomal proteins. Analysis of the Gene Ontology terms of the upregulated proteins revealed a strong enrichment of terms associated with histidine biosynthesis (Figure 29). Together with the isoDTB-ABPP data these results suggest a polypharmacological mode-of-action for **DGS** leading to the alteration of multiple essential pathways, which is reflected by complex changes in the overall proteome.

GeneOntology term (biological process)	corr. p-value
histidine biosynthetic process	3.16E-07
imidazole-containing compound metabolic process	3.27E-06
histidine metabolic process	3.27E-06
aromatic amino acid family biosynthetic process	3.05E-05
aromatic amino acid family metabolic process	1.36E-04

Figure 29. Enrichment analysis of Gene Ontology terms of the category "biological process" comparing the upregulated proteins to all proteins detected in the whole proteome analysis. The five terms with the lowest corrected p-value are shown. All data results from four independent biological replicates.

3. Summary and outlook

In summary, we identified degрасyn as a novel antibiotically active compound against *S. aureus* and clinically isolated MRSA strains. SAR studies unraveled a strong dependence of this antibiotic activity on the substitution pattern. In line with the essential role of the α -cyanoacrylamide as *Michael* acceptor covalent capture of target proteins failed due to limited stability of the linkage throughout the chemoproteomic protocol. Competitive residue-specific proteomics using the isoDTB-ABPP method turned out as an excellent complementary strategy to identify the targeted cysteines in vitro. 31 of these cysteines were labelled in proteins essential for viability of *S. aureus* highlighting a polypharmacological mode-of-action which was further corroborated by the up- or down-regulation of several proteins in a whole proteome study. These results encourage the repurposing of other human inhibitors or drugs for exploiting their antibacterial potential.

IV. **LK1602** as a potent inhibitor against gram positive and negative bacteria

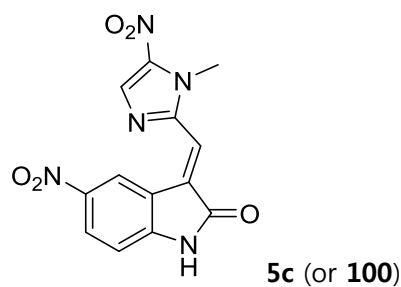
1. Introduction

1.1. The crisis caused by multidrug resistant microbes

The number of people facing antibiotic resistance has been high, since antibiotic resistant bacteria emerged. The threat of antibiotic resistance undermines progress in health care, food production, and life expectancy. Among these drug resistant bacteria, ESKAPE pathogens (*Enterococcus faecium*, *Staphylococcus aureus*, *Klebsiella pneumoniae*, *Acinetobacter baumannii*, *Pseudomonas aeruginosa*, and *Enterobacter species*) are leading cause of notorious hospital infections.^{89,92,93,94} Moreover, most of them are multidrug resistant microbes, which leads to increased risk of failure of clinical treatment and finally death.⁹⁵ Therefore, much more study and investment are required to develop new antimicrobial drugs, and vaccines by improvement of existing drugs or discovery of new scaffold.⁹⁶

1.2. Discovery of hybrids of indolin-2-one and nitroimidazole

The indolin-2-one moiety plays an important role in the pharmaceutical field, as numerous compounds containing it have good biological and pharmacological activities, such as kinase inhibitory activity,^{97, 98} anti-cancer,^{99, 100} anti-inflammatory,^{101, 102} anti-Alzheimer's,^{103,104} neuroprotective,^{105,106} antioxidant,^{107,108} and antimicrobial activity.^{109,110} Imidazole is also ubiquitous scaffold in natural products, and possesses good stability in acid, base, oxidation and reduction conditions.¹¹¹ It is component of several compounds having activities including antibacterial,¹¹² antinociceptive and anti-inflammatory,^{113,114,115} antifungal,¹¹⁶ antiparasitic,^{117,118,119} Tc-L14DM inhibitory,¹²⁰ antiviral,¹²¹ anticancer,^{122,123,124} and antidepressant activity.¹²⁵



Bacteria	MSSA ATCC25923	MRSA ATCC33591	<i>E. coli</i> ATCC25922	<i>P. aeruginosa</i> ATCC27853	VRE B148
MIC (μM)	0.2-0.4	0.2-0.4	0.8	0.8-1.6	12.8

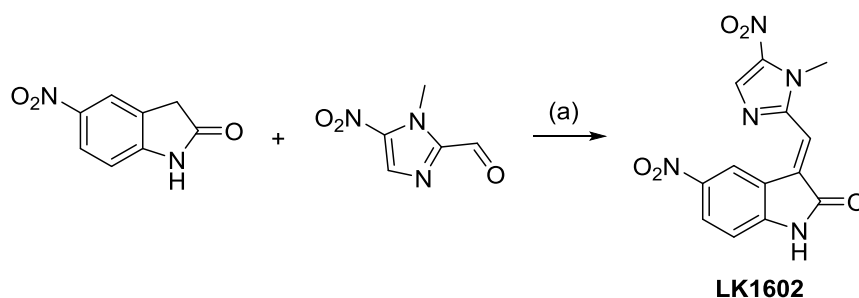
Figure 30. Structure of **5c** (or **LK1602**) and its activity (MIC) against various bacteria.

A nitroimidazole compound, **5c**, has recently been discovered by Y. Zhou *et al.* in 2018,¹²⁶ and it shows remarkable antibacterial activities with a low MIC against MRSA, gram negative bacteria and VRE strain. (Figure 30) According to the paper, this compound is a novel hybrid of indolin-2-one and nitroimidazole, (*E*)-3-((1-methyl-5-nitro-1*H*-imidazol-2-yl)methylene)-5-nitroindolin-2-one, and its low hemolytic rate implies promising safety profile. However, other biological information, target protein(s), mode of action and so on, are still elusive.

2. Result and Discussion

2.1. Synthesis and biological validation of **LK1602**

We synthesized the published compound (Scheme 15), renamed **LK1602**, and confirmed its activity against various bacteria. As depicted in the reference, **LK1602** is shown to exhibit remarkable antibacterial activity with submicromolar MIC against gram positive bacteria, *S. aureus* and *L. monocytogenes* and single digit micromolar activity against gram negative bacteria, *A. baumannii*, *P. aeruginosa*, and *S. typhimurium*. (Figure 31) Since its antimicrobial activity was confirmed in our lab, an alkyne probe of **LK1602** was needed to investigate potential target protein(s).



Scheme 15. Synthesis of **LK1602** (a) piperidine, EtOH, reflux, 77%.

Bacteria (gram positive)	<i>S. aureus</i> NCTC8325	<i>L. monocytogenes</i> EGD-e		
MIC (μ M)	0.13	0.5		
Bacteria (gram negative)	<i>A. baumannii</i> DSM30007	<i>P. aeruginosa</i> DSM19882	<i>P. aeruginosa</i> PAO1	<i>S. typhimurium</i> LT2
MIC (μ M)	2.5	2.5	1.3	0.5

Figure 31. MIC of **LK1602** against various species.

2.2. Synthesis of alkyne probe of **LK1602**

LK1602 has only a few positions available to introduce the alkyne moiety since the compound itself is small and compact. The key requirement, the alkyne, has to fulfill is that the molecule maintains the biological activity with little or no changes, thereby tracing

target protein(s) of the original compound. Keeping the backbone of the compound intact, three positions might be rationally considered; (1) nitrogen of amide functional group in the indolin-2-one, (2) phenyl ring in the indolin-2-one, and (3) 1-position of imidazole. (Figure 32)

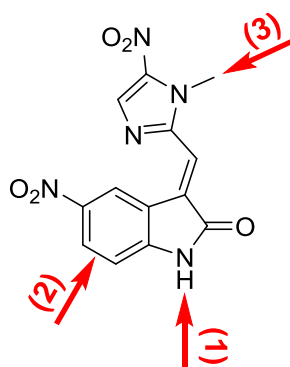
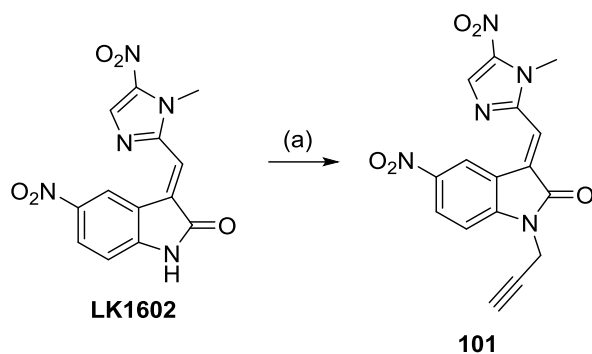


Figure 32. Three positions accessible for the introduction of an alkyne moiety.

2.2.1 Nitrogen of amide

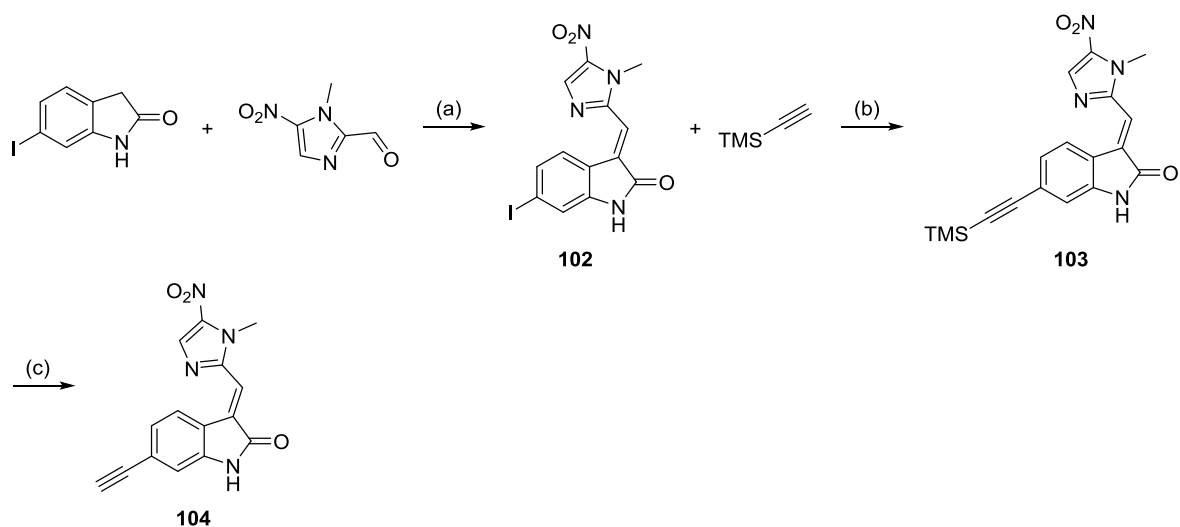
The nitrogen of the amide represents the easiest position for modification since already synthesized **LK1602** is a perfect starting material. Although the nucleophilicity of the nitrogen of the amide tends to be weak and only reacts as a nucleophile under strong basic conditions.¹²⁷ Sodium hydride appears to be a proper base to deprotonate an amide proton by literature search, and thereby the alkylation was conducted with 3-bromopropyne in THF. Nothing could be obtained from the organic phase except for a few faint spots on the TLC probably due to poor solubility of product. Therefore, precipitation was chosen as an alternative for an extraction step,¹²⁸ resulting in successful isolation of the desired product, **101**. (Scheme 16)



Scheme 16. Synthesis of **101** (a) 3-bromopropyne, NaH, DMF, 32%.

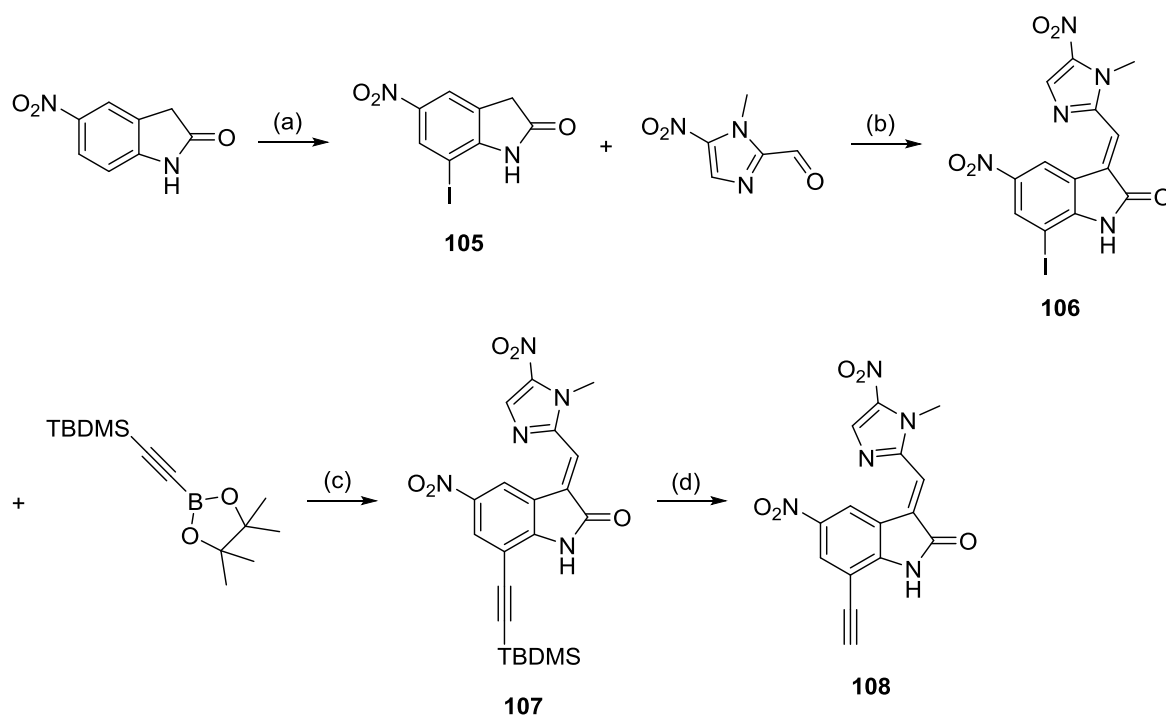
2.2.2. Phenyl ring of indolin-2-one

Second, the phenyl ring of indolin-2-one is suitable for modification, such as 6- or 7-position of indolin-2-one. In order to make a carbon-carbon bond between the sp^2 and sp^1 hybridized carbons, a halogen atom should be implanted into the phenyl ring of indolin-2-one, thereby affording a desired product by metal coupling reaction. Bromine was implanted into the phenyl ring (data not shown) at the beginning, however, a brominated intermediate wasn't able to give the desired product probably due to lacking reactivity.



Scheme 17. Synthesis of **104** (a) 2,2,6,6-tetramethylpiperidine, EtOH, reflux, 91%. (b) $\text{Pd}(\text{PPh}_3)_2\text{Cl}_2$, CuI, TEA, DMF, 51% (c) AgNO_3 , KCN, EtOH, THF, H_2O , 60%

Generally, iodine is more active than bromine in metal coupling reactions since the carbon-iodine bond can be easily cleaved by a metal catalyst, sometimes even at room temperature.¹²⁹ **102** was generated from 6-iodoindolin-2-one by a known procedure¹³⁰ and 1-methyl-5-nitro-1*H*-imidazole-2-carbaldehyde by Knoevenagel condensation. (Scheme 17) It was coupled with ethynyltrimethylsilane by Sonogashira coupling, which was followed by TMS deprotection to afford the alkyne probe **104**. However, this probe lost one nitro functional group, which might lead to activity loss. Hence, the other alkyne probe is needed to keep the structural difference from **LK1602** minimized. To preserve the nitro group, 5-nitroindolin-2-one was selected as a starting material, which is then iodinated with *N*-iodosuccinimide under conc. sulfuric acid condition. (Scheme 18)



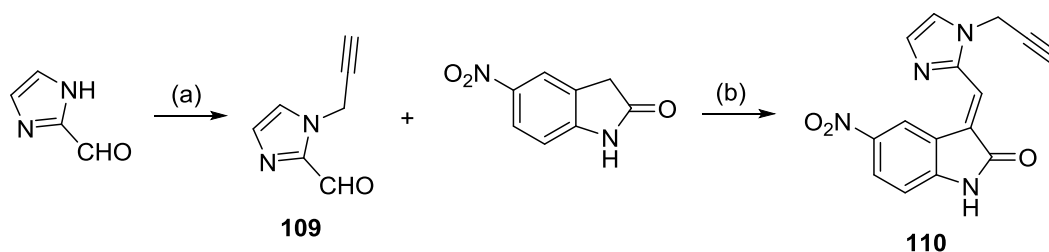
Scheme 18. Synthesis of **108** (a) *N*-iodosuccinimide, conc. H_2SO_4 , 91%. (b) 2,2,6,6-tetramethylpiperidine, EtOH, reflux, 82%. (c) $\text{Pd}(\text{PPh}_3)_4$, Cs_2CO_3 , 1,4-dioxane, 70 °C, 50%. (d) TBAF, THF, 53%.

This resulted in only one iodinated isomer 7-iodo-5-nitroindolin-2-one, **105**, as expected, since the nitro group is meta directing. Then **105** was condensed with the same imidazole reagent as in scheme 17 to afford **106**. It is similar to intermediate **102**, but only different in the presence of nitro group and the position of iodine. However, these changes reduced

reactivity of Sonogashira coupling reaction. Suzuki coupling may be a rational alternative since it tends to be working well even sometimes with poorly reactive compounds. **107** was successfully generated by Suzuki coupling in reasonable yield with *tert*-butyldimethyl((4,4,5,5-tetramethyl-1,3,2-dioxaborolan-2-yl)ethynyl)silane. The TBDMS protecting group was easily removed by TBAF to give another desired alkyne product **108**.

2.2.3. 1-position of imidazole

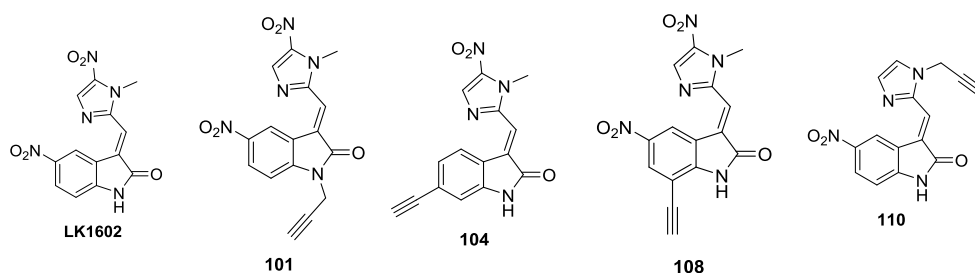
Third, the methyl group in 1-position of the imidazole could be replaced with alkyne moiety. Alkylation of 1*H*-imidazole-2-carbaldehyde with 3-bromopropyne gave **109** in 78% yield, and the product was subsequently condensed with 5-nitroindolin-2-one to afford the desired alkyne product **110**. (Scheme 19) As a result, four probes were obtained with an alkyne moiety at different positions. Having these compounds in hand additional insights into the structure activity relationship data can be gained.



Scheme 19. Synthesis of **110** (a) 3-bromopropyne, K₂CO₃, DMF, 78%. (b) piperidine, EtOH, reflux, 67%.

2.3. Biological validation of alkyne probes of **LK1602** by MIC assay

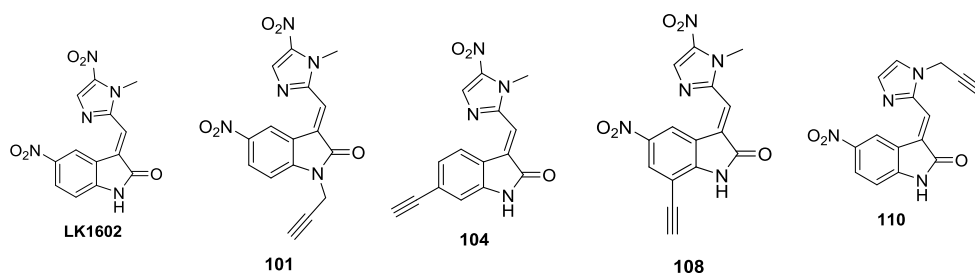
Next, all probes were tested by the MIC assay, so that the best one could be investigated via ABPP experiments. Two bacteria species; one from gram positive, *S. aureus* and the other one from gram negative, *P. aeruginosa* were chosen as representatives for MIC assay. Satisfyingly, two alkyne probes, **104** and **108**, retain antimicrobial activity against *S. aureus*, and **108** is even active as much as original compound **LK1602**. (Figure 33)



Bacteria	MIC (μM)				
<i>P. aeruginosa</i> PAO1	1.3	> 50	> 50	> 50	> 50
<i>S. aureus</i> NCTC8325	0.13	> 50	0.63	0.13	> 50

Figure 33. MIC of original compound, **LK1602**, and four alkyne probes **101**, **104**, **108** and **110** against *P. aeruginosa* PAO1 and *S. aureus* NCTC8325.

However, all probes lose their activity completely against *P. aeruginosa*, which is surprising since the only structural difference between **LK1602** and **108** is absence or presence of alkyne group. To trace the effect of alkyne, MIC of **108** on a lipopolysaccharide (LPS) deficient strain was measured. Lipopolysaccharide (LPS), also known as lipoglycans and endotoxin, is the part of outer membrane of gram negative bacteria, and it protects bacteria from particular kinds of antimicrobials by blocking them on outer membrane using its inherent high lipophobicity.¹³¹ So, if the alkyne probe recovers its activity over LPS deficient strain, at least we can guess that the permeability of the probe dropped sharply due to alkyne moiety. *E. coli* RFM795, as LPS deficient strain, was used for this experiment, and *E. coli* MM28, parental strain of *E. coli* RFM795, was also chosen as a control. Amazingly, except for **110**, the other three probes show two digits nanomolar activity against *E. coli* RFM795, and no activity against wild type, *E. coli* MM28. (Figure 34) Therefore, we can hypothesize both that the alkyne substitution increases the hydrophobicity of the compound and the nitroimidazole moiety is needed for activity in gram negatives.



Bacteria	MIC (μ M)				
<i>E. coli</i> MM28	1.25	> 10	> 10	> 10	> 10
<i>E. coli</i> RFM795	6.3 nM	78 nM	50 nM	25 nM	> 10

Figure 34. MIC of original compound, **LK1602**, and four alkyne probes **101**, **104**, **108** and **110** against *E. coli* MM28 and *E. coli* RFM795.

2.4. Gel-based ABPP for active and inactive probes

Further investigation was continued with *S. aureus* gram positive bacteria, since the alkyne moiety appeared to interrupt penetration of the probe across the outer membrane of gram negative bacteria. First, gel-based ABPP experiment was conducted to check if the alkyne probes covalently connect to its target protein(s). Otherwise, a photocrosslinker probe should be needed. *S. aureus* NCTC8325 was incubated with the active probes each, **104** and **108**, and lysed, the alkyne moiety of the probe attached to the proteins was clicked by rhodamine azide. Satisfyingly, proteins were detected through SDS-PAGE analysis, but there were too many fluorescent bands on the gel, (Figure 35) which implies both compounds are not selective enough to figure out significant target protein(s). So, the same experiment was conducted with inactive probes, **101** and **110**. Intriguingly, a number of bands were detected with them as well, (Figure 36) which indicates that meaningful target protein(s) can be figured out through further gel-free ABPP experiment by excluding overlapped proteins between active and inactive probes.

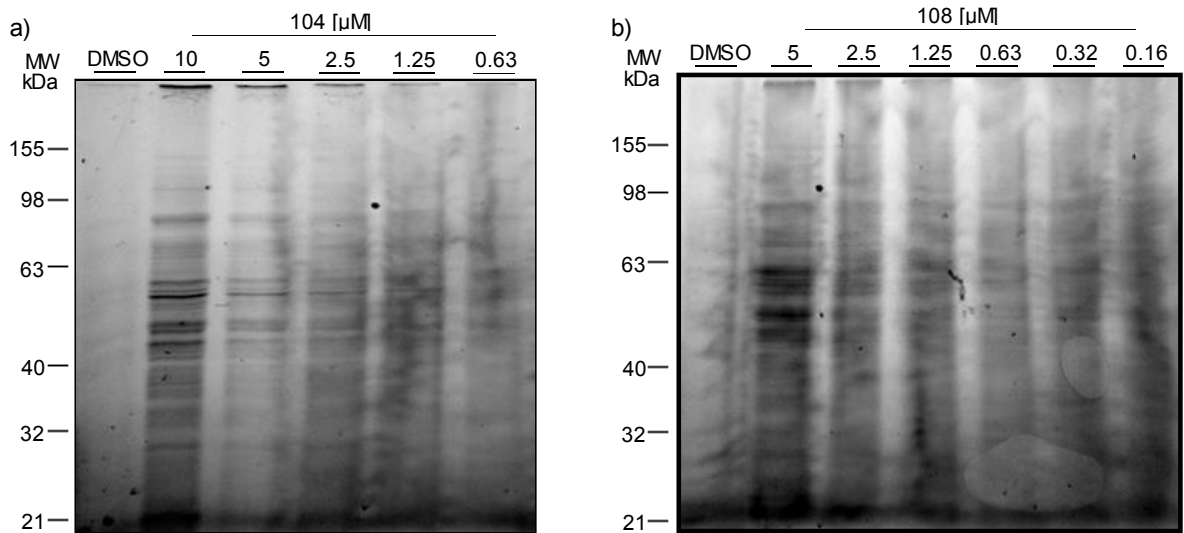


Figure 35. SDS-PAGE analysis of *S. aureus* NCTC8325 incubated with active probes a) **104** and b) **108**.

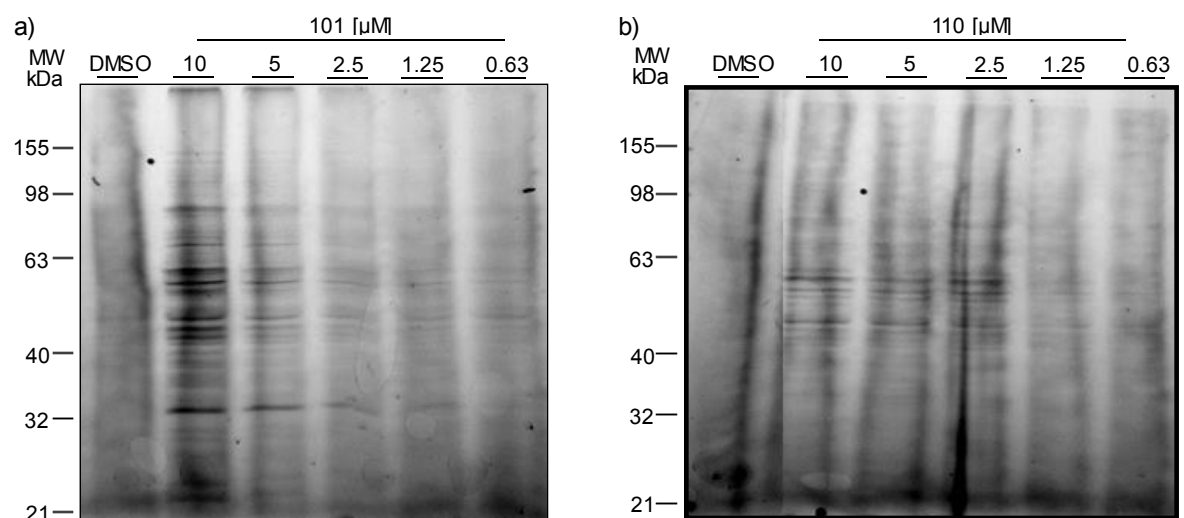


Figure 36. SDS-PAGE analysis of *S. aureus* NCTC8325 incubated with inactive probes a) **101** and b) **110**.

3. Summary and outlook

It has been found that the novel compound, **LK1602**, has remarkable activity against various bacteria, e.g. submicromolar MIC value against gram positive bacteria, *S. aureus* and *L. monocytogenes* and single digit micromolar activity against gram negative bacteria, *A. baumannii*, *P. aeruginosa*, and *S. typhimurium*. In order to better understand the mechanism-of-action of the compound, an alkyne moiety was successfully implemented into the compound; one at nitrogen of amide, two at aromatic ring in indolin-2-one, and one instead of methyl group of 1-position of imidazole, thereby four different alkyne probes in total. Two, **104** and **108**, are active against *S. aureus*, and the others, **101** and **110**, do not show any activity. Subsequently, it was confirmed that two active alkyne probes appear to form covalent bonds with target protein(s) since bands appeared on SDS-PAGE gel after incubation *S. aureus* with each probe. In spite of a number of bands on the gel implying some background there, the probes are likely going to be suitable for gel-free ABPP study since inactive probes also make covalent bonds with proteins. Therefore, we are likely going to be able to unravel molecular targets of **LK1602** by ABPP study excluding overlapped proteins between active and inactive probes in near future.



V. Experimental section

1. Chemistry

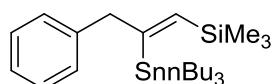
1.1 General remarks

All air or water sensitive reactions were carried out under argon in oven-dried glassware. Chemicals and solvents were purchased from Sigma-Aldrich, Alfa Aesar, Acros Organics, TCI Europe and Merck, were of reagent grade or better and were used without further purification. In all reactions, temperatures were measured externally. Solvents removed under reduced pressure were evaporated at 40 °C. Flash column chromatography was performed on silica gel (40-63 μm) by VWR, elution solvents were distilled prior to use. Analytical thin-layer chromatography was carried out on aluminium-baked TLC Silica gel plates by Merck. Components were visualized by UV detection ($\lambda=254$ nm, 312 nm) or stained via aqueous KMnO_4 or aqueous cerium molybdate (Hanessian's stain). ^1H NMR and ^{13}C spectra of small molecules were recorded on Bruker instruments (300MHz, 400 MHz or 500 MHz) and referenced to the residual proton signal of the deuterated solvent. (CDCl_3 , DMSO-d_6). Carbon samples were referenced externally against the residual ^{13}C signal of the solvent. HR-MS-ESI spectra were recorded with a Thermo Scientific LTQ FT Ultra.

1.2 Synthesis of smenothiazole A and photoprobe of smenothiazole B

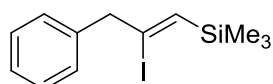
Compound **19** – **28** were synthesized according to *X. Ma et al.*⁵⁸

(*Z*)-trimethyl(3-phenyl-2-(tributylstannyl)prop-1-en-1-yl)silane (**1**)



A solution of triphenylphosphine (564 mg, 2.15 mmol), tris(dibenzylideneacetone)-dipalladium(0)-CHCl₃ complex (445 mg, 0.430 mmol) was stirred for 10 min in THF (7 mL). To the mixture was added trimethyl(tributylstannyl)silane (3.28 g, 9.04 mmol) and the prop-2-yn-1-ylbenzene (1.00 g, 8.61 mmol) in THF (5 mL). The resulting solution was refluxed overnight. The dark brown reaction mixture was cooled to room temperature and diluted with Et₂O (10 mL), filtered through a pad of celite, and concentrated by rotary evaporation. The residue was purified by flash column chromatography on silica gel (100% HEX) to afford the silastannane (2.68 g, 65%). – ¹H NMR (500 MHz, CDCl₃): 7.30 – 7.12 (m, 5H), 6.42 (s, 1H), 3.71 (d, *J* = 21.7 Hz, 1H), 3.66 (d, *J* = 21.7 Hz, 1H), 1.56 – 1.22 (m, 12H), 0.88 – 0.79 (m, 15H), 0.16 (s, 9H).

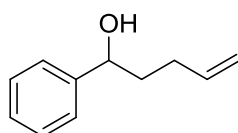
(*Z*)-(2-iodo-3-phenylprop-1-en-1-yl)trimethylsilane (**3**)



To a solution of (*Z*)-trimethyl(3-phenyl-2-(tributylstannyl)prop-1-en-1-yl)silane (817 mg, 1.70 mmol) in Et₂O (6 mL) was added a solution of I₂ (519 mg, 2.04 mmol) in Et₂O (6 mL)

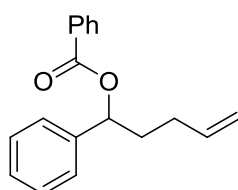
dropwise at 0 °C. After the mixture was stirred for 1 h at 0 °C, 0.5 M aqueous solution of $\text{Na}_2\text{S}_2\text{O}_3$ and sat. aqueous solution of KF were successively added to the reaction mixture. The organic materials were extracted with Et_2O , and the solvent was evaporated to give the title compound (272 mg, 51%). – ^1H NMR (500 MHz, CDCl_3): 7.37 – 7.22 (m, 5H), 6.43 (s, 1H), 3.94 (s, 2H), 0.22 (s, 9H).

1-phenylpent-4-en-1-ol (5)



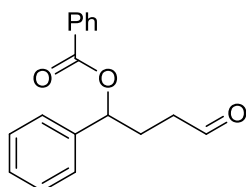
To the solution of benzaldehyde (1.01 mL, 9.89 mol) in dry THF (20 mL) was added 2 M homoallyl magnesium bromide solution in Et_2O (13.1 mL, 9.89 mol) at -78 °C. The mixture was warmed to room temperature over 1 h and sat. NH_4Cl solution was added, followed by extraction with EtOAc . The organic phase was separated, washed with brine and dried over Na_2SO_4 . The crude product was purified by column chromatography to yield the titled compound (1.50 g, 94%). – ^1H NMR (400 MHz, CDCl_3): 7.38 – 7.28 (m, 5H), 5.91 – 5.83 (m, 1H), 5.09 – 5.00 (m, 2H), 4.74 – 4.71 (m, 1H), 2.21 – 2.12 (m, 2H), 1.95 – 1.82 (m, 3H). – ^{13}C NMR (100 MHz, CDCl_3): 144.61, 138.18, 128.48, 127.59, 125.89, 74.05, 38.08, 30.07.

1-phenylpent-4-en-1-yl benzoate (6)



Benzoyl chloride (1.10 mL, 9.49 mmol) was added to a solution of 1-phenylpent-4-en-1-ol (1.40 g, 8.63 mmol), pyridine (2.04 g, 25.8 mmol) and 4,4-dimethylaminopyridine (105 mg, 0.863 mmol) in 23 mL of dry dichloromethane. The resulting solution was stirred overnight at room temperature. Dichloromethane was added and the solution was washed once with 1N HCl, once with sat. aqueous NaHCO₃, and once with brine. The final treatment afforded a crude oil, which was purified by column chromatography to give the titled compound (1.95 g, 85%). – ¹H NMR (400 MHz, CDCl₃): 8.13 – 8.10 (m, 2H), 7.60 – 7.28 (m, 10H), 6.05 – 6.02 (m, 1H), 5.91 – 5.81 (m, 1H), 5.08 – 5.00 (m, 2H), 2.24 – 2.00 (m, 4H). – ¹³C NMR (100 MHz, CDCl₃): 165.79, 140.63, 137.43, 132.94, 130.46, 129.65, 128.51, 128.37, 127.94, 126.45, 115.32, 76.08, 35.70, 29.74.

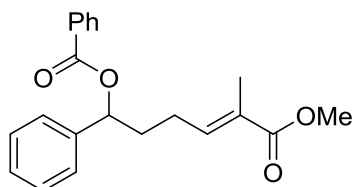
4-oxo-1-phenylbutyl benzoate (7)



To the solution of 1-phenylpent-4-en-1-yl benzoate (1.76 g, 6.61 mmol) in ethyl acetate (30 mL) was added sodium periodate (3.11 g, 14.5 mmol), 4% (w/w) OsO₄ in water (4.40 mL) and water (30 mL). The reaction mixture was stirred at room temperature for 2 h and then transferred into a separation funnel. After extraction with ether, the organic layer was combined, dried over magnesium sulfate and concentrated. The crude product was purified by column chromatography to yield the titled compound (1.27 g, 72%). – ¹H NMR (400 MHz, CDCl₃): 9.79 (s, 1H), 8.11 – 8.08 (m, 2H), 7.61 – 7.28 (m, 8H), 6.08 – 6.05 (m, 1H), 2.61 – 2.31 (m, 4H). – ¹³C NMR (100 MHz, CDCl₃): 200.91, 165.68, 139.80, 133.16, 130.08, 129.67,

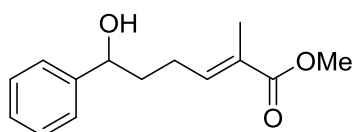
128.68, 128.46, 128.23, 126.29, 75.52, 39.95, 28.92.

(*E*)-6-methoxy-5-methyl-6-oxo-1-phenylhex-4-en-1-yl benzoate (9)



To a cooled solution (5 °C) of methyl (triphenylphosphoranylidene)propionate (1.76 g, 5.05 mmol) in DCM (32 mL), 4-oxo-1-phenylbutyl benzoate (1.13 g, 4.21 mmol) dissolved in DCM (13 mL) was added dropwise over a period of 30 min. The reaction was stirred for additional 10 min at 5 °C and then the mixture was warmed to room temperature. The reaction mixture was stirred for 3 h and then quenched with a 1N aqueous solution of NaHSO₄. The organic layer was separated and washed with brine, dried over Na₂SO₄, filtered and concentrated in vacuo. The crude was purified by column chromatography to give titled compound (1.32 g, 93%). – ¹H NMR (400 MHz, CDCl₃): 8.12 – 8.09 (m, 2H), 7.60 – 7.28 (m, 8H), 6.82 – 6.78 (m, 1H), 6.02 (t, *J* = 7.6 Hz, 1H), 3.73 (s, 3H), 2.34 – 2.09 (m, 4H), 1.78 (s, 3H). – ¹³C NMR (100 MHz, CDCl₃): 168.39, 165.73, 140.86, 140.20, 133.03, 130.27, 129.65, 128.59, 128.39, 128.34, 128.09, 126.37, 76.01, 51.70, 35.30, 24.93, 12.40.

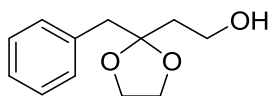
Methyl (*E*)-6-hydroxy-2-methyl-6-phenylhex-2-enoate (10)



A solution of the (*E*)-6-methoxy-5-methyl-6-oxo-1-phenylhex-4-en-1-yl benzoate (2.82 g,

8.33 mmol) in MeOH (27 mL), THF (27 mL), and aqueous 1N NaOH (30 mL) was stirred at 35 °C for 8 h. After the mixture was concentrated under reduced pressure, the residue was extracted with CH₂Cl₂. The organic layer was dried over Na₂SO₄ and concentrated under reduced pressure. The resulting residue was purified by column chromatography to afford the titled compound (925 mg, 50%). – ¹H NMR (300 MHz, CDCl₃): 7.41 – 7.28 (m, 5H), 6.97 – 6.90 (m, 1H), 4.72 (dd, *J* = 7.7, 5.5 Hz, 1H), 2.31 (q, *J* = 7.4 Hz, 2H), 2.06 – 1.82 (m, 5H). – ¹³C NMR (100 MHz, CDCl₃): 173.23, 144.20, 144.11, 128.59, 127.82, 127.59, 125.85, 73.93, 37.41, 25.24, 12.02.

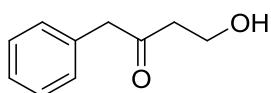
2-(2-benzyl-1,3-dioxolan-2-yl)ethan-1-ol (14)



To a solution of methyl 3-oxo-4-phenylbutanoate (724 mg, 3.77 mmol) and 1,2-bis-[trimethylsilyl(oxy)]ethane (1.15 mL, 4.71 mmol) in CH₂Cl₂ (10 ml) was added Trimethylsilyl trifluoromethanesulfonate (0.14 mL, 0.75 mmol) drop wise slowly at 0 °C. The mixture was warmed to room temperature. After 8h, the reaction was quenched with TEA (0.18 mL, 1.32 mmol) and washed with 5% aqueous NaHCO₃ solution, water, and brine, and dried over magnesium sulfate. The residue obtained after concentration was used for the next reaction without any further purification. To a solution of the residue in anhydrous THF (14 ml) was added 1.0 M LiAlH₄ in THF solution (4.0 mL, 3.96 mmol) dropwise at 0 °C. The mixture was warmed to room temperature. After 2h, excess of LiAlH₄ was quenched with EtOAc followed by saturated brine solution at 0 °C. The slurry obtained was passed through pad of celite and concentrated. The crude product obtained was dissolved in EtOAc, washed with 1N

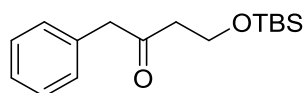
HCl, water, and brine, dried over magnesium sulfate and concentrated. The residue was purified by column chromatography to afford the titled compound (536 mg, 68%). – ¹H NMR (500 MHz, CDCl₃): 7.32 – 7.23 (m, 5H), 3.99 – 3.95 (m, 2H), 3.83 – 3.76 (m, 4H), 2.96 (s, 2H), 1.94 (t, *J* = 5.5 Hz, 2H). – ¹³C NMR (100 MHz, CDCl₃): 136.18, 130.51, 128.07, 126.57, 111.84, 65.11, 58.70, 43.75, 38.94.

4-hydroxy-1-phenylbutan-2-one (15)



To a stirred solution of 2-(2-benzyl-1,3-dioxolan-2-yl)ethan-1-ol (430 mg, 2.07 mmol) in acetone (5.0 mL) and H₂O (0.5 mL) was added p-TsOH monohydrate (98 mg, 0.52 mmol). The reaction mixture was stirred at room temperature for 16 h. After extraction with EtOAc, the organic phase was washed with brine and aqueous NaHCO₃ and dried over Na₂SO₄. After evaporation of the solvents the residue was purified by column chromatography to gain the title compound (293 mg, 86%). – ¹H NMR (500 MHz, CDCl₃): 7.39 – 7.22 (m, 5H), 3.86 – 3.75 (m, 4H), 2.74 (q, *J* = 5.6 Hz, 2H), 2.40 (s, 1H). – ¹³C NMR (75 MHz, CDCl₃): 209.00, 133.76, 129.45, 128.81, 127.19, 57.77, 50.55, 43.83.

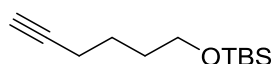
4-((*tert*-butyldimethylsilyl)oxy)-1-phenylbutan-2-one (17)



4-hydroxy-1-phenylbutan-2-one (160 mg, 0.97 mmol) was dissolved in CH₂Cl₂ (10 mL) and

cooled to 0 °C. Imidazole (358 mg, 5.26 mmol) was then added, followed by TBSCl (293.73 mg, 1.95 mmol), and DMAP (24 mg, 0.20 mmol). The reaction was stirred at room temperature overnight. The mixture was quenched with 1M HCl and extracted with CH₂Cl₂. The combined organic layers were dried over Na₂SO₄ and purified by column chromatography to yield the titled compound (264 mg, 97%). – ¹H NMR (300 MHz, CDCl₃): 7.37 – 7.20 (m, 5H), 3.89(t, *J* = 6.3 Hz, 2H), 3.76 (s, 2H), 2.66 (t, *J* = 6.3 Hz, 2H), 0.90 (s, 9H), 0.06 (s, 6H). – ¹³C NMR (75 MHz, CDCl₃): 207.21, 134.06, 129.50, 128.68, 126.98, 58.88, 51.01, 44.84, 25.88, 18.24, 5.46.

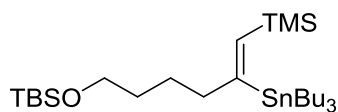
***tert*-butyl(hex-5-yn-1-yloxy)dimethylsilane (19)**



Hex-5-yn-1-ol (3.4 mL, 30.8 mmol) was dissolved in CH₂Cl₂ (30 mL) and cooled to 0 °C. Imidazole (4.2 g, 61.7 mmol) was then added, followed by TBSCl (6.98 g, 46.3 mmol), and DMAP (754 mg, 6.17 mmol). The reaction was stirred at room temperature overnight, quenched with 2M HCl, and extracted with CH₂Cl₂. The combined organic layers were washed with brine and dried over Na₂SO₄. The crude mixture was purified by column chromatography to give the titled compound (6.35 g, 97%). – ¹H NMR (300 MHz, CDCl₃): 3.66 (t, *J* = 4.3 Hz, 2H), 2.26 – 2.20 (m, 2H), 1.96 (t, *J* = 2.6 Hz, 1H), 1.66 – 1.58 (m, 4H), 0.92 (s, 9H), 0.07 (s, 6H). – ¹³C NMR (100 MHz, CDCl₃): 84.52, 68.23, 62.58, 31.81, 25.95, 24.96, 18.21, -5.31.

(*Z*)-*tert*-butyldimethyl((5-(tributylstannyl)-6-(trimethylsilyl)hex-5-en-1-yl)oxy)silane

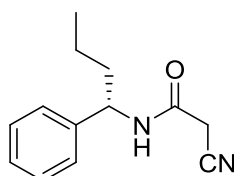
(20)



A solution of triphenylphosphine (617 mg, 2.35 mmol), tris(dibenzylideneacetone)-dipalladium(0) CHCl₃ complex (487 mg, 0.47 mmol) was stirred for 10 min in THF(10 mL). To the mixture was added trimethyl(tributylstannyl)silane (3.59 g, 9.89 mmol) and the *tert*-butyl(hex-5-yn-1-yloxy)dimethylsilane (2.0 g, 9.42 mmol) in THF (5 mL). The resulting solution was refluxed overnight. The dark brown reaction mixture was cooled to room temperature and diluted with EtOAc, filtered through a pad of celite, and concentrated by rotary evaporation. The residue was purified by column chromatography to afford the titled compound (4.01 g, 74%). – ¹H NMR (300 MHz, CDCl₃): 6.35 (s, 1H), 3.62 (t, *J* = 6.5 Hz, 2H), 2.31 (td, *J* = 7.6, 1.2 Hz, 2H), 1.56 – 1.28 (m, 16H), 0.98 – 0.85 (m, 24H), 0.11 (s, 9H), 0.07 (s, 6H). – ¹³C NMR (100 MHz, CDCl₃): 165.49, 143.41, 63.22, 47.33, 32.47, 29.24, 27.49, 26.28, 26.00, 18.37, 13.64, 11.19, 0.22, -5.25.

1.3 Degrasyn exhibits antibiotic activity against multi-resistant *Staphylococcus aureus* by modifying several essential cysteines

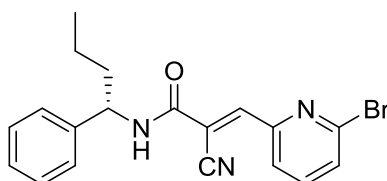
(*S*)-2-cyano-*N*-(1-phenylbutyl)acetamide (51)



To a stirred solution of (*S*)-1-phenylbutan-1-amine (500 mg, 3.35 mmol) in toluene (30 mL) was added 3-(3,5-dimethyl-1H-pyrazol-1-yl)-3-oxopropanenitrile (547 mg, 1.34 mmol) and refluxed for 2 h. After cooled to room temperature, the mixture was evaporated, and purified by column chromatography to afford the titled compound (540 mg, 75%).^{132,133} – ¹H NMR (300 MHz, *CDCl*₃): 7.31 – 7.18 (m, 5H), 6.30 (s, 1H), 4.85 (q, *J* = 7.6 Hz, 1H), 3.28 (d, *J* = 19.1 Hz, 1H), 3.22 (d, *J* = 19.1 Hz, 1H), 1.83 – 1.65 (m, 2H), 1.34 – 1.13 (m, 2H), 0.85 (t, *J* = 7.3 Hz, 3H). – ¹³C NMR (100 MHz, *CDCl*₃): 160.16, 141.29, 128.98, 127.94, 126.67, 114.92, 54.54, 38.10, 26.06, 19.55, 13.85. – HRMS (ESI) calcd. for C₁₃H₁₆N₂O [M+H]⁺ 217.1335, found 217.1336.

DGS

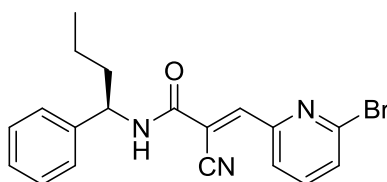
(*S,E*)-3-(6-bromopyridin-2-yl)-2-cyano-*N*-(1-phenylbutyl)acrylamide



To a solution of (*S*)-2-cyano-*N*-(1-phenylbutyl)acetamide (100 mg, 0.462 mmol) in EtOH (4.5 mL) was added 6-Bromo-2-pyridinecarboxaldehyde (95 mg, 0.509 mmol) and piperidine (9 μ L, 0.092 mmol). The reaction mixture was refluxed for 3 h, then cooled to room temperature. The solvent was evaporated in vacuo, and the residue was purified by column chromatography to afford the titled compound (85 mg, 65%).¹³⁴ – ¹H NMR (300 MHz, *CDCl*₃): 8.18 (s, 1H), 7.68 – 7.55 (m, 3H), 7.39 – 7.26 (m, 5H), 6.78 (d, *J* = 8.0 Hz, 1H), 5.08 (q, *J* = 7.6 Hz, 1H), 1.93 – 1.82 (m, 2H), 1.47 – 1.24 (m, 2H), 0.95 (t, *J* = 7.3 Hz, 3H). – ¹³C NMR (75 MHz, *CDCl*₃): 158.75, 151.03, 148.39, 142.60, 141.47, 139.27, 130.78, 128.97, 127.86, 126.65, 125.57, 115.95, 109.64, 54.79, 38.33, 19.59, 13.88. – HRMS (ESI) calcd. for C₁₉H₁₈BrN₃O [M+H]⁺ 384.0706, found 384.0704.

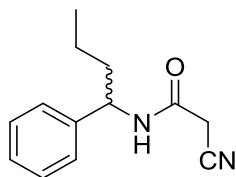
(*R*)-DGS

(*R,E*)-3-(6-bromopyridin-2-yl)-2-cyano-*N*-(1-phenylbutyl)acrylamide



Yield (142 mg, 63%). – ¹H NMR (300 MHz, *CDCl*₃): 8.18 (s, 1H), 7.68 – 7.55 (m, 3H), 7.39 – 7.26 (m, 5H), 6.78 (d, *J* = 8.0 Hz, 1H), 5.08 (q, *J* = 7.6 Hz, 1H), 1.93 – 1.82 (m, 2H), 1.47 – 1.24 (m, 2H), 0.95 (t, *J* = 7.3 Hz, 3H). – ¹³C NMR (75 MHz, *CDCl*₃): 158.75, 151.03, 148.39, 142.60, 141.47, 139.27, 130.78, 128.97, 127.86, 126.65, 125.57, 115.95, 109.64, 54.79, 38.33, 19.59, 13.88. – HRMS (ESI) calcd. for C₁₉H₁₈BrN₃O [M+H]⁺ 384.0706, found 384.0706.

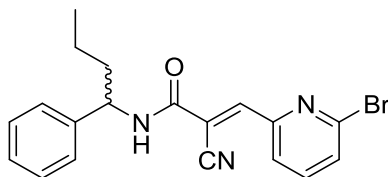
2-cyano-*N*-(1-phenylbutyl)acetamide (52)



To a solution of 1-phenylbutan-1-one (5.00 g, 33.7 mmol) in EtOH (53 mL) was added hydroxylamine hydrochloride (4.69 g, 67.5 mmol) and sodium hydroxide (5.40 g, 135 mmol) in H₂O (17 mL). The mixture was refluxed for 3 h, cooled to room temperature, and evaporated under the vacuum. The aqueous phase was extracted with EtOAc, and then the organic phase was washed with brine, dried over Na₂SO₄, filtered and concentrated in vacuo. The residue was dissolved in MeOH (100 mL) and then hydrogenated (H₂ balloon) using 10 wt% Pd/C catalyst (500 mg) at room temperature for 24 h. The reaction mixture was filtered through a pad of celite, and the combined filtrate was concentrated in vacuo, to provide the crude residue. Subsequently, to a stirred solution of the crude product in toluene (30 mL) was added 3-(3,5-dimethyl-1*H*-pyrazol-1-yl)-3-oxopropanenitrile (5.51 g, 33.7 mmol) and refluxed for 2 h. After cooled to room temperature, the mixture was evaporated, and purified by column chromatography to afford the titled compound (5.02 g, 69%).^[1,2] – ¹H NMR (300 MHz, CDCl₃): 7.31 – 7.18 (m, 5H), 6.30 (s, 1H), 4.85 (q, *J* = 7.6 Hz, 1H), 3.28 (d, *J* = 19.1 Hz, 1H), 3.22 (d, *J* = 19.1 Hz, 1H), 1.83 – 1.65 (m, 2H), 1.34 – 1.13 (m, 2H), 0.85 (t, *J* = 7.3 Hz, 3H). – ¹³C NMR (100 MHz, CDCl₃): 160.16, 141.29, 128.98, 127.94, 126.67, 114.92, 54.54, 38.10, 26.06, 19.55, 13.85. – HRMS (ESI) calcd. for C₁₃H₁₆N₂O [M+H]⁺ 217.1335, found 217.1335.

(*R,S*)-DGS

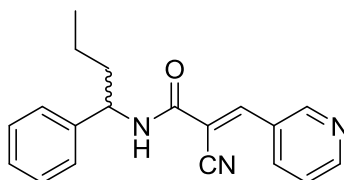
(*E*)-3-(6-bromopyridin-2-yl)-2-cyano-*N*-(1-phenylbutyl)acrylamide



To a solution of 2-cyano-*N*-(1-phenylbutyl)acetamide (70 mg, 0.324 mmol) in EtOH (3.0 mL) was added 6-Bromo-2-pyridinecarboxaldehyde (66 mg, 0.356 mmol) and piperidine (6 μ L, 0.065 mmol). The reaction mixture was refluxed for 3 h, then cooled to room temperature. The solvent was evaporated in vacuo, and the residue was purified by column chromatography to afford the titled compound. (59 mg, 64%). – ^1H NMR (300 MHz, CDCl_3): 8.18 (s, 1H), 7.68 – 7.55 (m, 3H), 7.39 – 7.26 (m, 5H), 6.78 (d, $J = 8.0$ Hz, 1H), 5.08 (q, $J = 7.6$ Hz, 1H), 1.93 – 1.82 (m, 2H), 1.47 – 1.24 (m, 2H), 0.95 (t, $J = 7.3$ Hz, 3H). – ^{13}C NMR (75 MHz, CDCl_3): 158.75, 151.03, 148.39, 142.60, 141.47, 139.27, 130.78, 128.97, 127.86, 126.65, 125.57, 115.95, 109.64, 54.79, 38.33, 19.59, 13.88. – HRMS (ESI) calcd. for $\text{C}_{19}\text{H}_{18}\text{BrN}_3\text{O}$ $[\text{M}+\text{H}]^+$ 384.0706, found 384.0706.

LK01

(*E*)-2-cyano-*N*-(1-phenylbutyl)-3-(pyridin-3-yl)acrylamide

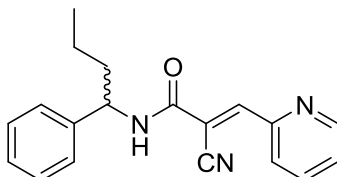


Yield (48 mg, 33%). – ^1H NMR (300 MHz, CDCl_3): 8.90 (d, $J = 2.3$ Hz, 1H), 8.71 – 8.69 (m, 1H), 8.40 – 8.36 (m, 1H), 8.30 (s, 1H), 7.44 – 7.27 (m, 6H), 6.63 (d, $J = 8.0$ Hz, 1H), 5.08 (q,

$J = 7.6$ Hz, 1H), 1.97 – 1.78 (m, 2H), 1.46 – 1.27 (m, 2H), 0.95 (t, $J = 7.3$ Hz, 3H). – ^{13}C NMR (75 MHz, CDCl_3): 158.75, 152.94, 152.31, 149.56, 141.38, 135.87, 128.92, 127.96, 127.83, 126.62, 124.02, 116.41, 106.76, 54.76, 38.15, 19.52, 13.81. – HRMS (ESI) calcd. for $\text{C}_{19}\text{H}_{19}\text{N}_3\text{O}$ $[\text{M}+\text{H}]^+$ 306.1601, found 306.1600.

LK02

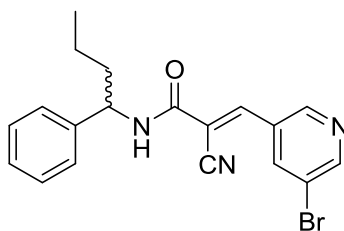
(*E*)-2-cyano-*N*-(1-phenylbutyl)-3-(pyridin-2-yl)acrylamide



Yield (41 mg, 42%). – ^1H NMR (300 MHz, CDCl_3): 8.82 – 8.79 (m, 1H), 8.27 (s, 1H), 7.82 – 7.76 (m, 1H), 7.60 – 7.57 (m, 1H), 7.41 – 7.26 (m, 6H), 6.80 (d, $J = 7.6$ Hz, 1H), 5.08 (q, $J = 7.6$ Hz, 1H), 1.97 – 1.79 (m, 2H), 1.47 – 1.25 (m, 2H), 0.95 (t, $J = 7.3$ Hz, 3H). – ^{13}C NMR (75 MHz, CDCl_3): 159.18, 150.65, 150.44, 150.27, 141.59, 137.07, 128.94, 127.80, 127.22, 126.66, 126.10, 116.85, 108.09, 54.71, 38.39, 19.59, 13.89. – HRMS (ESI) calcd. for $\text{C}_{19}\text{H}_{19}\text{N}_3\text{O}$ $[\text{M}+\text{H}]^+$ 306.1601, found 306.1600.

LK03

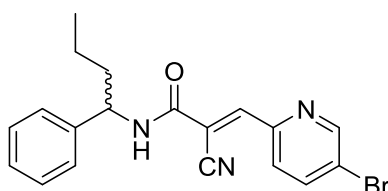
(*E*)-3-(5-bromopyridin-3-yl)-2-cyano-*N*-(1-phenylbutyl)acrylamide



Yield (48 mg, 36%). – ^1H NMR (300 MHz, CDCl_3): 8.85 (d, $J = 2.0$ Hz, 1H), 8.77 (d, $J = 2.2$ Hz, 1H), 8.44 (t, $J = 2.2$ Hz, 1H), 8.24 (s, 1H), 7.39 – 7.29 (m, 5H), 6.59 (d, $J = 8.0$ Hz, 1H), 5.07 (q, $J = 7.6$ Hz, 1H), 1.94 – 1.82 (m, 2H), 1.44 – 1.27 (m, 2H), 0.95 (t, $J = 7.3$ Hz, 3H). – ^{13}C NMR (75 MHz, CDCl_3): 158.25, 153.99, 149.92, 147.82, 141.23, 138.21, 129.39, 129.02, 127.99, 126.68, 121.40, 115.98, 108.11, 54.92, 38.19, 19.59, 13.87. – HRMS (ESI) calcd. for $\text{C}_{19}\text{H}_{18}\text{BrN}_3\text{O}$ $[\text{M}+\text{H}]^+$ 384.0706, found 384.0704.

LK04

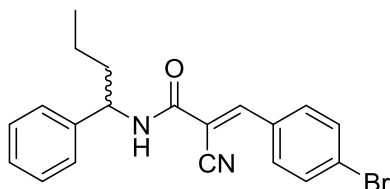
(*E*)-3-(5-bromopyridin-2-yl)-2-cyano-*N*-(1-phenylbutyl)acrylamide



Yield (45 mg, 51%). – ^1H NMR (300 MHz, CDCl_3): 8.85 (d, $J = 2.3$ Hz, 1H), 8.21 (s, 1H), 7.92 (dd, $J = 8.3, 2.3$ Hz, 1H), 7.48 – 7.25 (m, 6H), 6.77 (d, $J = 8.1$ Hz, 1H), 5.07 (q, $J = 7.6$ Hz, 1H), 1.97 – 1.78 (m, 2H), 1.47 – 1.25 (m, 2H), 0.95 (t, $J = 7.3$ Hz, 3H). – ^{13}C NMR (75 MHz, CDCl_3): 158.93, 151.74, 149.16, 148.58, 141.47, 139.69, 128.95, 127.93, 127.83, 126.65, 123.80, 116.52, 108.58, 54.77, 38.33, 19.57, 13.87. – HRMS (ESI) calcd. for $\text{C}_{19}\text{H}_{18}\text{BrN}_3\text{O}$ $[\text{M}+\text{H}]^+$ 384.0706, found 384.0711.

LK05

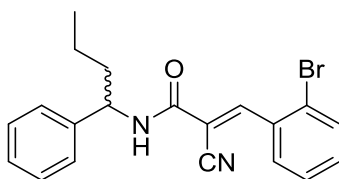
(*E*)-3-(4-bromophenyl)-2-cyano-*N*-(1-phenylbutyl)acrylamide



Yield (50 mg, 56%). – ^1H NMR (300 MHz, CDCl_3): 8.23 (s, 1H), 7.78 – 7.74 (m, 2H), 7.64 – 7.59 (m, 2H), 7.39 – 7.26 (m, 5H), 6.55 (d, $J = 8.1$ Hz, 1H), 5.07 (q, $J = 7.6$ Hz, 1H), 1.97 – 1.78 (m, 2H), 1.47 – 1.25 (m, 2H), 0.95 (t, $J = 7.3$ Hz, 3H). – ^{13}C NMR (75 MHz, CDCl_3): 159.23, 151.86, 141.53, 132.75, 131.94, 130.77, 128.99, 127.88, 127.73, 126.68, 116.94, 104.77, 54.75, 38.32, 19.59, 13.89. – HRMS (ESI) calcd. for $\text{C}_{20}\text{H}_{19}\text{BrN}_2\text{O}$ $[\text{M}+\text{H}]^+$ 383.0754, found 383.0755.

LK06

(*E*)-3-(2-bromophenyl)-2-cyano-*N*-(1-phenylbutyl)acrylamide

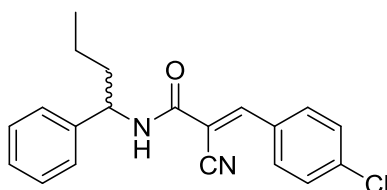


Yield (62 mg, 70%). – ^1H NMR (300 MHz, CDCl_3): 8.67 (s, 1H), 8.03 (dd, $J = 7.8, 1.7$ Hz, 1H), 7.68 (dd, $J = 7.8, 1.4$ Hz, 1H), 7.46–7.26 (m, 7H), 6.57 (d, $J = 8.4$ Hz, 1H), 5.08 (q, $J = 7.6$ Hz, 1H), 1.99 – 1.79 (m, 2H), 1.45 – 1.23 (m, 2H), 0.96 (t, $J = 7.3$ Hz, 3H). – ^{13}C NMR (75 MHz, CDCl_3): 158.76, 152.38, 141.48, 133.78, 133.30, 132.37, 129.78, 129.01, 128.06, 127.91, 126.75, 126.56, 116.42, 107.66, 54.84, 38.31, 19.62, 13.89. – HRMS (ESI) calcd. for $\text{C}_{20}\text{H}_{19}\text{BrN}_2\text{O}$

[M+H]⁺ 383.0754, found 383.0754.

LK07

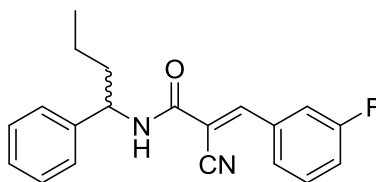
(*E*)-3-(4-chlorophenyl)-2-cyano-*N*-(1-phenylbutyl)acrylamide



Yield (42 mg, 54%). – ¹H NMR (300 MHz, *CDCl*₃): 8.26 (s, 1H), 7.78 – 7.82 (m, 2H), 7.48 – 7.27 (m, 7H), 6.56 (d, *J* = 8.1 Hz, 1H), 5.07 (q, *J* = 7.6 Hz, 1H), 1.96 – 1.78 (m, 2H), 1.47 – 1.23 (m, 2H), 0.95 (t, *J* = 7.3 Hz, 3H). – ¹³C NMR (75 MHz, *CDCl*₃): 159.24, 151.74, 141.54, 139.10, 131.87, 130.37, 129.74, 128.97, 127.85, 126.66, 116.93, 104.61, 54.73, 38.32, 19.59, 13.99. – HRMS (ESI) calcd. for C₂₀H₁₉ClN₂O [M+H]⁺ 339.1259, found 339.1257.

LK08

(*E*)-2-cyano-3-(3-fluorophenyl)-*N*-(1-phenylbutyl)acrylamide

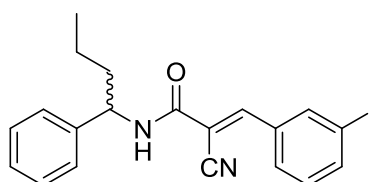


Yield (50 mg, 67%). – ¹H NMR (400 MHz, *CDCl*₃): 8.26 (s, 1H), 7.67 – 7.60 (m, 2H), 7.48 – 7.20 (m, 7H), 6.58 (d, *J* = 8.2 Hz, 1H), 5.07 (q, *J* = 7.6 Hz, 1H), 1.96 – 1.81 (m, 2H), 1.45 – 1.27 (m, 2H), 0.95 (t, *J* = 7.3 Hz, 3H). – ¹³C NMR (100 MHz, *CDCl*₃): 162.85 (d, ¹*J*_{C-F} = 330

Hz), 159.18, 151.74, 141.50, 133.91, 133.81, 131.02, 130.91, 128.96, 127.85, 126.67, 119.80 (d, $^2J_{C-F} = 28$ Hz), 116.83 (d, $^2J_{C-F} = 30$ Hz), 105.71, 54.76, 38.28, 19.58, 13.87. – HRMS (ESI) calcd. for $C_{20}H_{19}FN_2O$ $[M+H]^+$ 323.1554, found 323.1554.

LK09

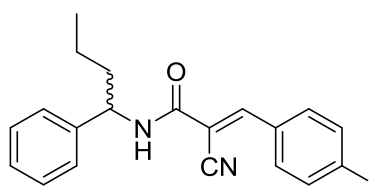
(*E*)-2-cyano-3-(3-iodophenyl)-*N*-(1-phenylbutyl)acrylamide



Yield (34 mg, 34%). – 1H NMR (300 MHz, $CDCl_3$): 8.11 (s, 1H), 8.07 (t, $J = 1.8$ Hz, 1H), 7.85-7.75 (m, 2H), 7.32-7.11 (m, 6H), 6.50 (d, $J = 8.1$ Hz, 1H), 5.00 (q, $J = 7.6$ Hz, 1H), 1.90 – 1.71 (m, 2H), 1.39 – 1.18 (m, 2H), 0.88 (t, $J = 7.3$ Hz, 3H). – ^{13}C NMR (75 MHz, $CDCl_3$): 158.99, 151.36, 141.47, 139.43, 133.93, 130.85, 129.14, 128.97, 127.87, 126.68, 116.62, 116.60, 105.65, 94.79, 54.75, 38.29, 19.58, 13.87. – HRMS (ESI) calcd. for $C_{20}H_{19}IN_2O$ $[M+H]^+$ 431.0615, found 431.0613.

LK10

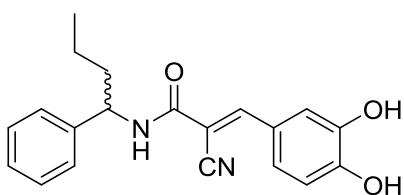
(*E*)-2-cyano-3-(4-iodophenyl)-*N*-(1-phenylbutyl)acrylamide



Yield (75 mg, 75%). – ^1H NMR (300 MHz, CDCl_3): 8.14 (s, 1H), 7.75 (d, $J = 8.5$ Hz, 1H), 7.53 (d, $J = 8.5$ Hz, 1H), 7.31-7.18 (m, 5H), 6.49 (d, $J = 8.1$ Hz, 1H), 4.99 (q, $J = 7.6$ Hz, 1H), 1.89 – 1.71 (m, 2H), 1.39 – 1.18 (m, 2H), 0.87 (t, $J = 7.3$ Hz, 3H). – ^{13}C NMR (75 MHz, CDCl_3): 159.21, 152.04, 141.51, 138.71, 131.77, 131.26, 128.96, 127.85, 126.66, 116.91, 104.84, 100.28, 54.73, 38.30, 19.58, 13.88. – HRMS (ESI) calcd. for $\text{C}_{20}\text{H}_{19}\text{IN}_2\text{O}$ $[\text{M}+\text{H}]^+$ 431.0615, found 431.0613.

LK11

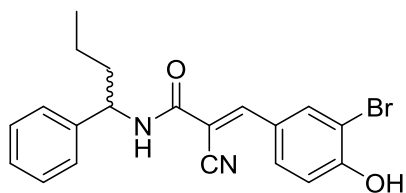
(*E*)-2-cyano-3-(3,4-dihydroxyphenyl)-*N*-(1-phenylbutyl)acrylamide



Yield (85 mg, 68%). – ^1H NMR (400 MHz, $\text{DMSO}-d_6$): 9.83 (brs, 2H), 8.61 (d, $J = 8.2$ Hz, 1H), 7.91 (s, 1H), 7.54 (s, 1H), 7.38 – 7.20 (m, 6H), 6.88 (d, $J = 8.2$ Hz, 1H), 4.88 (q, $J = 6.0$ Hz, 1H), 1.90 – 1.65 (m, 2H), 1.41 – 1.17 (m, 2H), 0.89 (t, $J = 7.3$ Hz, 3H). – ^{13}C NMR (100 MHz, $\text{DMSO}-d_6$): 161.56, 150.59, 150.27, 145.67, 143.53, 128.23, 126.76, 126.56, 125.06, 123.34, 117.14, 116.10, 115.91, 101.33, 53.48, 37.71, 19.37, 13.59. – HRMS (ESI) calcd. for $\text{C}_{20}\text{H}_{20}\text{N}_2\text{O}_3$ $[\text{M}+\text{H}]^+$ 337.1547, found 337.1546.

LK12

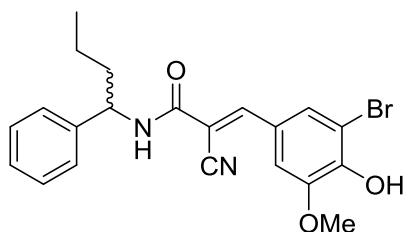
(*E*)-3-(3-bromo-4-hydroxyphenyl)-2-cyano-*N*-(1-phenylbutyl)acrylamide



Yield (100 mg, 67%). – ^1H NMR (400 MHz, $\text{DMSO}-d_6$): 11.42 (s, 1H), 8.69 (d, $J = 8.2$ Hz, 1H), 8.17 (q, $J = 2.2$ Hz, 1H), 8.00 (s, 1H), 7.86 (dd, $J = 8.6, 2.2$ Hz, 1H), 7.38 – 7.21 (m, 5H), 7.10 (d, $J = 8.6$ Hz, 1H), 4.88 (q, $J = 7.8$ Hz, 1H), 1.89 – 1.65 (m, 2H), 1.41 – 1.20 (m, 2H), 0.89 (t, $J = 7.3$ Hz, 3H). – ^{13}C NMR (100 MHz, $\text{DMSO}-d_6$): 161.08, 157.91, 148.55, 143.37, 135.25, 131.31, 128.22, 126.78, 126.55, 126.54, 124.46, 116.71, 116.69, 109.96, 103.45, 53.53, 37.70, 19.33, 13.58. – HRMS (ESI) calcd. for $\text{C}_{20}\text{H}_{19}\text{BrN}_2\text{O}_2$ $[\text{M}+\text{H}]^+$ 399.0703, found 399.0703.

LK13

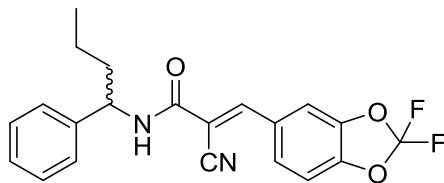
(*E*)-3-(3-bromo-4-hydroxy-5-methoxyphenyl)-2-cyano-*N*-(1-phenylbutyl)acrylamide



Yield (62 mg, 63%). – ^1H NMR (300 MHz, CDCl_3): 8.13 (s, 1H), 7.61 (d, $J = 2.0$ Hz, 1H), 7.56 (d, $J = 2.0$ Hz, 1H), 7.39 – 7.25 (m, 5H), 6.51 (brs, 1H), 6.49 (s, 1H), 5.07 (q, $J = 7.6$ Hz, 1H), 3.96 (s, 3H), 1.92 – 1.80 (m, 2H), 1.45 – 1.25 (m, 2H), 0.95 (t, $J = 7.3$ Hz, 3H). – ^{13}C NMR (75 MHz, CDCl_3): 159.63, 151.76, 147.49, 147.39, 141.64, 130.18, 128.94, 127.81, 126.67, 125.17, 117.48, 110.16, 108.77, 102.05, 56.71, 54.62, 28.36, 19.60, 13.90. – HRMS (ESI) calcd. for $\text{C}_{21}\text{H}_{21}\text{BrN}_2\text{O}_3$ $[\text{M}+\text{H}]^+$ 429.0808, found 429.0807.

LK14

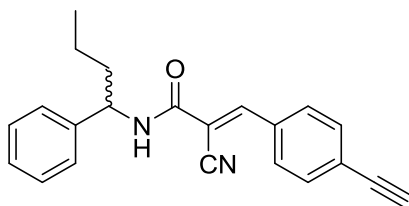
(*E*)-2-cyano-3-(2,2-difluorobenzo[*d*][1,3]dioxol-5-yl)-*N*-(1-phenylbutyl)acrylamide



Yield (40 mg, 40%). – ^1H NMR (300 MHz, CDCl_3): 8.16 (s, 1H), 7.70 (d, $J = 1.8$ Hz, 1H), 7.52-7.48 (m, 1H), 7.32-7.18 (m, 5H), 7.09 (d, $J = 8.4$ Hz, 1H), 6.48 (d, $J = 8.1$ Hz, 1H), 4.99 (q, $J = 7.6$ Hz, 1H), 1.90 – 1.71 (m, 2H), 1.39 – 1.18 (m, 2H), 0.88 (t, $J = 7.3$ Hz, 3H). – ^{13}C NMR (75 MHz, CDCl_3): 159.15, 151.50, 146.61, 144.48, 141.51, 131.75 (t, $^1J_{\text{C-F}} = 257$ Hz), 129.01, 128.94, 128.22, 127.84, 126.65, 116.83, 110.24, 110.17, 104.15, 54.76, 38.27, 19.57, 13.84. – HRMS (ESI) calcd. for $\text{C}_{21}\text{H}_{18}\text{F}_2\text{N}_2\text{O}_3$ $[\text{M}+\text{H}]^+$ 385.1358, found 385.1356.

DGSp

(*E*)-2-cyano-3-(4-ethynylphenyl)-*N*-(1-phenylbutyl)acrylamide

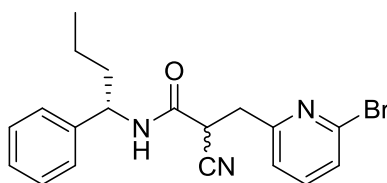


Yield (49 mg, 65%). – ^1H NMR (300 MHz, CDCl_3): 8.27 (s, 1H), 7.88-7.84 (m, 2H), 7.59-7.55 (m, 2H), 7.39-7.25 (m, 5H), 6.57 (d, $J = 8.1$ Hz, 1H), 5.08 (q, $J = 7.6$ Hz, 1H), 3.27 (s, 1H), 1.98 – 1.79 (m, 2H), 1.50 – 1.24 (m, 2H), 0.96 (t, $J = 7.3$ Hz, 3H). – ^{13}C NMR (75 MHz, CDCl_3): 159.24, 151.96, 141.54, 132.87, 132.00, 130.47, 128.94, 127.82, 126.65, 126.62, 116.94, 104.89, 82.83, 81.02, 54.71, 38.29, 19.57, 13.87. – HRMS (ESI) calcd. for $\text{C}_{22}\text{H}_{20}\text{N}_2\text{O}$ $[\text{M}+\text{H}]^+$ 329.1648,

found 329.1648.

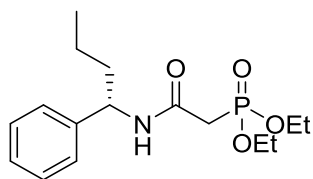
DGS-re

(*R,S*)-3-(6-bromopyridin-2-yl)-2-cyano-*N*-((*S*)-1-phenylbutyl)propenamide



To a solution of (*S,E*)-3-(6-bromopyridin-2-yl)-2-cyano-*N*-(1-phenylbutyl)acrylamide (83 mg, 0.216 mmol) in THF (2.0 mL) was added NaBH₄ (5.0 mg, 0.130 mmol) at 0 °C. The mixture was warmed to room temperature after 24h and quenched with water. The aqueous phase was extracted with EtOAc three times, and combined organic layers were dried over Na₂SO₄. The residue was concentrated under reduced pressure and purified by column chromatography to afford the titled diastereomers (48 mg, 58%). – ¹H NMR (500 MHz, CDCl₃): 7.51 – 7.21 (m, 12H), 7.18 – 7.14 (m, 4H), 6.67 (d, *J* = 8.2 Hz, 1H), 6.58 (d, *J* = 8.2 Hz, 1H), 4.88 (q, *J* = 7.7 Hz, 2H), 4.12 (t, *J* = 6.8 Hz, 1H), 4.07 (t, *J* = 6.8 Hz, 1H), 3.51 – 3.41 (m, 2H), 3.35 – 3.27 (m, 2H), 1.85 – 1.70 (m, 4H), 1.34 – 1.16 (m, 4H), 0.91 (t, *J* = 7.3 Hz, 3H), 0.86 (t, *J* = 7.3 Hz, 3H). – ¹³C NMR (125 MHz, CDCl₃): 163.31, 157.11, 157.03, 141.74, 141.73, 141.51, 141.49, 139.44, 139.37, 127.76, 127.67, 127.07, 127.04, 122.92, 122.84, 117.75, 117.66, 54.52, 54.47, 38.31, 38.27, 37.20, 37.09, 36.75, 36.65, 19.58, 19.51, 13.91, 13.87. – HRMS (ESI) calcd. for C₁₉H₂₀BrN₃O [M+H]⁺ 386.0863, found 386.0865.

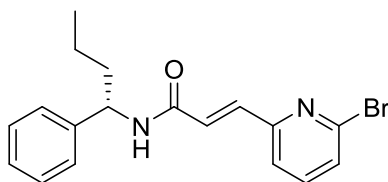
diethyl (*S*)-(2-oxo-2-((1-phenylbutyl)amino)ethyl)phosphonate (53)



A mixture of 4-dimethylaminopyridine (77 mg, 0.630 mmol) and 1-ethyl-3-(3-dimethylaminopropyl)carbodiimide hydrochloride (121 mg, 0.630 mmol) was added to a stirred solution of diethylphosphonoacetic acid (62 mg, 0.315 mmol) and (*S*)-1-phenylbutan-1-amine (47 mg, 0.315 mmol) in DMF. The resulting mixture was stirred under argon for 3 h at room temperature, and then poured into EtOAc. The solution was washed with 1N HCl twice and brine, dried over Na₂SO₄, and concentrated. The crude was purified by column chromatography to yield the titled compound. (58 mg, 56%). – ¹H NMR (300 MHz, CDCl₃): 7.31 – 7.15 (m, 5H), 4.95 (q, *J* = 7.9 Hz, 2H), 4.16 – 3.97 (m, 4H), 2.96 – 2.76 (m, 2H), 1.85 – 1.67 (m, 2H), 1.42 – 1.18 (m, 8H), 0.91 (t, *J* = 7.3 Hz, 3H).

DGS-CN

(*S,E*)-3-(6-bromopyridin-2-yl)-*N*-(1-phenylbutyl)acrylamide



To a solution of sodium hydride (60% wt. in mineral oil, 13 mg, 0.317 mmol) in dry THF (0.5 mL) was added a solution of diethyl (*S*)-(2-oxo-2-((1-phenylbutyl)amino)ethyl)phosphonate (34 mg, 0.104 mmol) in THF (1.0 mL) at 0 °C. The mixture was warmed to room temperature and stirred for 30 min. Then a solution of 6-bromopicolinaldehyde (19 mg, 0.104 mmol) in dry THF (1 mL) was added dropwise and

stirred overnight. The reaction was quenched with water, and the aqueous phase was extracted with EtOAc three times. The combined organic layers were dried over Na₂SO₄ and concentrated under reduced pressure. The residue was purified by column chromatography to afford the titled diastereomers (21 mg, 56%). – ¹H NMR (300 MHz, CDCl₃): 7.47 – 7.14 (m, 9H), 6.96 (d, *J* = 15.0 Hz, 1H), 6.01 (d, *J* = 8.4 Hz, 1H), 5.02 (q, *J* = 7.7 Hz, 2H), 4.12 (t, *J* = 6.8 Hz, 1H), 4.07 (t, *J* = 6.8 Hz, 1H), 1.79 – 1.68 (m, 2H), 1.37 – 1.16 (m, 2H), 0.85 (t, *J* = 7.3 Hz, 3H). – ¹³C NMR (75 MHz, CDCl₃): 164.41, 154.48, 142.53, 142.26, 139.23, 137.85, 128.80, 128.27, 127.51, 126.67, 126.59, 123.54, 53.66, 38.54, 19.60, 13.96. – HRMS (ESI) calcd. for C₁₈H₁₉BrN₂O [M+H]⁺ 359.0754, found 359.0759.

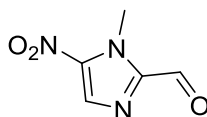
1.4. **LK1602** as a potent inhibitor against gram positive and negative bacteria

General method for the condensation of imidazole and indolin-2-one

To a solution of indolin-2-one compound (1 equiv.) in EtOH (0.3 M), piperidine or 2,2,6,6-tetramethylpiperidine (1.5 equiv.) as a base and imidazole compound (1.05 equiv.) were added. The reaction mixture was heated to reflux and stirred for 4 h, then cooled to room temperature. The mixture was filtered, and the filter cake was washed with EtOH three times. Then the filter cake was collected and dried under vacuum to remove the residual solvent to give the titled compounds

LK1601

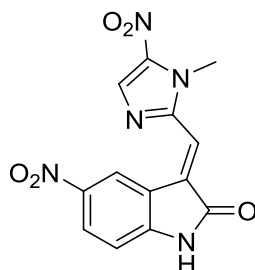
1-methyl-5-nitro-1*H*-imidazole-2-carbaldehyde



(1-methyl-5-nitro-1*H*-imidazol-2-yl)methanol (1.00 g, 6.36 mmol) in toluene (17 mL) and activated manganese dioxide (4.60 g, 53.5 mmol) were refluxed for 4 h. After filtration, the mixture was evaporated. The residue was purified by column chromatography to afford the titled compound (617 mg, 63%). – ¹H NMR (300 MHz, *CDCl*₃): 9.86 (s, 1H), 8.27 (s, 1H), 4.21 (s, 3H). – ¹³C NMR (100 MHz, *CDCl*₃): 184.05, 143.19, 141.01, 132.30, 33.88. – HRMS (ESI) calcd. for C₅H₆N₃O₃ [M+H]⁺ 156.0404, found 156.0402.

LK1602

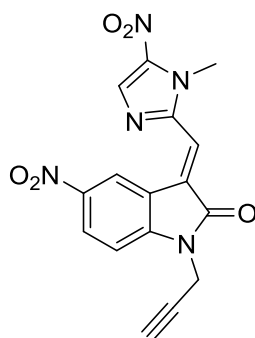
(E)-3-((1-methyl-5-nitro-1H-imidazol-2-yl)methylene)-5-nitroindolin-2-one



Prepared according to general method using 5-nitroindolin-2-one, piperidine, and 1-methyl-5-nitro-1H-imidazole-2-carbaldehyde (150 mg, 77%). – ^1H NMR (500 MHz, $\text{DMSO-}d_6$): 11.35 (s, 1H), 9.86 (d, $J = 2.5$ Hz, 1H), 8.43 (s, 1H), 8.19 (dd, $J = 8.7, 2.5$ Hz, 1H), 7.36 (s, 1H), 6.97 (d, $J = 8.7$ Hz, 1H), 4.10 (s, 3H). – ^{13}C NMR (75 MHz, $\text{DMSO-}d_6$): 168.72, 149.37, 145.62, 141.96, 139.93, 133.50, 129.74, 127.88, 123.18, 120.67, 118.93, 109.93, 33.70. – HRMS (ESI) calcd. for $\text{C}_{13}\text{H}_9\text{N}_5\text{O}_5$ $[\text{M}+\text{H}]^+$ 316.0676, found 316.0674.

101

(E)-3-((1-methyl-5-nitro-1H-imidazol-2-yl)methylene)-5-nitro-1-(prop-2-yn-1-yl)indolin-2-one

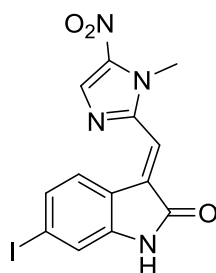


To a solution of (E)-3-((1-methyl-5-nitro-1H-imidazol-2-yl)methylene)-5-nitroindolin-2-one

(100 mg, 0.320 mmol) in DMF (1.5 mL) was added NaH 60% dispersion in mineral oil (27 mg, 0.750 mmol) were added. The mixture turned black and was stirred 15 min at rt. 3-bromoprop-1-yne (29 μ L, 0.380 mmol) were added and the reaction mixture was stirred at room temperature for 1.5 h. The mixture was diluted with EtOAc and quenched with water. Three phases occurred, an organic, an aqueous and a slurry/solid phase. The organic phase was discarded, and diethyl ether was added to precipitate orange solid. After vacuum filtration the solid was washed with water and diethyl ether to obtain the titled compound (36 mg, 32%). – ^1H NMR (500 MHz, $\text{DMSO-}d_6$): 10.08 (s, 1H), 8.52 (s, 1H), 8.41 (d, $J = 8.7$ Hz, 1H), 7.61 (s, 1H), 7.39 (d, $J = 8.7$ Hz, 1H), 4.74 (s, 2H), 4.14 (s, 3H), 3.38 (s, 1H). – ^{13}C NMR (75 MHz, $\text{DMSO-}d_6$): 168.72, 149.37, 145.62, 141.96, 139.93, 133.50, 129.74, 127.88, 123.18, 120.67, 118.93, 109.93, 33.70. – HRMS (ESI) calcd. for $\text{C}_{16}\text{H}_{11}\text{N}_5\text{O}_5$ $[\text{M}+\text{H}]^+$ 354.0833, found 354.0834.

102

(*E*)-6-iodo-3-((1-methyl-5-nitro-1*H*-imidazol-2-yl)methylene)indolin-2-one



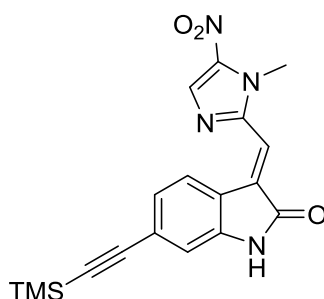
Prepared according to general method using 6-iodoindolin-2-one, 2,2,6,6-tetramethylpiperidine, and 1-methyl-5-nitro-1*H*-imidazole-2-carbaldehyde (200 mg, 91%). – ^1H NMR (300 MHz, $\text{DMSO-}d_6$): 10.81 (s, 1H), 8.80 (d, $J = 8.2$ Hz, 1H), 8.41 (s, 1H), 7.40 – 7.35 (m, 2H), 7.21 (d, $J = 1.6$ Hz, 1H), 4.07 (s, 3H). – ^{13}C NMR (75 MHz, $\text{DMSO-}d_6$): 168.20,

146.24, 145.05, 139.70, 133.59, 131.11, 130.19, 129.25, 120.12, 118.38, 116.96, 98.56, 33.59.

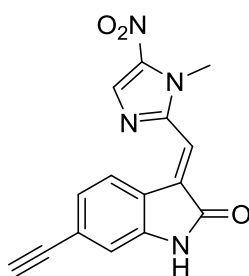
– HRMS (ESI) calcd. for $C_{13}H_9IN_4O_3$ $[M+H]^+$ 396.9792, found 396.9791.

103

**(*E*)-3-((1-methyl-5-nitro-1*H*-imidazol-2-yl)methylene)-6-
((trimethylsilyl)ethynyl)indolin-2-one**

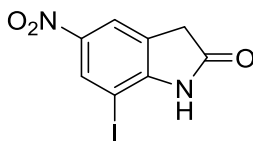


(Trimethylsilyl)acetylene (84 mg, 0.858 mmol) and (*E*)-6-iodo-3-((1-methyl-5-nitro-1*H*-imidazol-2-yl)methylene)indolin-2-one (170 mg, 0.429 mmol) were dissolved in DMF (1.0 mL) and triethylamine (1.5 mL). The solution was degassed for 10 minutes by bubbling argon through the solution. At this time CuI (12 mg, 0.064 mmol) and Bis(triphenylphosphine)palladium(II) dichloride (30 mg, 0.043 mmol) were added, and the reaction was heated, under argon, at 70 °C. for 22 h. Water was then added and the precipitate was filtered off and dried. The crude was purified by column chromatography to afford the titled compound (80 mg, 51%). – 1H NMR (300 MHz, $DMSO-d_6$): 10.83 (s, 1H), 9.00 (d, $J = 8.1$ Hz, 1H), 8.43 (s, 1H), 7.35 (s, 1H), 7.08 (d, $J = 8.1$ Hz, 1H), 6.85 (s, 1H), 4.09 (s, 3H), 0.24 (s, 9H). – ^{13}C NMR (75 MHz, $DMSO-d_6$): 168.35, 145.14, 143.95, 139.72, 133.61, 131.05, 127.89, 124.86, 124.74, 121.11, 117.07, 112.26, 105.22, 96.53, 33.59, -0.19. – HRMS (ESI) calcd. for $C_{18}H_{18}N_4O_3Si$ $[M+H]^+$ 367.1221, found 367.1219.

(*E*)-6-ethynyl-3-((1-methyl-5-nitro-1*H*-imidazol-2-yl)methylene)indolin-2-one

To a solution of (*E*)-3-((1-methyl-5-nitro-1*H*-imidazol-2-yl)methylene)-6-((trimethylsilyl)ethynyl)indolin-2-one (50 mg, 0.136 mmol) in EtOH (2.3 mL) and THF (0.7 mL) was added dropwise a solution of silver nitrate (53 mg, 0.314 mmol) in water (0.5 mL) and EtOH (0.7 mL), during which time a precipitate formed. The mixture was stirred at room temperature for 45 min, after which a solution of potassium cyanide (96 mg, 1.47 mmol) in water (0.34 mL) was added and the precipitated dissolved. To the solution was then added a saturated aqueous sodium bicarbonate solution followed by water. The product was then filtered off and dried to give the crude product, which was recrystallized from EtOAc/HEX to yield the titled compound (24 mg, 60%). – ¹H NMR (300 MHz, *DMSO-d*₆): 10.82 (s, 1H), 9.02 (d, *J* = 8.0 Hz, 1H), 8.42 (s, 1H), 7.35 (s, 1H), 7.11 (dd, *J* = 8.0, 1.5 Hz, 1H), 6.89 (d, *J* = 1.5 Hz, 1H), 4.36 (s, 1H), 4.08 (s, 3H). – ¹³C NMR (75 MHz, *DMSO-d*₆): 168.36, 146.14, 143.99, 139.71, 133.59, 131.08, 127.90, 125.09, 124.37, 121.09, 117.03, 112.31, 83.63, 82.76, 33.57. – HRMS (ESI) calcd. for C₁₅H₁₀N₄O₃ [M+H]⁺ 295.0826, found 295.0824.

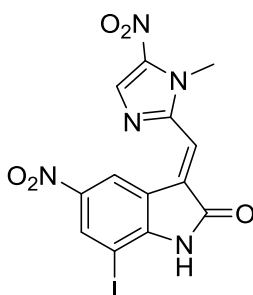
7-iodo-5-nitroindolin-2-one



5-nitroindolin-2-one (500 mg, 2.81 mmol) was dissolved in conc. sulfuric acid (5mL). Consequently, *N*-iodosuccinimide (755 mg, 3.37 mmol) was added in small portions to the solution. The mixture was stirred 17 hours at room temperature and the reaction then quenched with water. The resulting suspension was filtered, and the filter cake washed with water to afford the titled compound (766 mg, 91%). – ¹H NMR (500 MHz, *DMSO-d*₆): 11.05 (s, 1H), 8.39 (d, *J* = 2.1 Hz, 1H), 8.05 (d, *J* = 2.1 Hz, 1H), 3.77 (s, 2H). – ¹³C NMR (75 MHz, *DMSO-d*₆): 176.10, 153.08, 142.31, 132.85, 127.07, 119.28, 72.97, 37.20. – HRMS (ESI) calcd. for C₈H₅IN₂O₃ [M-H]⁻ 302.9272, found 302.9270.

106

(*E*)-7-iodo-3-((1-methyl-5-nitro-1*H*-imidazol-2-yl)methylene)-5-nitroindolin-2-one

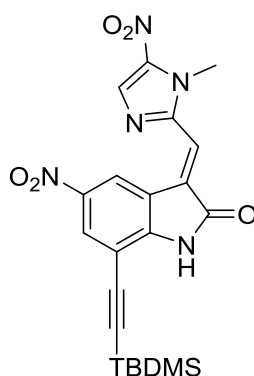


Prepared according to general method using 7-iodo-5-nitroindolin-2-one, 2,2,6,6-tetramethylpiperidine, and 1-methyl-5-nitro-1*H*-imidazole-2-carbaldehyde (594 mg, 82%). – ¹H NMR (300 MHz, *DMSO-d*₆): 11.35 (s, 1H), 9.94 (d, *J* = 2.3 Hz, 1H), 8.45 (s, 1H), 8.44 (d,

$J = 2.3$ Hz, 1H), 7.42 (s, 1H), 4.13 (s, 3H). – ^{13}C NMR (75 MHz, $\text{DMSO-}d_6$): 168.45, 151.73, 145.26, 142.31, 139.94, 135.51, 133.57, 129.93, 122.18, 120.66, 119.78, 74.53, 33.77. – HRMS (ESI) calcd. for $\text{C}_{13}\text{H}_8\text{IN}_5\text{O}_5$ $[\text{M}+\text{H}]^+$ 441.9643, found 441.9640.

107

(*E*)-7-((*tert*-butyldimethylsilyl)ethynyl)-3-((1-methyl-5-nitro-1*H*-imidazol-2-yl)methylene)-5-nitroindolin-2-one

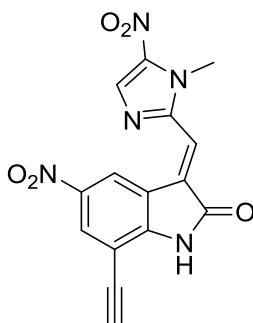


A mixture of (*E*)-7-iodo-3-((1-methyl-5-nitro-1*H*-imidazol-2-yl)methylene)-5-nitroindolin-2-one (100 mg, 0.227 mmol), ((*tert*-butyldimethylsilyl)ethynyl)boronic acid pinacol ester (77 mg, 0.289 mmol), and Cs_2CO_3 (222 mg, 0.680 mmol) in 1,4-dioxane (1.1 mL) was degassed with Argon for 5 min. Then, tetrakis(triphenylphosphine)palladium(0) (27mg, 23mmol) was added and the reaction was set under argon atmosphere, sealed and stirred at 70 °C for 24 h. The mixture was diluted with EtOAc and the reaction then quenched with water. The resulting emulsion was extracted three times with EtOAc and the combined organic fraction dried over Na_2SO_4 . The crude product was purified by column chromatography to afford the titled compound (51 mg, 50%). – ^1H NMR (300 MHz, $\text{DMSO-}d_6$): 11.85 (s, 1H), 10.03 (d, $J = 2.4$ Hz, 1H), 8.50 (s, 1H), 8.18 (d, $J = 2.4$ Hz, 1H), 7.56 (s, 1H), 4.14 (s, 3H), 1.00 (s,

9H), 0.24 (s, 6H). – ^{13}C NMR (75 MHz, $\text{DMSO}-d_6$): 169.14, 150.39, 145.42, 141.78, 140.08, 133.53, 129.90, 129.18, 123.02, 121.30, 120.04, 104.53, 99.70, 97.90, 33.78, 26.08, 16.36, -4.83. – HRMS (ESI) calcd. for $\text{C}_{21}\text{H}_{23}\text{N}_5\text{O}_5\text{Si}$ $[\text{M}+\text{H}]^+$ 454.1541, found 454.1540.

108

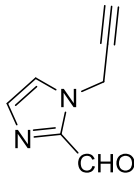
(*E*)-7-ethynyl-3-((1-methyl-5-nitro-1*H*-imidazol-2-yl)methylene)-5-nitroindolin-2-one



1.0 M TBAF solution in THF (177 μL , 0.177 mmol) was added to a solution of (*E*)-7-((*tert*-butyldimethylsilyl)ethynyl)-3-((1-methyl-5-nitro-1*H*-imidazol-2-yl)methylene)-5-nitroindolin-2-one (30 mg, 0.088 mmol) in THF (5 mL), whereupon the orange solution turned dark brown. The mixture was stirred for 1 h and the reaction then quenched with sat. NaHCO_3 solution. The residue was extracted with EtOAc three times and the combined organic phases were concentrated under reduced pressure. The crude product was purified by column chromatography to afford the titled compound (16 mg, 53%). – ^1H NMR (300 MHz, $\text{DMSO}-d_6$): 11.74 (s, 1H), 9.94 (s, 1H), 8.45 (s, 1H), 8.18 (s, 1H), 7.45 (s, 1H), 4.62 (s, 1H), 4.14 (s, 3H). – ^{13}C NMR (75 MHz, $\text{DMSO}-d_6$): 168.86, 150.86, 145.38, 141.71, 140.06, 133.54, 129.77, 129.11, 123.03, 121.12, 119.87, 103.92, 87.49, 76.46, 33.79. – HRMS (ESI) calcd. for $\text{C}_{15}\text{H}_9\text{N}_5\text{O}_5$ $[\text{M}+\text{H}]^+$ 340.0676, found 340.0674.

109

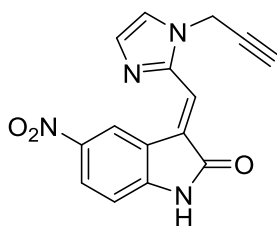
1-(prop-2-yn-1-yl)-1*H*-imidazole-2-carbaldehyde



To a suspension of 1*H*-imidazole-2-carbaldehyde (500 mg, 5.20 mmol) and potassium carbonate (863 mg, 6.24 mmol) in DMF (7 mL) was added 3-bromopropyne (743 mg, 6.24 mmol) and the mixture was heated at 50 °C for 5 h. The mixture was quenched with water and diluted with EtOAc, and then the residue was partitioned between water and EtOAc. The aqueous layer was extracted with ethyl acetate. The combined organic layers were washed with brine, dried over anhydrous sodium sulfate, and concentrated. The crude was purified by column chromatography to afford the titled compound (545 mg, 78%). – ¹H NMR (300 MHz, *CDCl*₃): 9.80 (s, 1H), 7.46 (s, 1H), 7.31 (s, 1H), 5.25 (d, *J* = 2.6 Hz, 1H), 2.52 (t, *J* = 2.6 Hz, 1H). – ¹³C NMR (75 MHz, *CDCl*₃): 182.27, 142.82, 131.78, 125.55, 76.20, 75.44, 37.34. – HRMS (ESI) calcd. for C₇H₇N₂O [M+H]⁺ 135.0553, found 135.0551.

110

(*E*)-5-nitro-3-((1-(prop-2-yn-1-yl)-1*H*-imidazol-2-yl)methylene)indolin-2-one



Prepared according to general method using 5-nitroindolin-2-one, piperidine, and 1-(prop-

2-yn-1-yl)-1*H*-imidazole-2-carbaldehyde (26 mg, 67%). – ¹H NMR (300 MHz, *DMSO-d*₆): 11.29 (s, 1H), 10.34 (d, *J* = 2.5 Hz, 1H), 8.21 (dd, *J* = 8.6, 2.5 Hz, 1H), 7.68 (d, *J* = 1.1 Hz, 1H), 7.62 (s, 1H), 7.50 (s, 1H), 7.03 (d, *J* = 8.6 Hz, 1H), 5.31 (d, *J* = 2.5 Hz, 2H), 3.61 (t, *J* = 2.5 Hz, 1H). – ¹³C NMR (75 MHz, *DMSO-d*₆): 169.62, 148.36, 142.00, 141.66, 131.29, 126.62, 125.10, 123.81, 122.71, 121.80, 120.40, 78.34, 77.01, 35.83. – HRMS (ESI) calcd. for C₁₅H₁₀N₄O₃ [M+H]⁺ 295.0826, found 295.0824.

2. Microbiology

2.1. Bacterial strains and media

Species	Strain	Medium for cultivation
<i>Staphylococcus aureus</i>	NCTC8325	B
	ACTT29213	B
	USA300	B
	MU50	B
<i>Listeria monocytogenes</i>	EGD-e	BHB
<i>Acinetobacter baumannii</i>	DSM30007	BHB
<i>Pseudomonas aeruginosa</i>	DSM19882	BHB
	PAO1	LB
<i>Salmonella Typhimurium</i>	LT2	LB
<i>Escherichia coli</i>	MM28	LB
	RFM795	LB
MRSA clinical isolate ⁸³		
<i>Staphylococcus aureus</i>	VA402525	B
	VA409044	B
	VA402923	B
	VA412350	B
	VA418879	B
	VA417350	B
	IS050611	B
	IS050678	B
	BK097296	B
	BK095395	B

Table 2. Bacterial strains and their appropriate cultivation media.

Media	Composition
B	10.0 g peptone ex casein 5.00 g NaCl 5.00 g yeast extract in 1 L ddH ₂ O, pH = 7.5
BHB	17.5 g brain heart infusion 2.50 g Na ₂ HPO ₄ 2.00 g <i>D</i> -(+)-glucose 10.0 g peptone ex casein 5.00 g NaCl in 1 L ddH ₂ O, pH = 7.4
LB	10.0 g peptone ex casein 5.00 g NaCl 5.00 g yeast extract 1.00 g K ₂ HPO ₄ in 1 L ddH ₂ O, pH = 7.5

Table 3. Composition of the different media used for the cultivation of bacteria. Amounts of the single ingredients were calculated for 1 L total volume.

2.2. Cultivation methods

Overnight culture

5 mL of the medium for cultivation were inoculated with 5 µL of the desired bacterial cryostock (1:1,000) in a plastic culture tube. The culture was incubated overnight (routinely 16 h) by shaking at 200 rpm at 37 °C. All overnight cultures were prepared freshly to avoid genetic variation. A sterile control was added each time (medium without bacteria).

Cryostock

5 mL of an overnight culture of the desired bacteria were harvested by centrifugation (6,000 g, 10 m, 4 °C) and the supernatant was removed. The living bacteria pellet was resuspended in 750 µL of fresh medium. Sterile glycerol was added to get a final

concentration of 50%. The stock was mixed and stored at -80 °C in 20 µL aliquots prior to use. After inoculating fresh media with the aliquot, the leftover of the cryostock was discarded.

Minimal inhibitory concentration (MIC) assay

The overnight culture was diluted to $OD_{600} = 0.001$ in fresh media and 100 µL aliquots were added to 96 well plates which contain various concentrations of compounds (1 µL in DMSO) and DMSO (1 µL) as a negative control. After 20 h incubation at 200 rpm at 37 °C, the optical density was measured at 600 nm with a plate reader (infinite M200Pro plate reader).

3. Proteomics

3.1. Activity-based protein profiling experiments

3.1.1 Analytical gel-based ABPP

Bacterial strains were cultivated under defined growth conditions to stationary phase. Cultures were collected in a 50 mL falcon tube, pelleted at 6,000 rpm for 10 min at 4 °C and washed with PBS. The pellet was then resuspended in PBS to a final OD₆₀₀ = 40. Here the PBS buffer was always pH = 7.4 in the following steps. 200 µL of aliquots of bacterial suspension and 2 µL of various concentrations of the alkyne probe of the original compound (or just DMSO as a control) were mixed and incubated for 1 h at 200 rpm at 37 °C. The bacterial suspension was centrifuged at 6,000 g for 10 min at 4 °C. The supernatant was removed and the pellets were stored at -80 °C. Pellets were resuspended in 200 µL PBS (4 °C) and the suspension was lysed by sonication five times 20 sec pulses at 80% max. power on ice. The suspension was incubated two times for 0.5 h at 200 rpm at 37 °C after addition of 5 µL of lysostaphin (2 mg/mL) and then 25 µL of 10% (w/v) SDS in PBS solution in that order. And then click chemistry was carried out with 20 µL click reagent mix (4 µL RhN₃ (5 mM rhodamine-azide in DMSO), 4 µL TCEP (50 mM tris(2-carboxyethyl)phosphine in ddH₂O), 12 µL TBTA ligand (1.667 mM Tris(benzyltriazolylmethyl)amine in 80% tBuOH and 20% DMSO)). After shortly vortexing the samples, the cycloaddition reaction was initiated by adding 4 µL of CuSO₄ (50 mM in ddH₂O) solution. The mixture was incubated for 1 h at room temperature and quenched by 200 µL of 2x gel loading buffer. After the samples were heated up to 95 °C for 10 min at 600 rpm, they were shortly centrifugated to run down. 40 µL of each sample was applied on the analytical SDS-PAGE gel, which was developed for 3 h under 150 V under constant cooling. Fluorescent bands were visualized by Fujifilm Las-3000 Fluorescence Darkbox with a Fujinon VRF 43LMD Lens, 605DF40 filter and 520 nm EPI excitation wavelength.

3.1.2. Gel-free quantitative ABPP

An overnight culture of *S. aureus* was grown in 5 mL B medium in a plastic culture tube. After 1:100 dilution of the culture with fresh B medium, the cultures were grown until stationary phase. Cultures were collected in a 50 mL falcon tube and centrifuged at 6,000 g for 10 min at 4 °C. The supernatant was disposed and the pellet was resuspended in PBS to reach OD₆₀₀ = 40. 500 µL of this suspension and 5 µL of the alkyne probe of the original compound in DMSO (or just DMSO as a control) were mixed and incubated for 1 h at 200 rpm at 37 °C. The bacterial suspension was centrifuged at 6,000 g for 10 min at 4 °C. The supernatant was removed and the pellets were stored at –80 °C. Pellets were resuspended in 500 µL PBS (4 °C) and the suspension was lysed by sonication with 5 x 20 sec pulsed at 80% max. power on ice. The suspension was incubated two times for 0.5 h at 200 rpm at 37 °C after each addition of 5 µL of lysostaphin (2 mg/mL) and then 25 µL of 10% (w/v) SDS in PBS solution in order. Protein concentration was determined using a bicinchoninic acid (BCA) assay and the concentration was adjusted to 1 mg/mL with PBS. In a 15 mL falcon tube, 500 µL of solution were treated with 43 µL click reagent mix (3 µL Biotin-PEG3-N₃ (Jena Bioscience, CLK-AZ104P4-100; 10 mM in DMSO), 10 µL TCEP (50 mM in ddH₂O), 30 µL TBTA ligand (1.667 mM in 80% tBuOH and 20% DMSO)). Resulting in final concentrations of: 233 µM Biotin-PEG3-N₃, 581 µM TCEP and 58.2 µM TBTA Ligand. The lysates were mixed by vortexing and 10 µL CuSO₄ solution (50 mM in ddH₂O) were added to start the click reaction. The lysates were mixed by vortexing again and incubated for 1 h at RT in the dark. Subsequently 4 mL of cold acetone (–80° C, MS grade) were added and proteins were precipitated overnight at –80 °C. The precipitated proteins were thawed on ice, pelletized (10,000 g, 15 min, 4 °C) and the supernatant was disposed. Proteins were washed two times with 1 mL cold methanol (–80 °C, MS grade). Resuspension was achieved by sonication (10 sec at 10% intensity) and proteins were pelletized via centrifugation (10,000 g, 10 min, 4 °C). After the washing steps the supernatant was disposed and the pellet resuspended in 500 µL 0.4% SDS in PBS at RT by sonication (10 sec at 10% intensity). 50 µL avidin-agarose beads (Sigma-Aldrich) were prepared by washing three times with 1 mL 0.4% SDS in PBS. All centrifugation steps were conducted at 400 g for 3 min at RT. 500 µL protein solution was added to the washed avidin-agarose beads and incubated under continuous inverting (1 h, RT). Beads were washed three times with 1 mL 0.4% SDS in PBS, two times with 6 M urea in ddH₂O and three times with 1 mL PBS.

[Digestion]

The beads were resuspended in 200 μ L denaturation buffer (7 M urea, 2 M thiourea in 20 mM pH 7.5 HEPES buffer). For reduction, Dithiothreitol (DTT, 500 mM, 0.4 μ L) was added, the tubes were mixed by vortexing shortly and incubated in a thermoshaker (600 rpm, 60 min, RT). Then 2-iodoacetamide (IAA, 500 mM, 4 μ L) was added for alkylation, the tubes were mixed by vortexing shortly and incubated in a thermoshaker (600 rpm, 30 min, RT, in the dark). Remaining IAA was quenched by the addition of dithiothreitol (DTT, 500 mM, 4 μ L). The tubes were shortly mixed by vortexing and incubated in a thermoshaker (600 rpm, 30 min, RT). LysC (0.5 μ g/ μ L) was thawed on ice and 1 μ L was added to each microcentrifuge tube, the tubes were shortly mixed by vortexing and incubated in a thermoshaker (600 rpm, 2 h, RT, in the dark). Triethylammonium bicarbonate (TEAB) solution (600 μ L, 50 mM in water) and then trypsin (1.5 μ L, 0.5 μ g/ μ L in 50 mM acetic acid) were added to each tube with a short vortexing step after each addition. The microcentrifuge tubes were incubated in a thermoshaker (600 rpm, 15 h, 37 °C). The digest was stopped by adding 10 μ L formic acid (FA) and vortexing followed by centrifugation (13,000 g, 3 min, RT).

[Desalting]

50 mg SepPak C18 columns (Waters) were equilibrated by gravity flow two times with 1 mL acetonitrile and three times with 1 mL aqueous 0.1% trifluoroacetic acid (TFA) solution. Subsequently the samples were loaded by gravity flow, washed three times with 1 mL aqueous 0.1% TFA solution and once with 0.5 mL aqueous 0.5% FA solution. Elution of peptides into new 2.0 mL Protein LoBind Eppendorf tubes was performed by two times addition of 250 μ L elution buffer (80% ACN, 0.5% FA) by gravity flow followed by 250 μ L elution buffer by vacuum flow until all liquid was eluted from the column. The eluates were lyophilized.

[Filtering and MS measurement]

Before MS measurement the samples were dissolved in 30 μ L 1% FA by pipetting up and down, vortexing and sonication for 15 min (brief centrifugation after each step). 0.22 μ m centrifugal filter units (VWR) were equilibrated with 300 μ L 1% FA (13,000 g, 2 min, RT) and samples were filtered through the equilibrated filters (centrifugation: 13,000 g, 1 min, RT).

Samples were analyzed with an UltiMate 3000 nano HPLC system (Dionex) using Acclaim C18 PepMap100 75 μm ID x 2 cm trap and Acclaim PepMap RSLC C18 (75 μm ID x 50 cm) separation columns in an EASY-spray setting coupled to a Qexactive Plus (Thermo Fisher). 5 μL peptide samples were loaded on the trap and washed with 0.1% TFA, then transferred to the analytical column (buffer A: H_2O with 0.1% FA, buffer B: MeCN with 0.1% FA, flow 0.3 $\mu\text{L}/\text{min}$, gradient: to 5% buffer B in 7 min, from 5% to 22% buffer B in 105 min, then to 32% buffer B in 10 min, to 90% buffer B in 10 min and hold at 90% buffer B for 10 min, then to 5% buffer B in 0.1 min and hold 5% buffer B for 9.9 min) and ionized at spray voltage of 2.0 kV and a capillary temperature of 275 $^\circ\text{C}$. Q Exactive Plus was operated in a TOP12 data dependent mode with full scan acquisition in the orbitrap at a resolution of $R = 140,000$ and an AGC target of $3\text{e}6$ in a scan range of 300 - 1500 m/z with a maximum injection time of 80 ms. Monoisotopic precursor selection as well as dynamic exclusion (dynamic exclusion duration: 60 s) was enabled. Precursors with charge states >1 and intensities greater than $1\text{e}4$ were selected for fragmentation. Isolation was performed in the quadrupole using a window of 1.6 m/z . Precursors were analyzed in a scan range of 200 – 2000 m/z to an AGC target of $1\text{e}5$ and a maximum injection time of 100 ms. Peptide fragments were generated by higher-energy collisional dissociation (HCD) with a normalized collision energy of 27% and detected in the orbitrap.

Peptide and protein identifications were performed using MaxQuant 1.6.0.16 software with Andromeda as search engine using following parameters: Carbamidomethylation of cysteines as fixed and oxidation of methionine, trypsin as the proteolytic enzyme, 4.5 ppm for precursor mass tolerance (main search ppm) and 0.5 Da for fragment mass tolerance (ITMS MS/MS tolerance). Searches were performed against the Uniprot database for *S. aureus* NCTC8325 (taxon identifier: 93061, downloaded on 12.09.2018). Quantification was performed using label-free quantification (LFQ). The match between runs (default settings) option was used. Identification was done with at least 2 unique peptides and quantification only with unique peptides.

Statistical analysis was performed with Perseus 1.6.2.2. LFQ ratios were $\log_2(x)$ transformed. $-\log_{10}(p\text{-values})$ were obtained by a two sample t-test over three biological replicates. Putative contaminants, reverse peptides and peptides only identified by site were deleted. Valid values were filtered for three in at least one group and a missing values imputation was performed over the total matrix.

3.1.3. Competition ABPP experiment

Procedure was followed as described in Gel free ABPP in chapter 3.1.2, but for competition, the bacteria suspension was pretreated with original compound of alkyne probe in DMSO (or just DMSO as a control) for 45 min at 200 rpm at 37 °C, and then treated with probe in DMSO for 45 min at 200 rpm at 37 °C.

3.1.4. Competitive isoDTB-ABPP

[Sample preparation]

Overnight cultures of *S. aureus* NCTC8325 were inoculated with 5 mL of a corresponding glycerol stock into 5 mL of B- medium and grown overnight at 37 °C with shaking at 200 rpm. For preparation of lysates, the indicated medium was inoculated 1:100 with an overnight culture of the respective bacteria and incubated at 37 °C with shaking at 200 rpm until 1 h after it reached the stationary phase. The cells were harvested by centrifuging at 8,000 xg at 4 °C for 10 min, and the pellets were washed two times with PBS prior to the immediate use or storage at –80 °C. PBS was added to the bacterial pellets and the pellets were resuspended and transferred into 7 mL tubes containing 0.1 mm ceramic beads. Cells were lysed in a Precellys 24 bead mill using three 30 s cycles at 6,500 rpm while cooling with an airflow that was pre-cooled with liquid nitrogen. The suspension was transferred into an Eppendorf tube and centrifuged at 20,000 xg at 4 °C for 30 min. The supernatant of several samples was pooled and filtered through a 0.45 mm filter. Protein concentration of the lysate was determined using a bicinchoninic acid (BCA) assay and the concentration was adjusted to 1 mg/mL with PBS.

1.00 mL freshly prepared lysate were incubated with 10 µL 100x of compound in DMSO (e.g. 10 µL 10 mM stock for 100 µM final concentration or 10 µL 2 mM stock for 20 µM final concentration) at room temperature for 1 h. Another 1.00 mL sample of lysate was incubated with 10 µL of DMSO. After this incubation, 20 µL of 50 mM IA-alkyne in DMSO were separately added to the lysate with and without competitor and incubated at room temperature for 1 h. The samples were clicked to the heavy (DMSO-treated) and light (compound-treated) isoDTB tags by adding 120 µL of a solution consisting of 60 µL 0.9

mg/mL TBTA ligand in 4:1 tBuOH/DMSO, 20 μ L 12.5 mg/mL CuSO₄ in water, 20 μ L 13 mg/ml TCEP in water and 20 μ L 5 mM of the respective isoDTB tag in DMSO. After incubation of the samples at room temperature for 1 h, the light- and heavy-labeled samples were combined into 8 mL of cold acetone in order to precipitate all proteins. Precipitates were stored at -20 °C overnight.

[MS Sample Preparation]

The protein precipitates were centrifuged at 3,500 rpm at 25 °C for 10 min. The supernatant was removed, and precipitates resuspended in 1 mL cold methanol by sonification. After centrifugation at 20,000 xg at 4 °C for 10 min, the supernatant was removed. This wash step with methanol was repeated one more time. The pellets were dissolved in 300 μ L 8 M urea in 0.1 M triethylammonium bicarbonate (TEAB) by sonification. 900 μ L 0.1 M TEAB were added to obtain a concentration of 2 M urea. This solution was added to 1.2 mL of washed high capacity streptavidin agarose beads (50 μ L initial slurry, Fisher Scientific, 10733315) in 0.2% nonyl phenoxy polyethoxy ethanol (NP40). The samples were rotated at room temperature for 1 h in order to assure binding to the beads.

The beads were centrifuged (1 min, 1,000 xg) and the supernatant was removed. The beads were resuspended in 600 μ L 0.1% NP40 in PBS and transferred to a centrifuge column (Fisher Scientific, 11894131). Beads were washed two times with 0.1% NP40 in PBS, three times with PBS and three times with ddH₂O. The beads were resuspended in 600 μ L 8 M urea in 0.1 M TEAB, transferred to a Protein LoBind tube and centrifuged (1 min, 1,000 xg). The supernatant was removed, and the beads were resuspended in 300 μ L 8 M urea in 0.1 M TEAB. 15 μ L of dithiothreitol (DTT; 31 mg/mL in water) were added and the beads incubated at 37 °C with shaking at 200 rpm for 45 min. Free thiol groups were modified by adding 15 μ L of iodoacetamide (74 mg/mL in water) and incubation at 25 °C with shaking at 200 rpm for 30 min. Remaining iodoacetamide was quenched by adding 15 μ L DTT (31 mg/mL in water) and incubation at 25 °C with shaking at 200 rpm for another 30 min.

For trypsin digestion, 900 μ L TEAB were added to the samples after alkylation to obtain a urea concentration of 2 M. Samples were centrifuged (1 min, 1,000 xg) and the supernatant removed. The beads were resuspended in 200 μ L 2 M urea in 0.1 M TEAB. 4 μ L 0.5 mg/mL trypsin (Promega, V5113) were added and samples incubated at 37 °C with shaking

at 200 rpm overnight. After the digestion, samples were diluted by adding 400 μ L of 0.1% NP40 in PBS and transferred to a centrifuge column (Fisher Scientific, 11894131). Beads were washed three times with 0.1% NP40 in PBS, three times with PBS (MS grade) and three times with water (MS grade). Peptides were eluted by adding 200 mL 0.1% formic acid in 50% acetonitrile in water to the column. 100 mL of the elution buffer were added two times more to the column and peptides eluted into a Protein LoBind tube by centrifuging at 3,000 xg for 3 min. The solvent was removed in a vacuum concentrator by rotating at 30 °C for approximately 5 h. Samples were dissolved in 30 mL 1% formic acid in water by sonification for 5 min. Samples were filtered (Merck, UVC30GVNB) washed with the same solvent and transferred into MS sample vials. Samples were stored at -20 °C until measurement.

[Sample Analysis by LC-MS/MS]

10 μ L of the samples were analyzed using a Qexactive Plus mass spectrometer (ThermoFisher) coupled to an Ultimate 3000 nano HPLC system (Dionex). Samples were loaded on an Acclaim C18 PepMap100 trap column (75 μ m ID x 2 cm) and washed with 0.1% TFA. The subsequent separation was carried out on an Acclaim C18PepMapRSLC column (75 μ m ID x 50 cm) with a flow of 300 μ L/min and buffer A: 0.1% formic acid in water and B: 0.1% formic acid in acetonitrile. Analysis started with washing in 5% B for 7 min followed a gradient from 5% to 40% buffer B in 105 min, an increase to 60% B in 10 min and another increase to 90% B in 10 min. 90% B was held for 10 min, then decreased to 5% in 0.1 min and held at 5% for another 9.9 min. The Qexactive Plus mass spectrometer was run in a TOP10 data-dependent mode. In the orbitrap, full MS scans were collected in a scan range of 300-1500 m/z at a resolution of 70,000 and an AGC target of $3e6$ with 80 ms maximum injection time. The most intense peaks were selected for MS2 measurement with a minimum AGC target of $1e3$ and isotope exclusion and dynamic exclusion (exclusion duration: 60 s) enabled. Peaks with unassigned charge or a charge of +1 were excluded. MS2 spectra were collected at a resolution of 17,500 aiming at an AGC target of $1e5$ with a maximum injection time of 100 ms. Isolation was conducted in the quadrupole using a window of 1.6 m/z . Fragments were generated using higher-energy collisional dissociation (HCD, normalized collision energy: 27%) and finally detected in the orbitrap.

[Data evaluation using MaxQuant]

MS raw data were analyzed using MaxQuant software (version 1.6.1.0).¹³⁵ Standard settings were used with the following changes and additions: A modified FASTA database, based on the UniProt database for *S. aureus* NCTC8325 (taxon identifier: 93061, downloaded on 12.09.2018), with individual substitutions of cysteines with the placeholder "U" were used as described previously.¹³⁶ Labels were set on the placeholder amino acid "U" for the light isoDTB tag as light label (C₂₈H₄₆N₁₀O₆S₁Se₋₁) and the heavy isoDTB tag as heavy label (C₂₄¹³C₄H₄₆N₈¹⁵N₂O₆S₁Se₋₁). A multiplicity of 2 was set and a maximum number of labeled amino acids of 1. The digestion enzyme was set to trypsin with maximum number of missed cleavages of 2. No variable modifications were included. The "re-quantify" option was enabled. Carbamidomethyl (C₂H₃NO) was used as fixed modification on cysteine. Contaminants were included. Peptides were searched with a minimum peptide length of 7 and a maximum peptide mass of 4,600 Da. "Second peptides" and "dependent peptides" were disabled and the option "Match between run" was enabled with a match time window of 0.7 min and an alignment window of 20 min. An FDR of 0.01 was used for Protein FDR, PSM FDR and XPSM FDR.

[Data Processing]

The "peptides.txt" file of the MaxQuant analysis was used for further analysis. All peptide sequences without a modified cysteine (placeholder "U") and all reverse sequences were deleted. Only the columns "Sequence", "Leading Razor Protein", "Start Position" and the columns for "Ratio H/L" for all experiments were kept. The "Leading Razor Protein" was renamed to the Uniprot Code without the indicator for the number of the cysteine. All individual ratios were filtered out, if they were "NaN", and all other values were transformed into the log₂-scale. For each peptide in each condition, the data was filtered out, if there were not at least two data points for individual experiments or if the standard deviation between the experiments exceeded a value of 1.41. For each peptide, an identifier was generated in the form "Uniprot Code"_"C"_"residue number of the modified cysteine". The data for the same experiment for all peptides with the same identifier, and therefore the same modified cysteine, were combined. Here, the median of the data was used. The data was filtered out if the standard deviation exceeded a value of 1.41. Each modified cysteine was kept in the dataset once with the shortest peptide sequence as the reported sequence. For each modified cysteine, all values for the same condition were combined, but the individual values are also reported. The values were combined as the median and the data

was filtered out, if there were not at least two data points or if the standard deviation exceeded a value of 1.41. All modified cysteines were filtered out if they were not quantified for at least one condition. These are the final ratios that are reported. The information on the "Gene Name" and "Name" was linked back from the FASTA database.

[Downstream Analysis]

For the competitive experiments, all conditions were further analyzed using Perseus software.¹³⁷ All individual values for each modified cysteine for the same condition were loaded into Perseus and analyzed using a one-sample t-test against a value of $\log_2(R) = 0$. Conditions with $p < 0.05$ were considered significant and compounds were deemed to engage a certain cysteine at a specific condition and called a "hit" if the statistical significance was $p < 0.05$ and the median ratio was $\log_2(R) > 2$ according to the values described under "Data Processing".

[Analysis of Protein Essentiality]

The data for the database of essential genes (DEG)¹³⁸ was used. It was downloaded from aureowiki (aureowiki.med.uni-greifswald.de). The information was linked to the information in the FASTA database through the "ordered locus name" that is reported in aureowiki and in UniProt.¹³⁹

[Analysis of Functional Sites]

For all entries in the FASTA database for *S. aureus* NCTC8325 the information in the categories "Active site", "Binding Site", "DNA-binding", "Nucleotide-binding", "Site" and "Metal-binding" was downloaded from uniprot.org.¹³⁶ This information gives all amino acid residues that are in the respective functional sites. It was determined for all cysteines, whether they are in these functional sites or less than six amino acid residues in the primary sequence away from a residue in a functional site. If this is the case for any kind of functional site, the cysteine is considered as being at a functional site.

[Analysis of Functional Protein Classes]

Gene Ontology terms¹⁴⁰ for all entries in the FASTA database for *S. aureus* NCTC8325 in the category "GO - Molecular function" were downloaded from uniprot.org.¹³⁶ For each term that was present in the database at least once, a functional class was annotated manually. In this way, each term for each protein was assigned to a functional class. If a

protein was only associated with terms from one functional class, it was assigned to that functional class. If a protein was associated with terms from different functional classes, the functional class of the protein was assigned according to this order of priority: enzyme, modulator / scaffolding / adaptor, receptor / transporter / channel and then gene expression / nucleic acid-binding. If no functional class was assigned to any of the terms, the protein was classified as “not assigned”.

3.2. Global proteomics analysis

An overnight culture of *S. aureus* was grown in 5 mL B medium in a plastic culture tube. After 1:100 dilution of the culture with fresh B medium, the cultures were grown for 2 h until OD₆₀₀ value was between 0.4 and 0.6. Cultures were diluted into B medium to give a final OD₆₀₀ of 0.3 and then 12 mL diluted cultures were incubated with the ½ MIC concentration of original compound in DMSO and same amount of DMSO as a control until OD₆₀₀ value was reached around 3. The bacteria suspension was centrifuged at 6,000 g for 10 min at 4 °C and the supernatant was disposed. The pellet was resuspended in PBS and centrifuged at 6,000 g for 10 min at 4 °C again. The supernatant was removed and the pellets were stored at –80 °C. Pellets were resuspended in 200 µL 100 mM Tris pH 7.4 (lysis buffer) and lysed by sonication with 5 x 20 sec pulsed at 80% max. power on ice. 75 µL solution of 10% (w/v) SDS and 1.25% (w/v) sodium deoxycholate in lysis buffer was added and samples heated for 10 min at 90 °C. Lysates were sonicated for 10 s at 10% intensity to shear nucleic acids and centrifuged at 10,000 g for 15 min at 4 °C to pellet debris. Protein concentration was determined using a bicinchoninic acid (BCA) assay and the concentration was adjusted to 1 mg/mL with PBS, and the samples were adjusted to equal protein amounts (0.5 mg/mL). Subsequently, proteins were precipitated with 4 mL of cold acetone (–80 °C, MS grade) overnight at –80 °C. The precipitated proteins were thawed on ice, pelletized (12,000 g, 20 min, 4 °C) and the supernatant was disposed. Proteins were washed three times with 1 mL cold methanol (–80 °C, MS grade). Resuspension was achieved by sonication (10 sec at 10% intensity) and proteins were pelletized via centrifugation (12,000 g, 20 min, 4 °C). The following steps from digestion to filtering, were performed as described in Gel free ABPP in chapter 3.1.2.

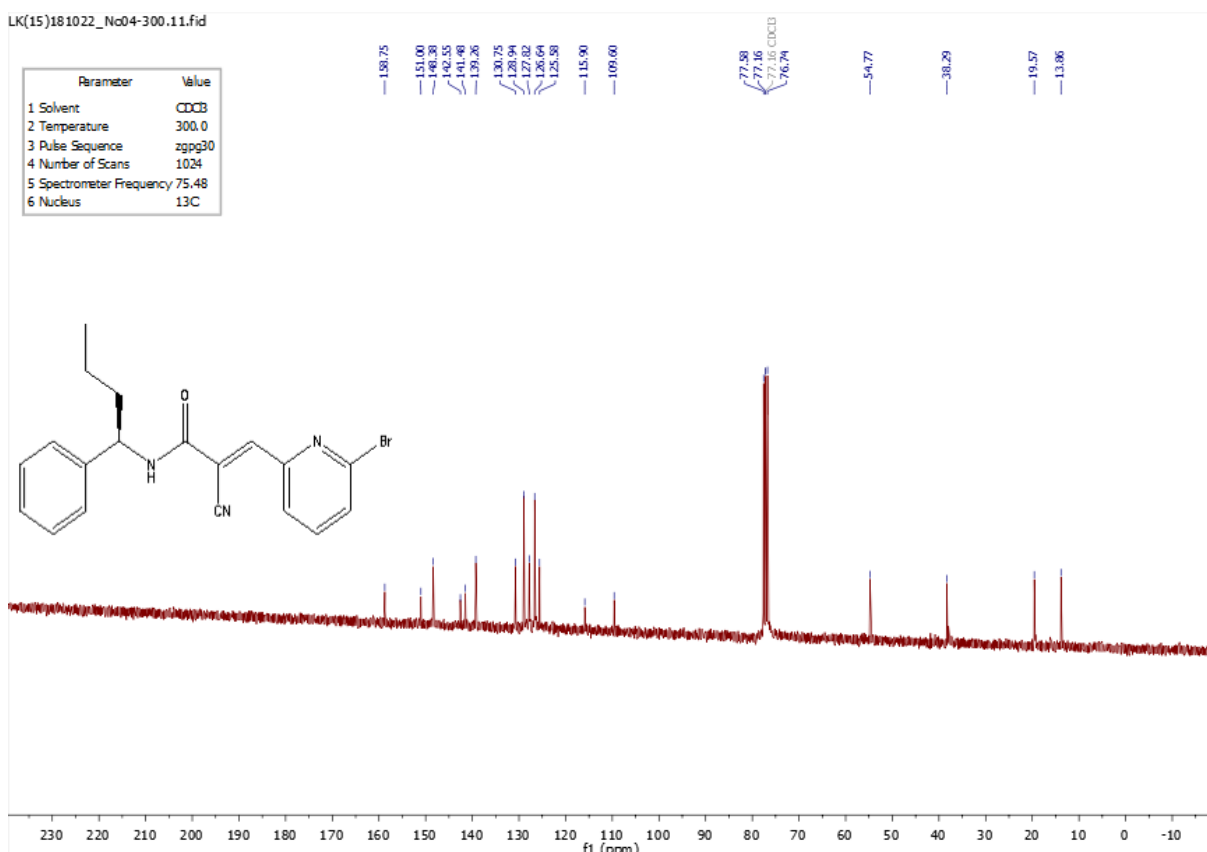
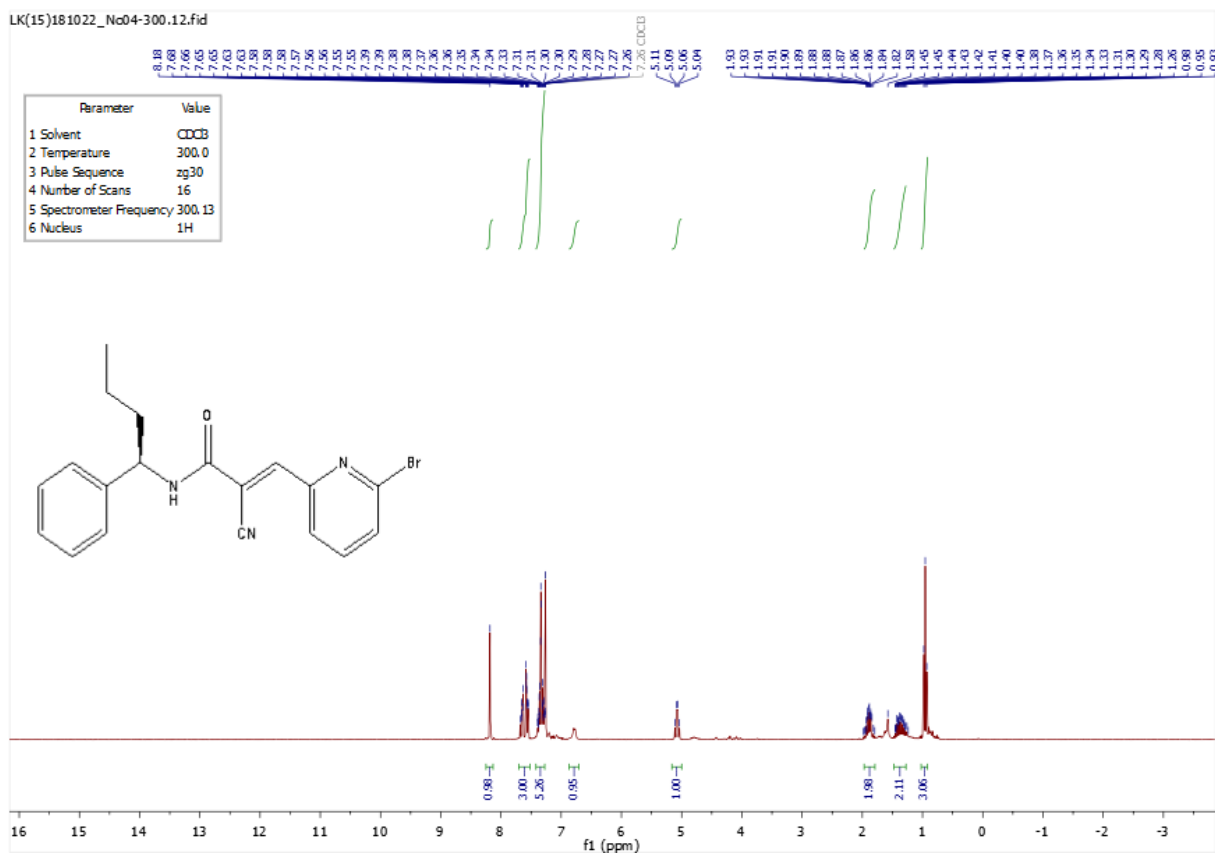
[MS measurement]

Samples were analyzed via HPLC-MS/MS using an UltiMate 3000 nano HPLC system (Dionex, Sunnyvale, California, USA) equipped with Acclaim C18 PepMap100 75 μ m ID x 2 cm trap and Acclaim C18 PepMap RSLC, 75 μ m ID x 15 cm separation columns coupled to Thermo Fischer LTQ Orbitrap Fusion (Thermo Fisher Scientific Inc., Waltham, Massachusetts, USA). Samples were loaded on the trap and washed for 10 min with 0.1% FA (at 5 μ L/min), then transferred to the analytical column and separated using a, 112 min gradient from 4% to 35% MeCN followed by 4 min at 80% MeCN in 0.1% FA (at 200 nL/min flow rate). LTQ Orbitrap Fusion was operated in a 3 second top speed data dependent mode. Full scan acquisition was performed in the orbitrap at a resolution of 120,000 and an ion target of $4e5$ in a scan range of 300 – 1700 m/z. Monoisotopic precursor selection as well as dynamic exclusion for 60 sec were enabled. Precursors with charge states of 2 – 7 and intensities greater than $5e3$ were selected for fragmentation. Isolation was performed in the quadrupole using a window of 1.6 m/z. Precursors were collected to a target of $1e2$ for a maximum injection time of 250 ms with “inject ions for all available parallelizable time” enabled. Fragments were generated using higher-energy collisional dissociation (HCD) and detected in the ion trap at a rapid scan rate. Internal calibration was performed using the ion signal of fluoranthene cations (EASY-ETD/IC source). MS raw files were processed with MaxQuant version 1.6.0.16 as described above. Statistical analysis was performed as described above using Perseus version 1.6.2.2.



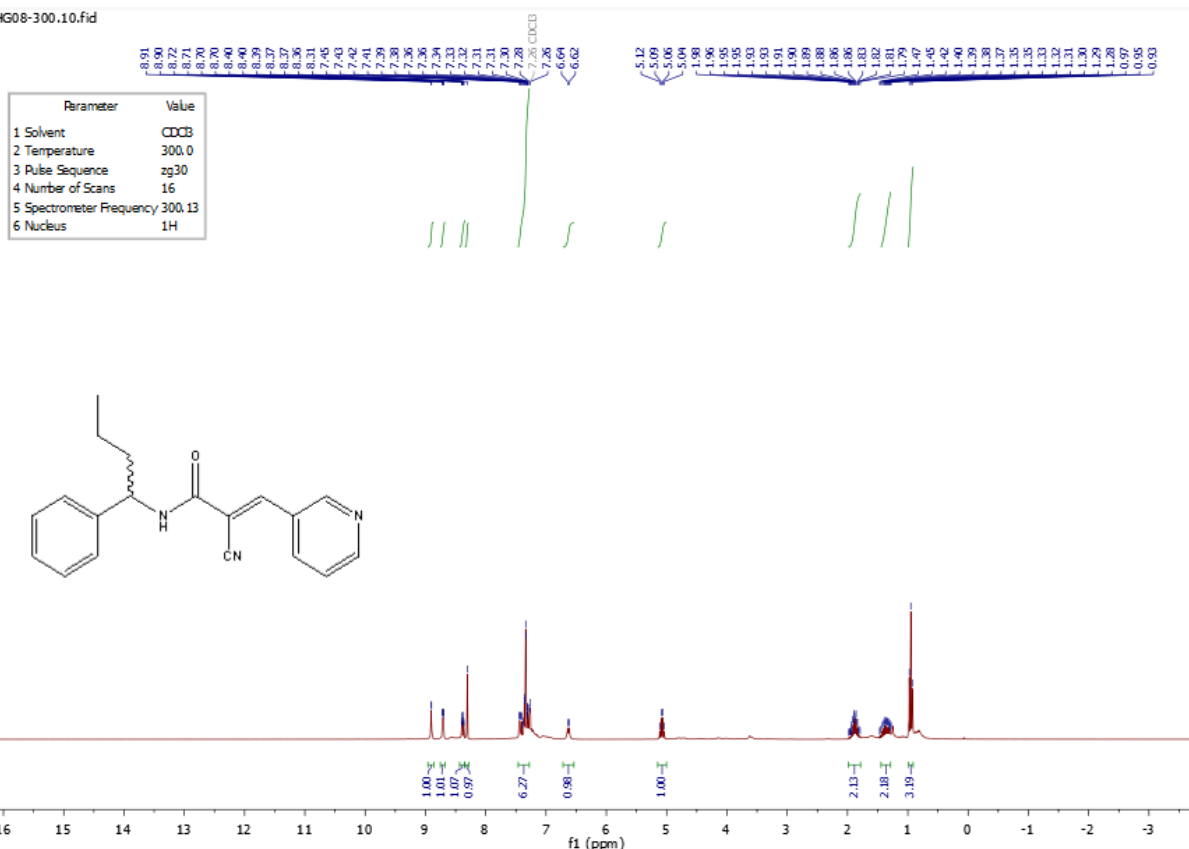
VI. NMR spectra

(*R,E*)-3-(6-bromopyridin-2-yl)-2-cyano-*N*-(1-phenylbutyl)acrylamide ((*R*)-DGS)

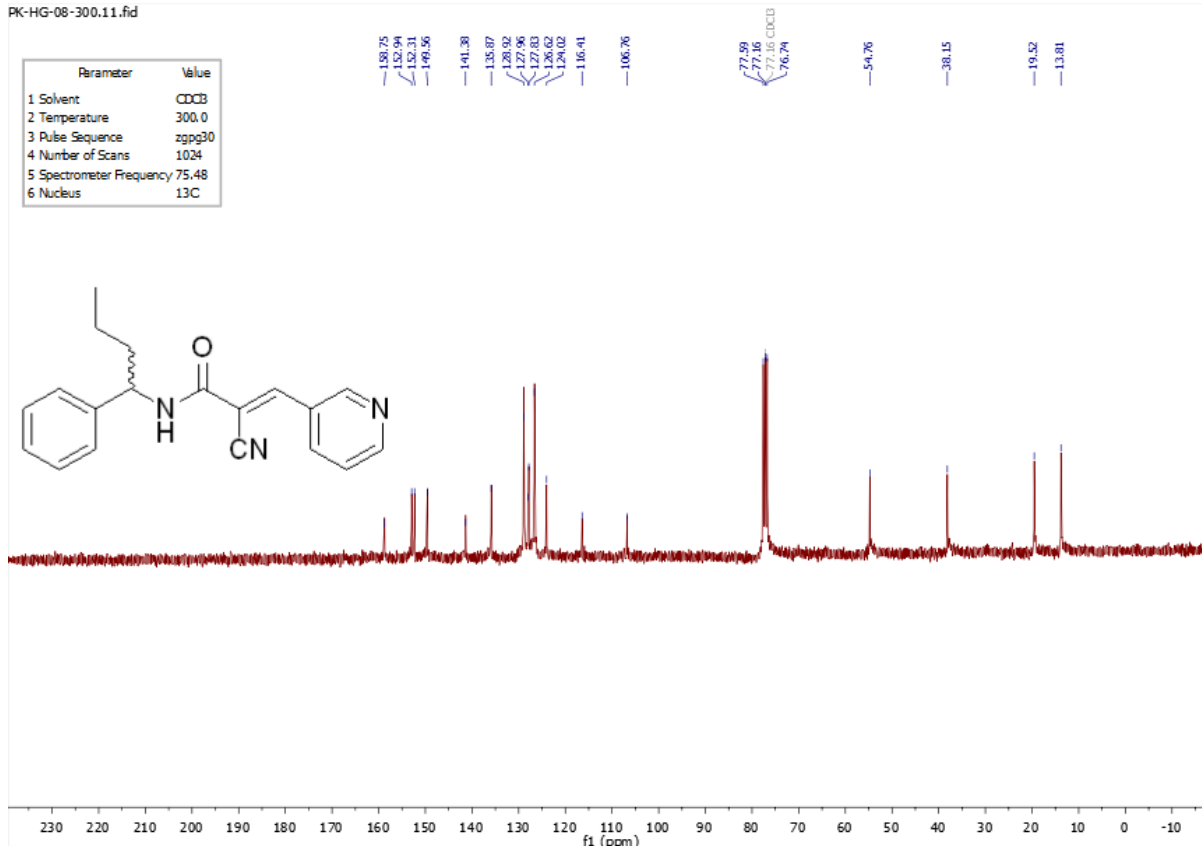


(E)-2-cyano-N-(1-phenylbutyl)-3-(pyridin-3-yl)acrylamide (LK01)

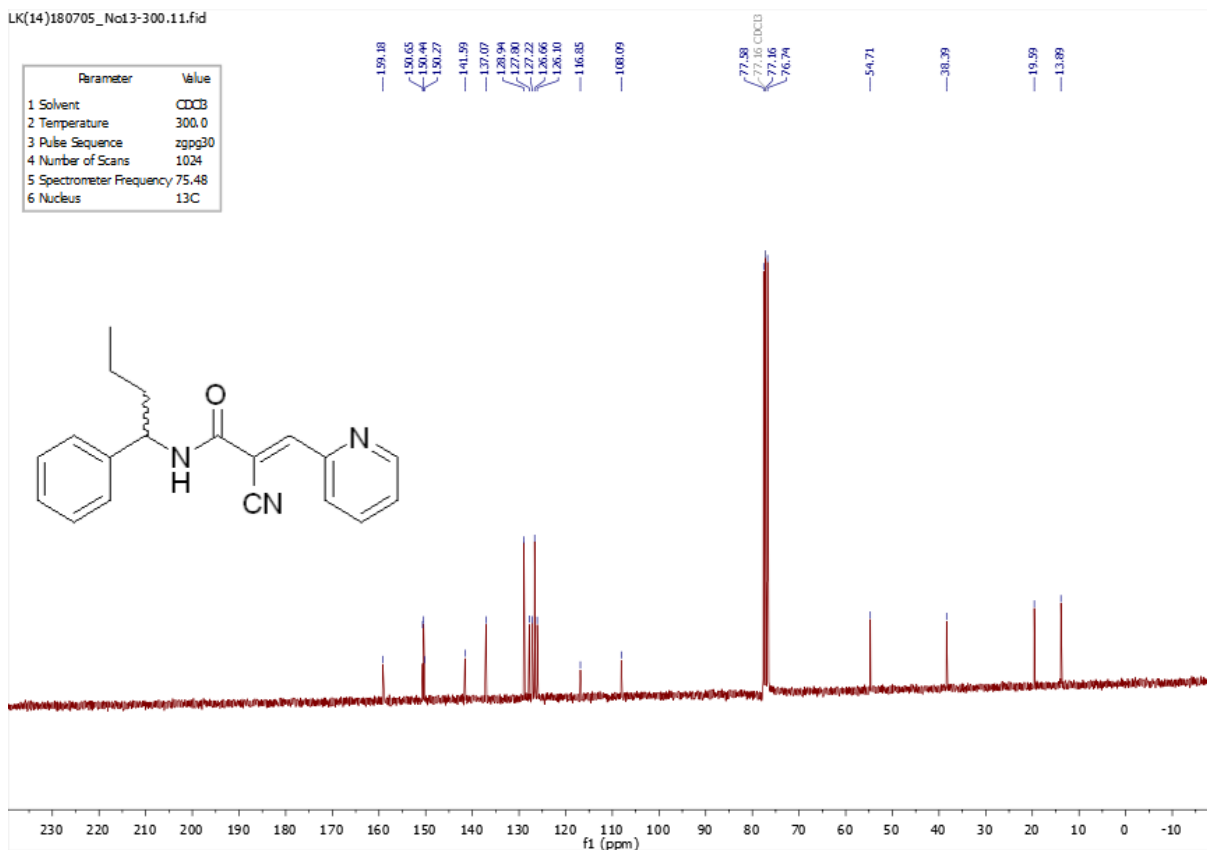
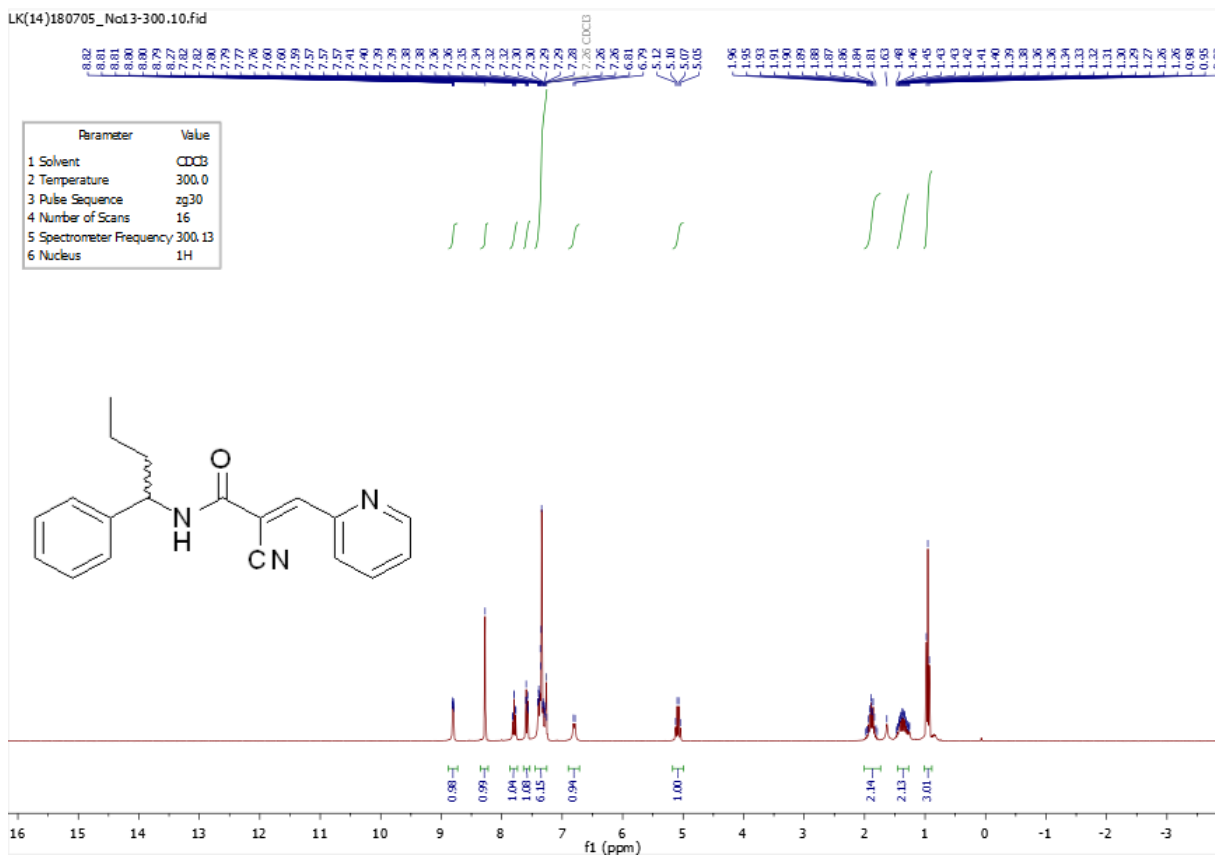
HG08-300.10.fid



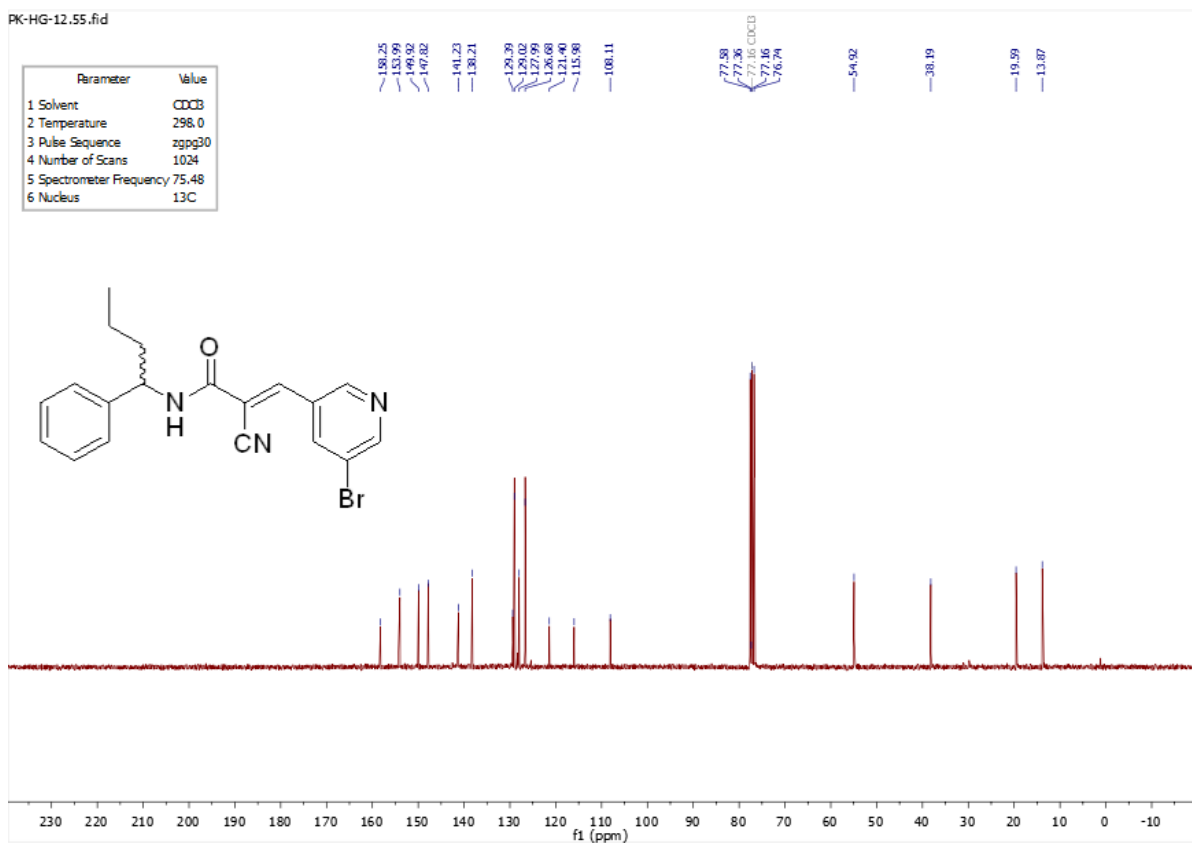
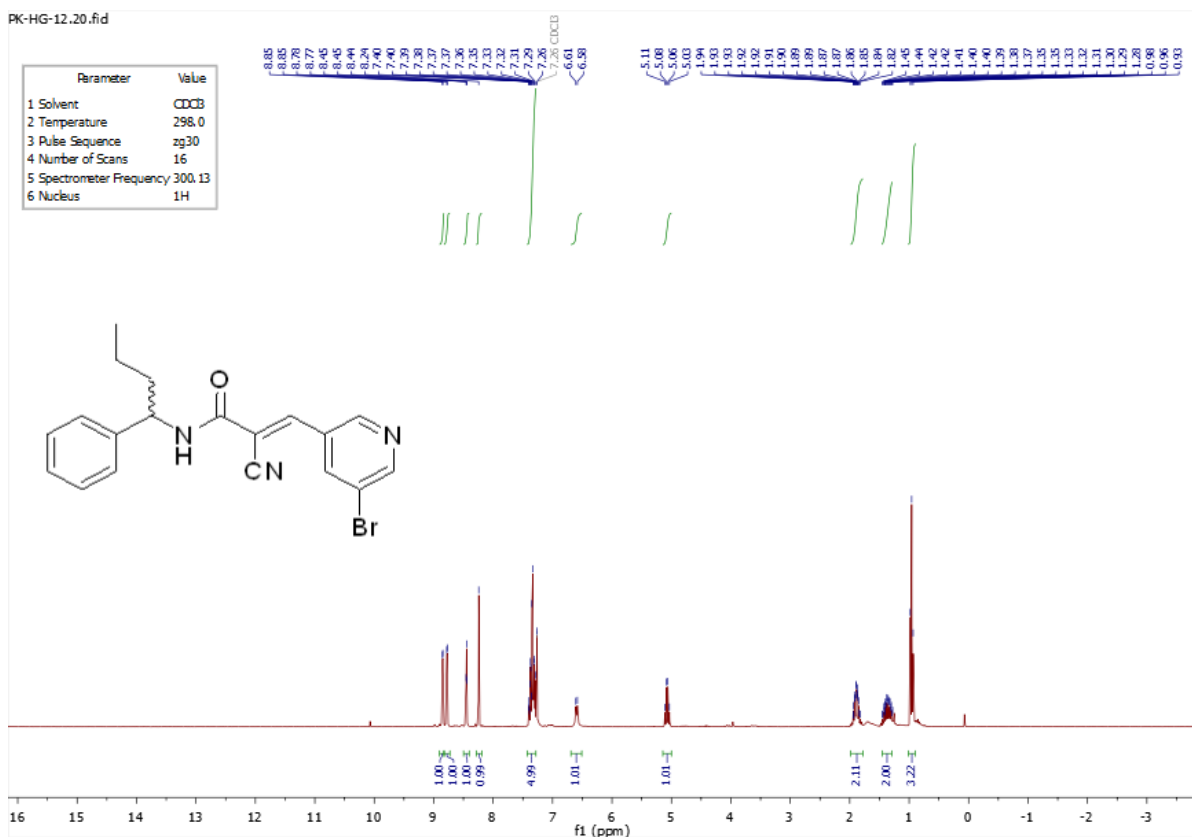
PK-HG-08-300.11.fid



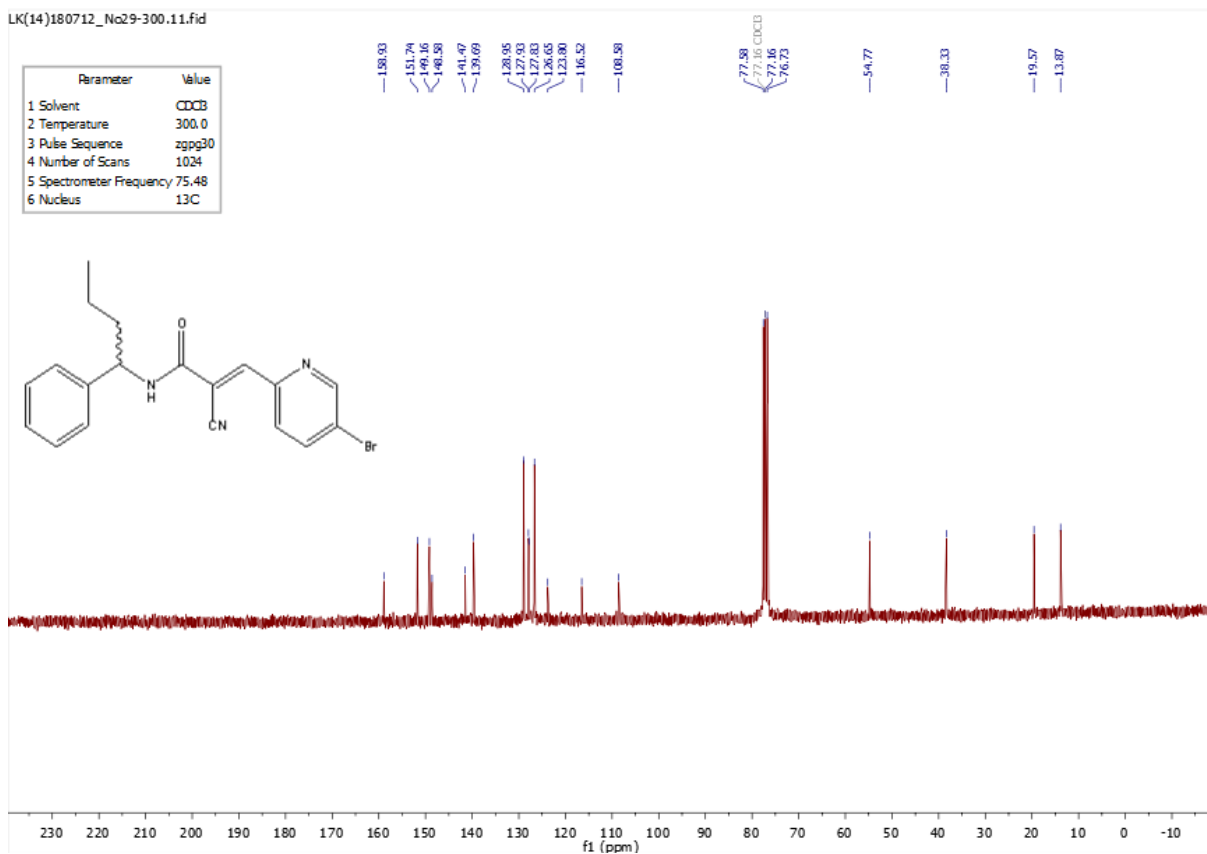
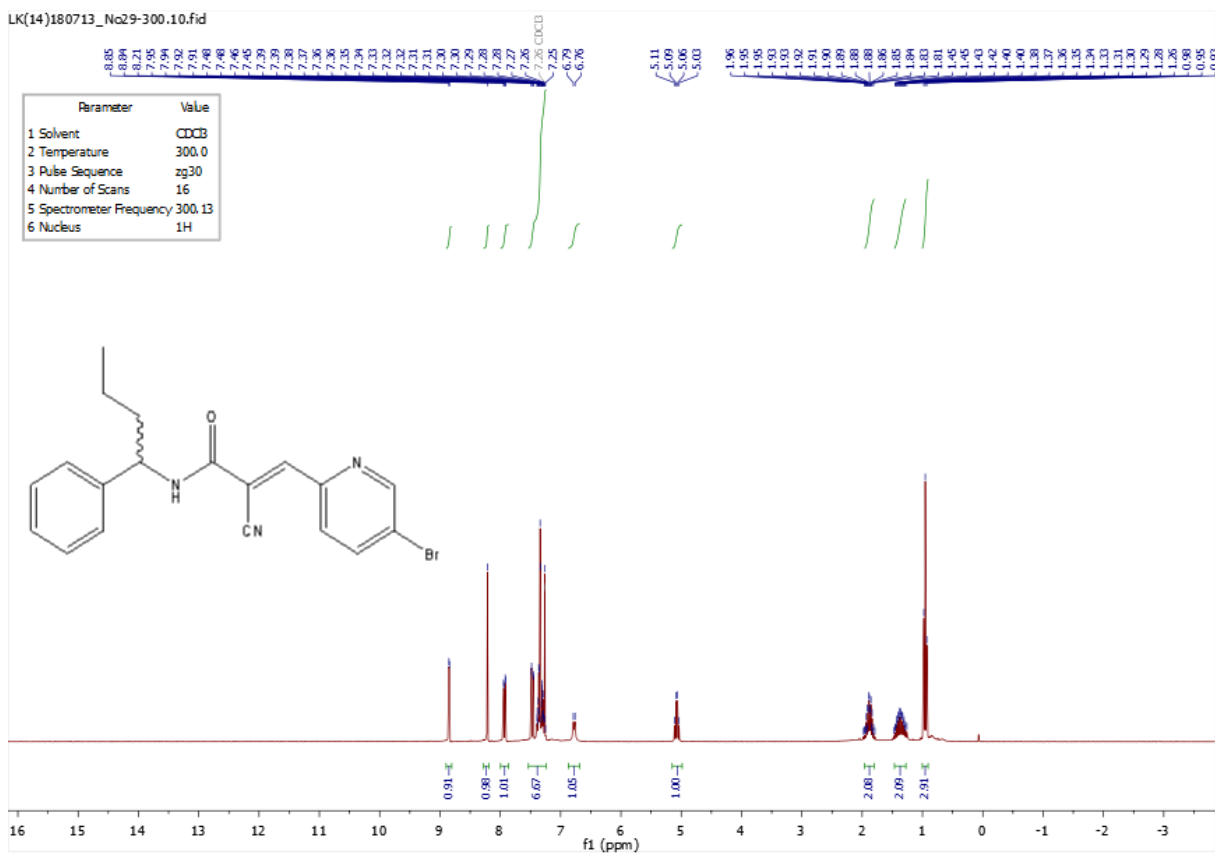
(E)-2-cyano-N-(1-phenylbutyl)-3-(pyridin-2-yl)acrylamide (LK02)



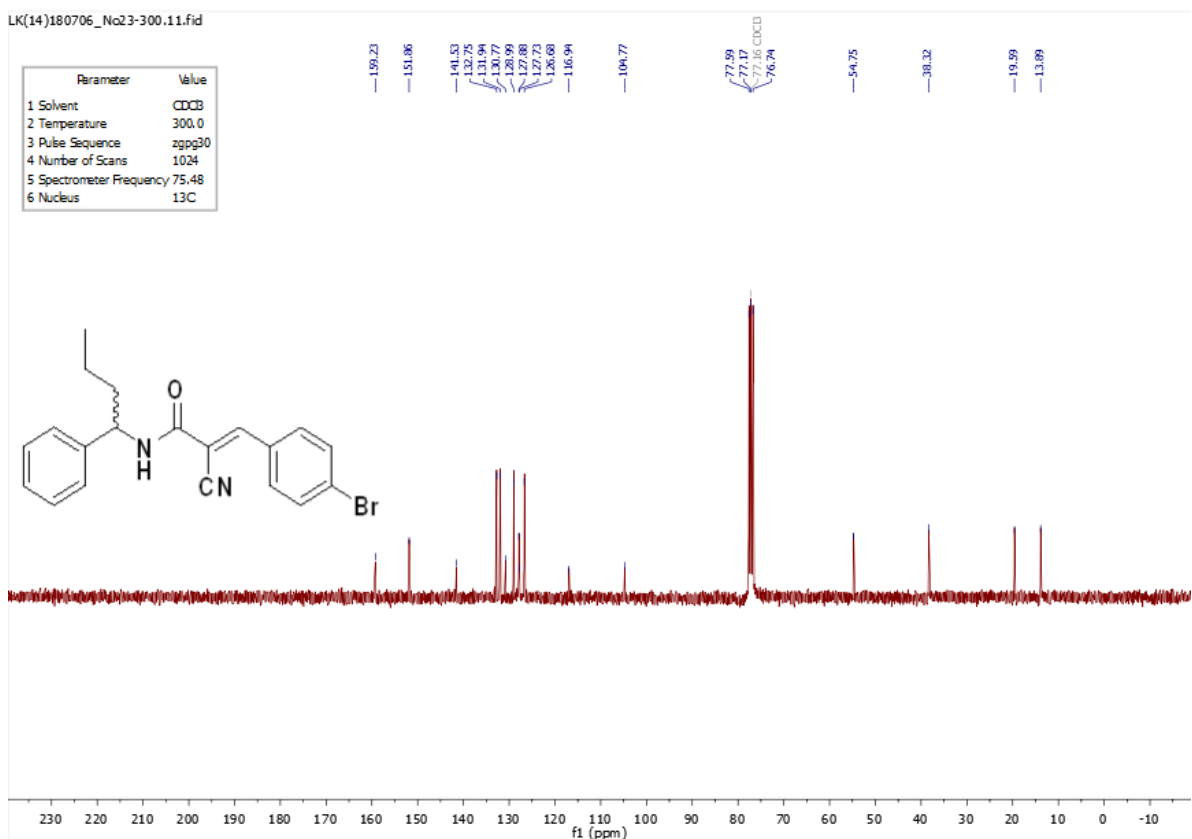
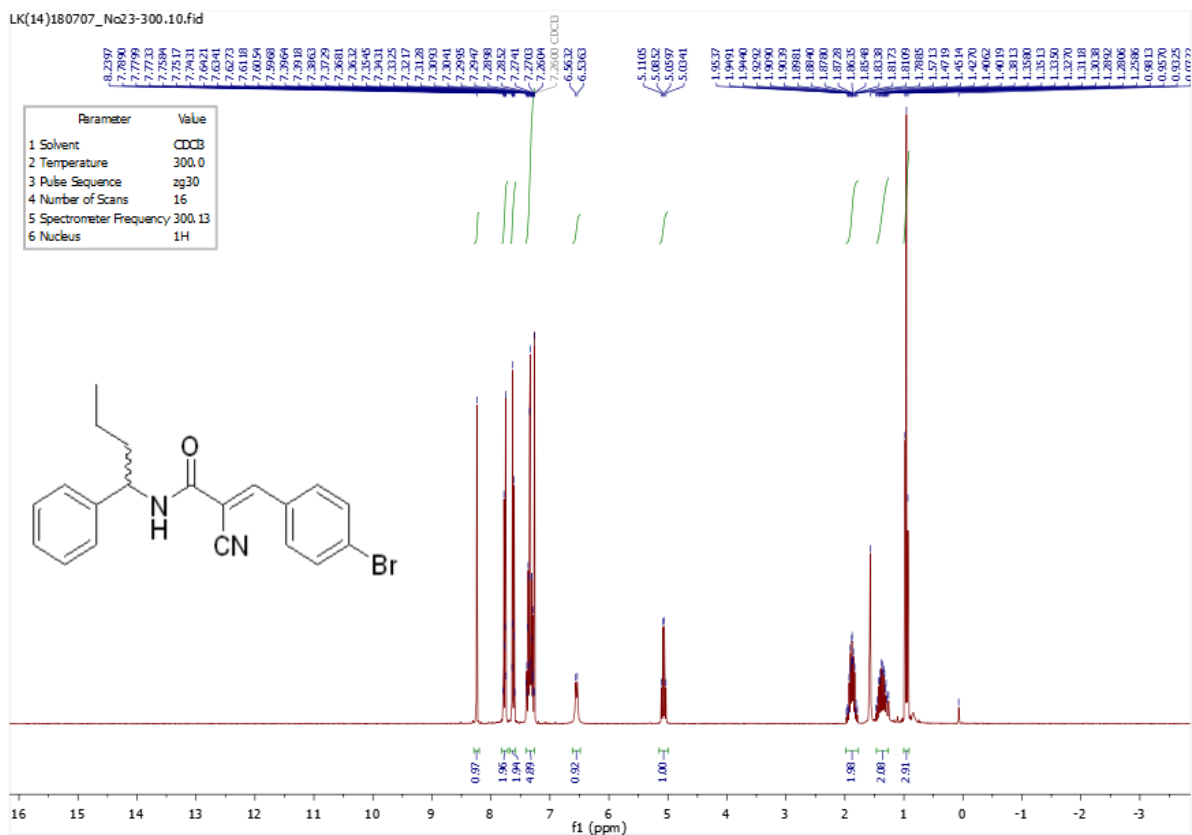
(E)-3-(5-bromopyridin-3-yl)-2-cyano-N-(1-phenylbutyl)acrylamide (LK03)



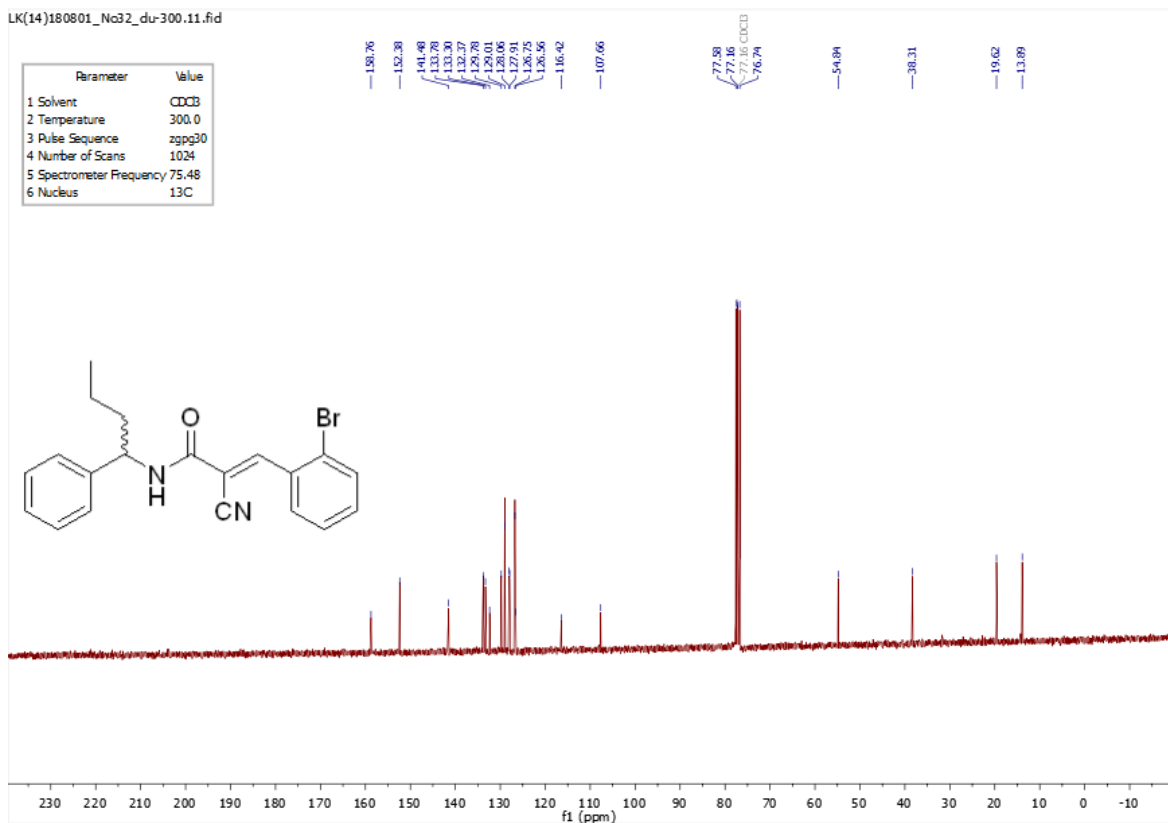
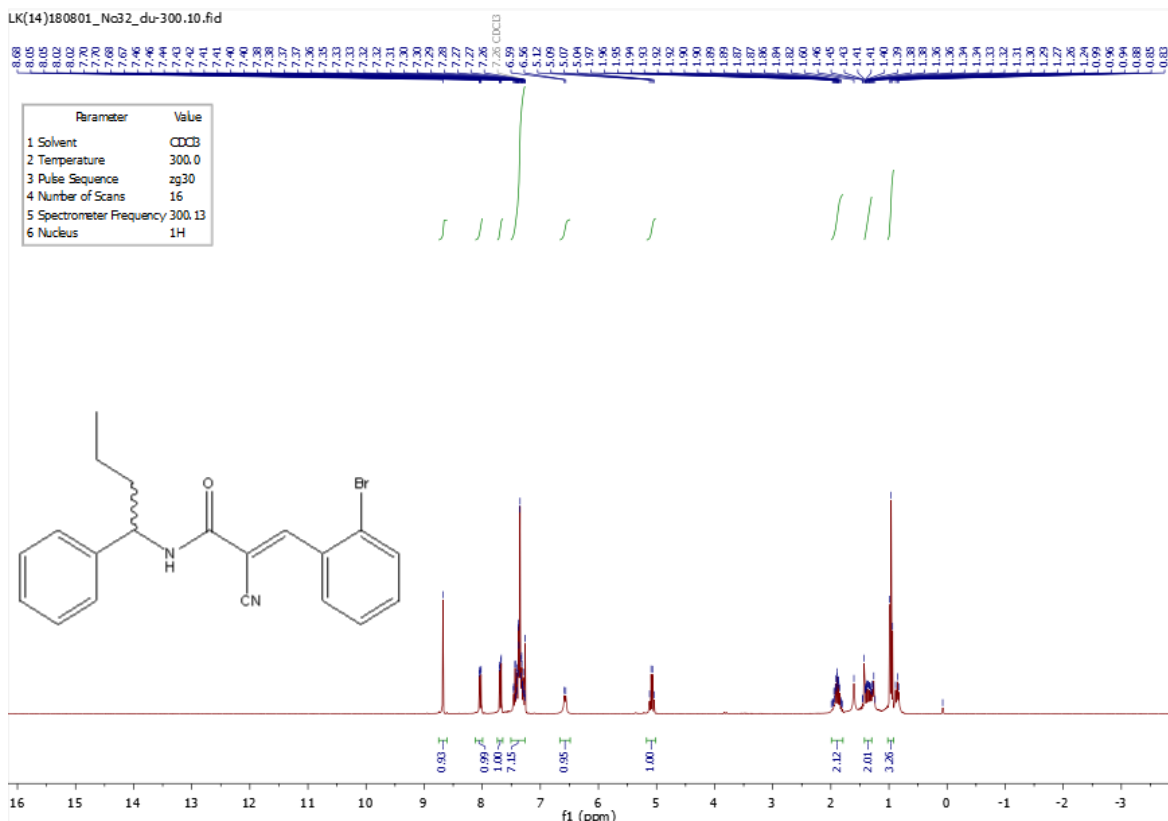
(E)-3-(5-bromopyridin-2-yl)-2-cyano-N-(1-phenylbutyl)acrylamide (LK04)



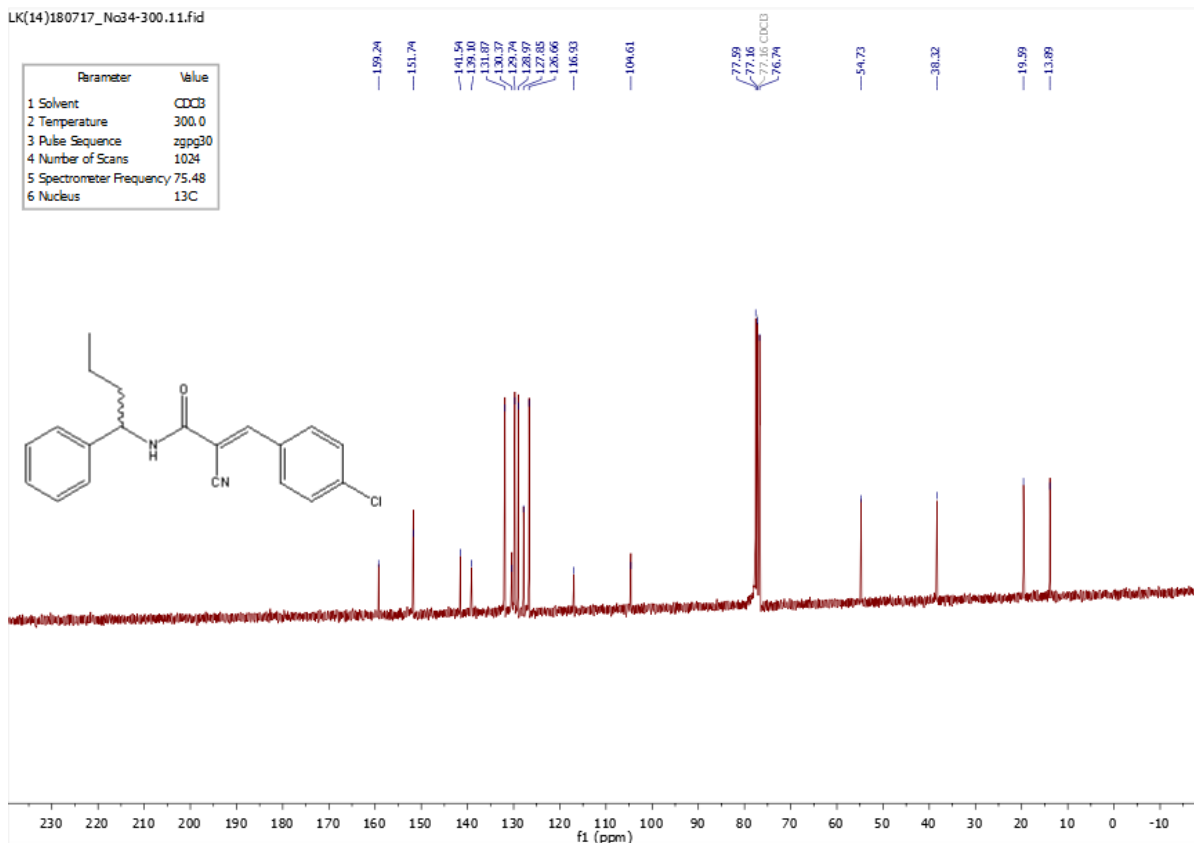
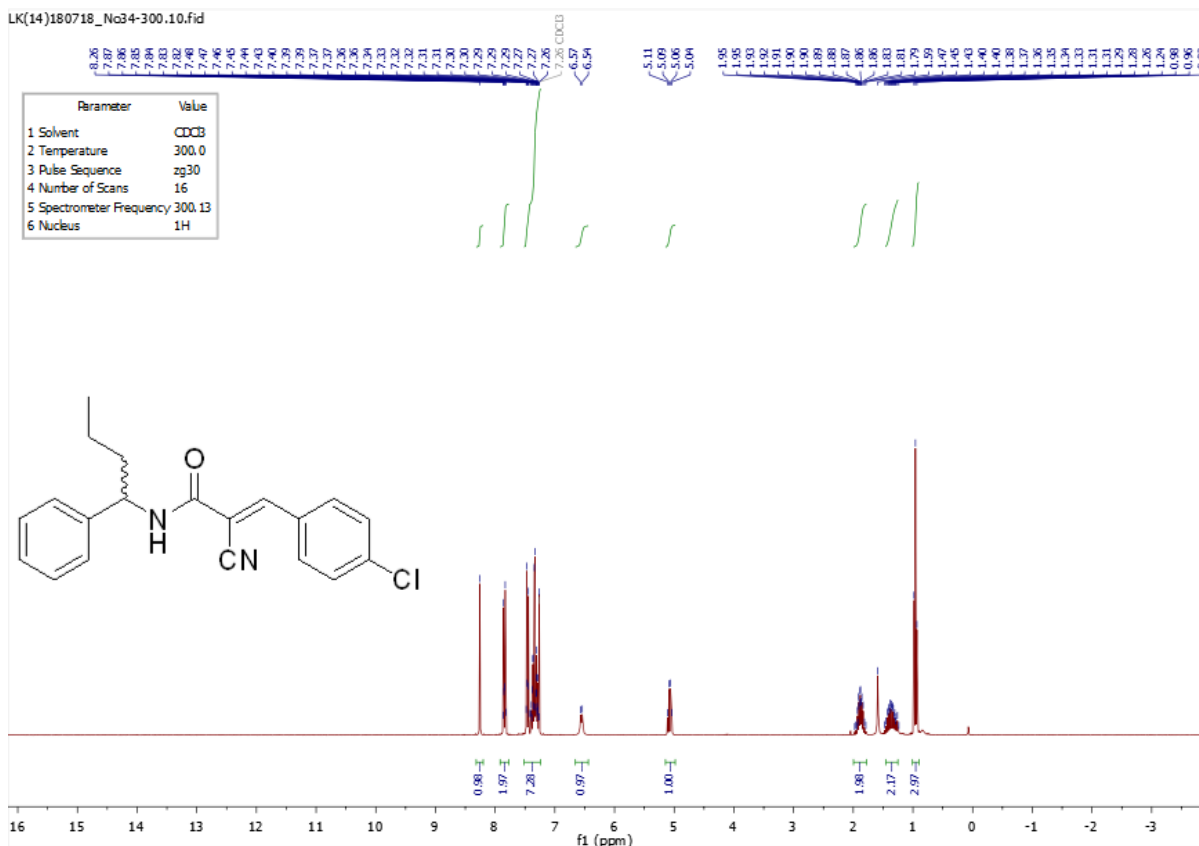
(E)-3-(4-bromophenyl)-2-cyano-N-(1-phenylbutyl)acrylamide (LK05)



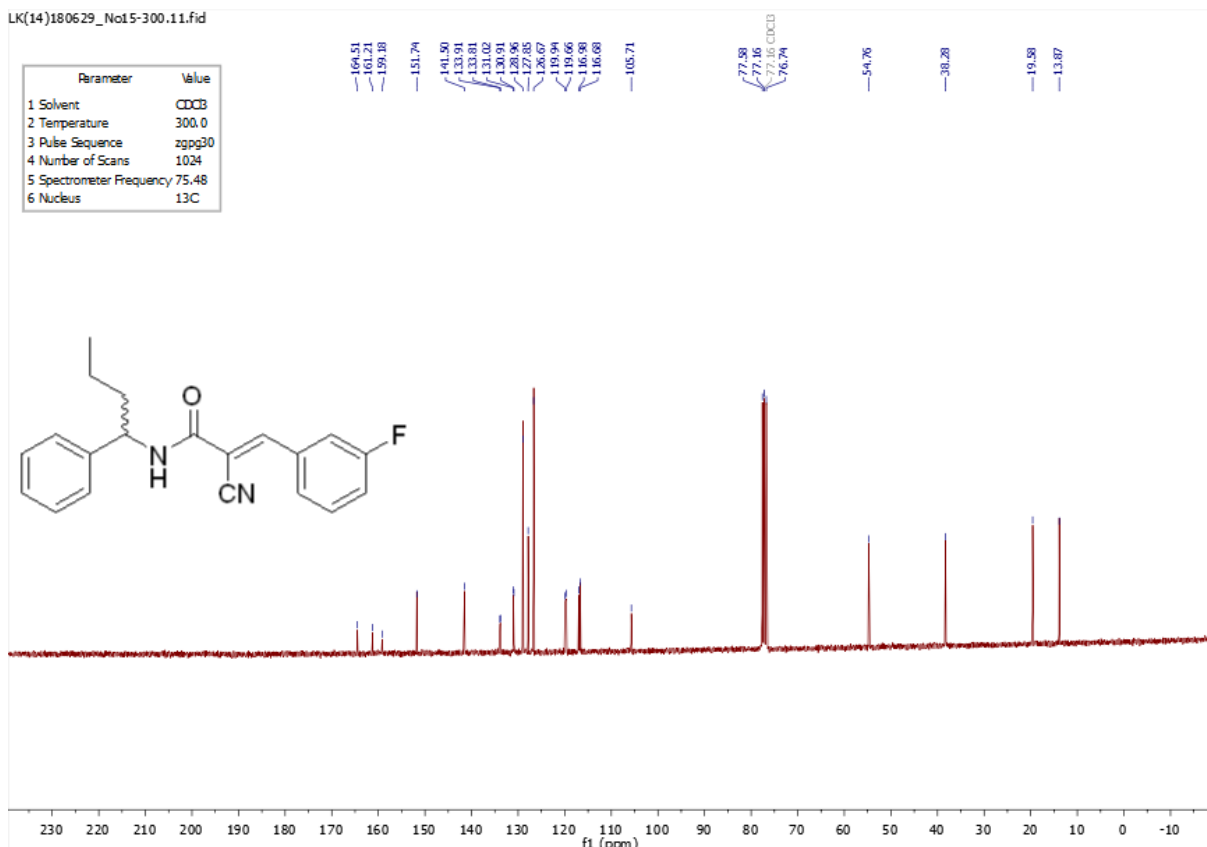
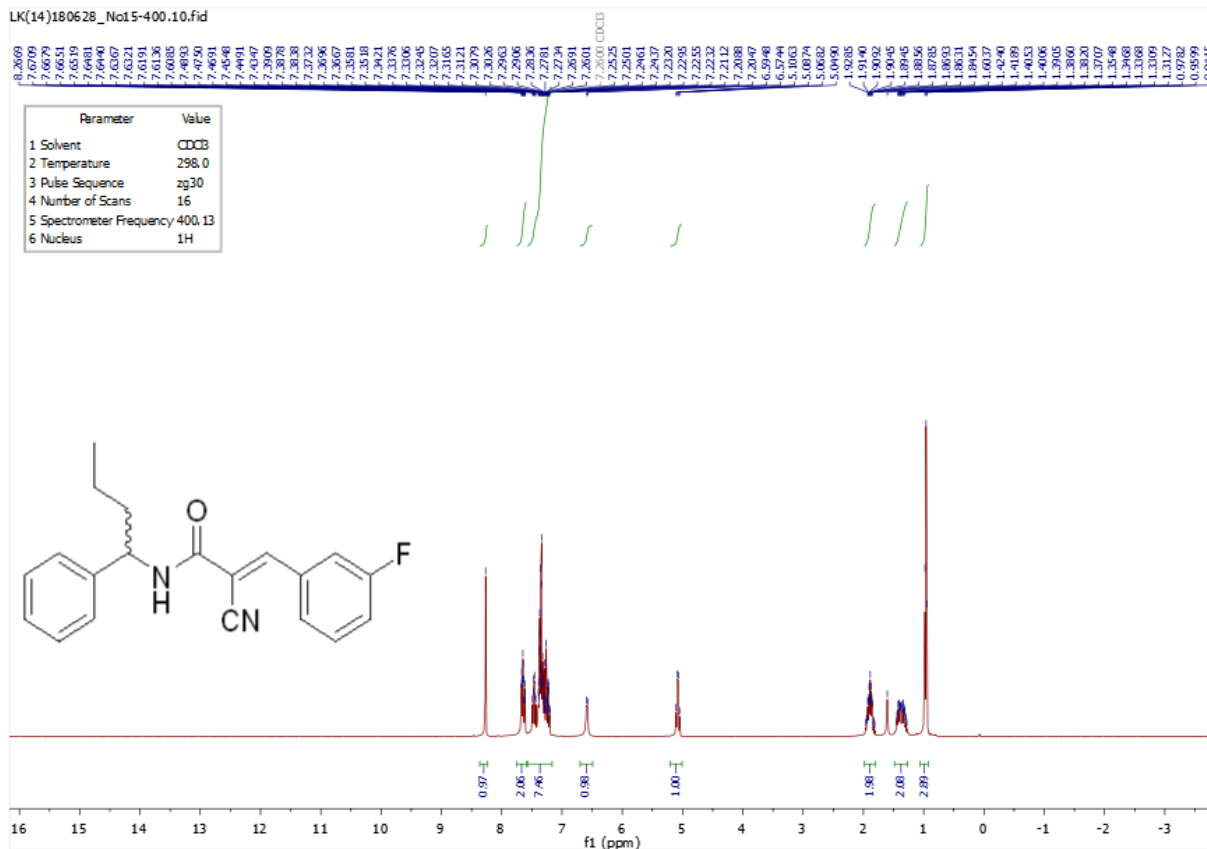
(E)-3-(2-bromophenyl)-2-cyano-N-(1-phenylbutyl)acrylamide (LK06)



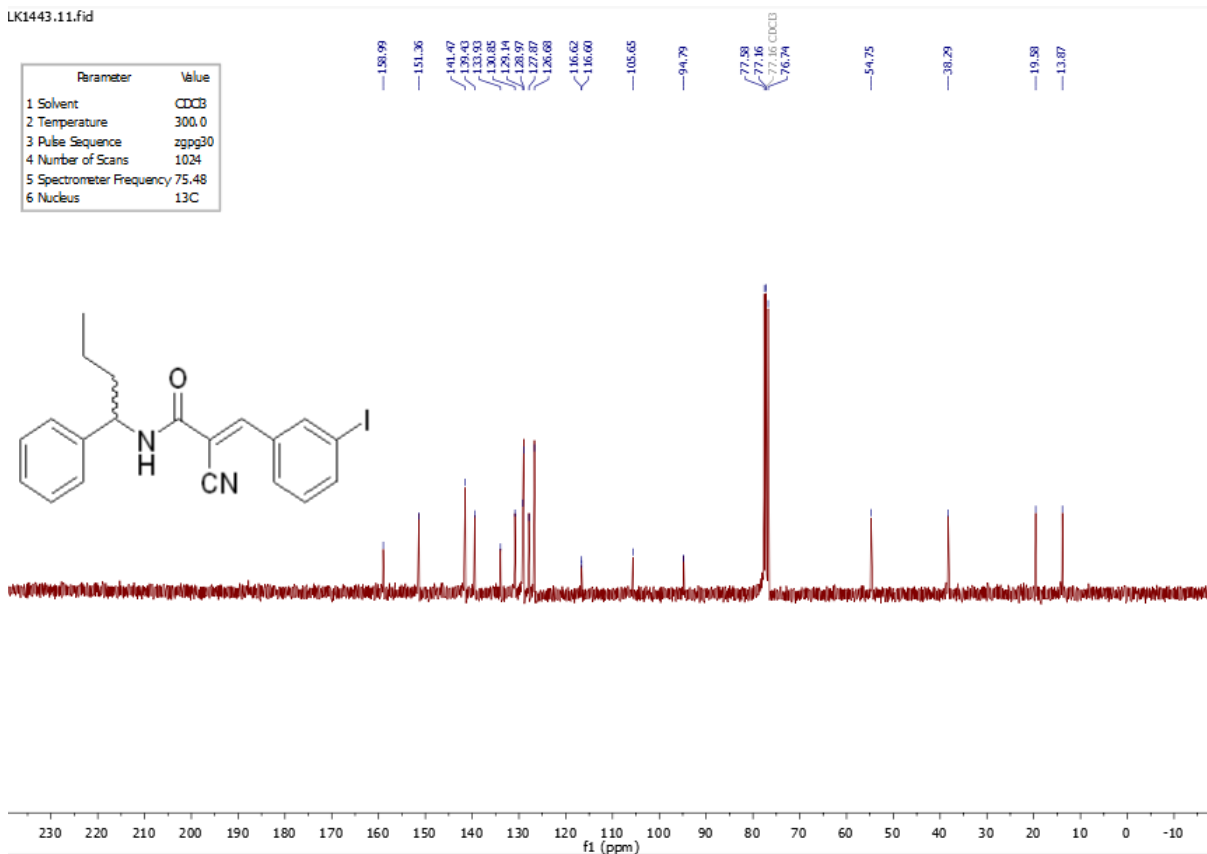
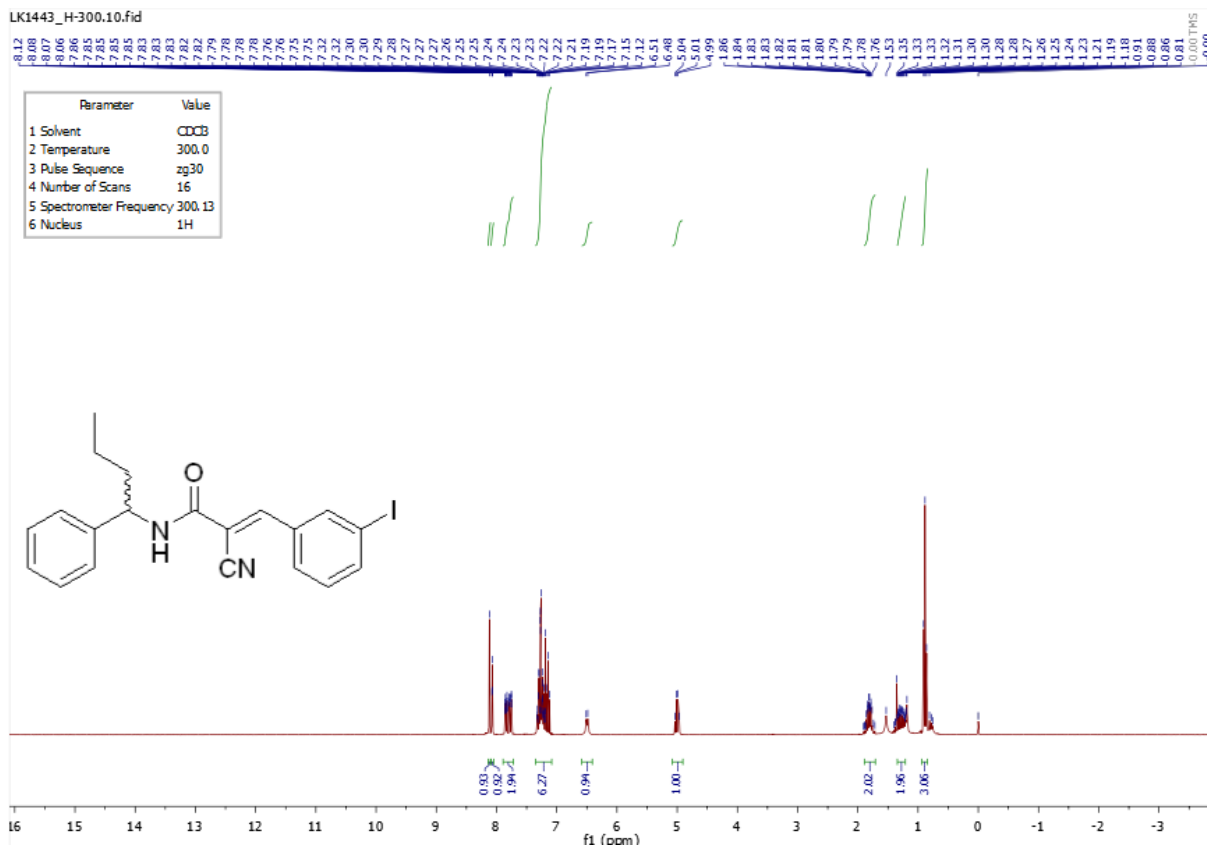
(E)-3-(4-chlorophenyl)-2-cyano-N-(1-phenylbutyl)acrylamide (LK07)



(E)-2-cyano-3-(3-fluorophenyl)-N-(1-phenylbutyl)acrylamide (LK08)



(E)-2-cyano-3-(3-iodophenyl)-N-(1-phenylbutyl)acrylamide (LK09)

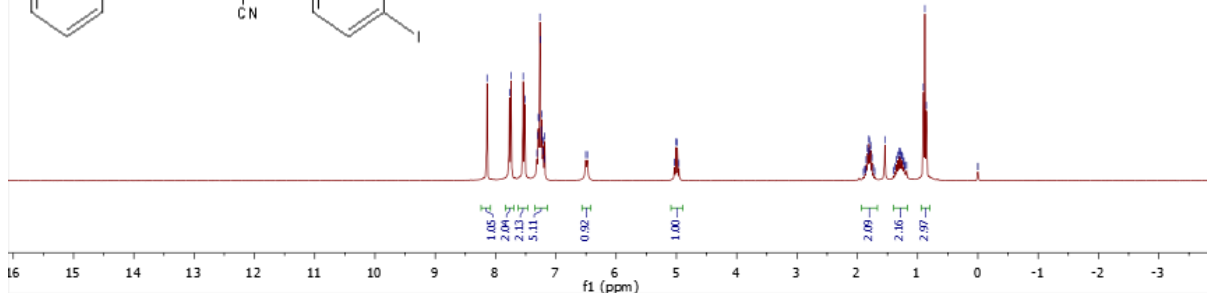
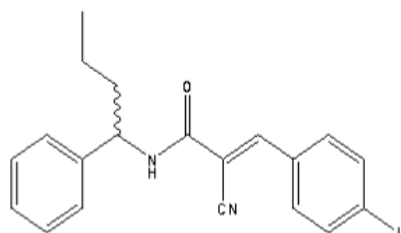


(E)-2-cyano-3-(4-iodophenyl)-N-(1-phenylbutyl)acrylamide (LK10)

LK(14)180806_No46-300.10.fid

Parameter	Value
1 Solvent	CDCl ₃
2 Temperature	300.0
3 Pulse Sequence	zg30
4 Number of Scans	16
5 Spectrometer Frequency	300.13
6 Nucleus	¹ H

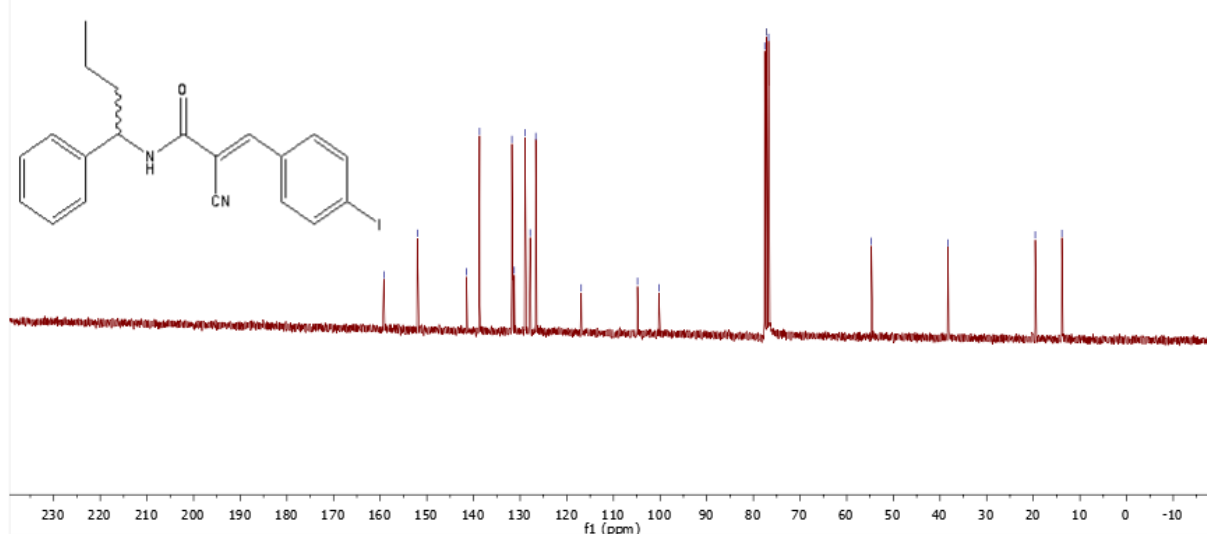
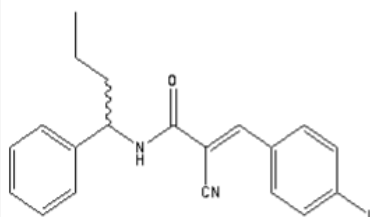
8.14, 7.74, 7.54, 7.51, 7.31, 7.29, 7.28, 7.28, 7.26, 7.24, 7.23, 7.23, 7.22, 7.21, 7.19, 7.18, 6.98, 5.03, 5.01, 4.98, 4.96, 1.90, 1.89, 1.87, 1.85, 1.83, 1.82, 1.81, 1.80, 1.79, 1.78, 1.76, 1.73, 1.71, 1.54, 1.40, 1.37, 1.35, 1.32, 1.30, 1.30, 1.28, 1.27, 1.25, 1.25, 1.24, 1.24, 1.21, 1.20, 1.18, 1.08, 1.06, 0.00, 0.00, 0.00, 0.00



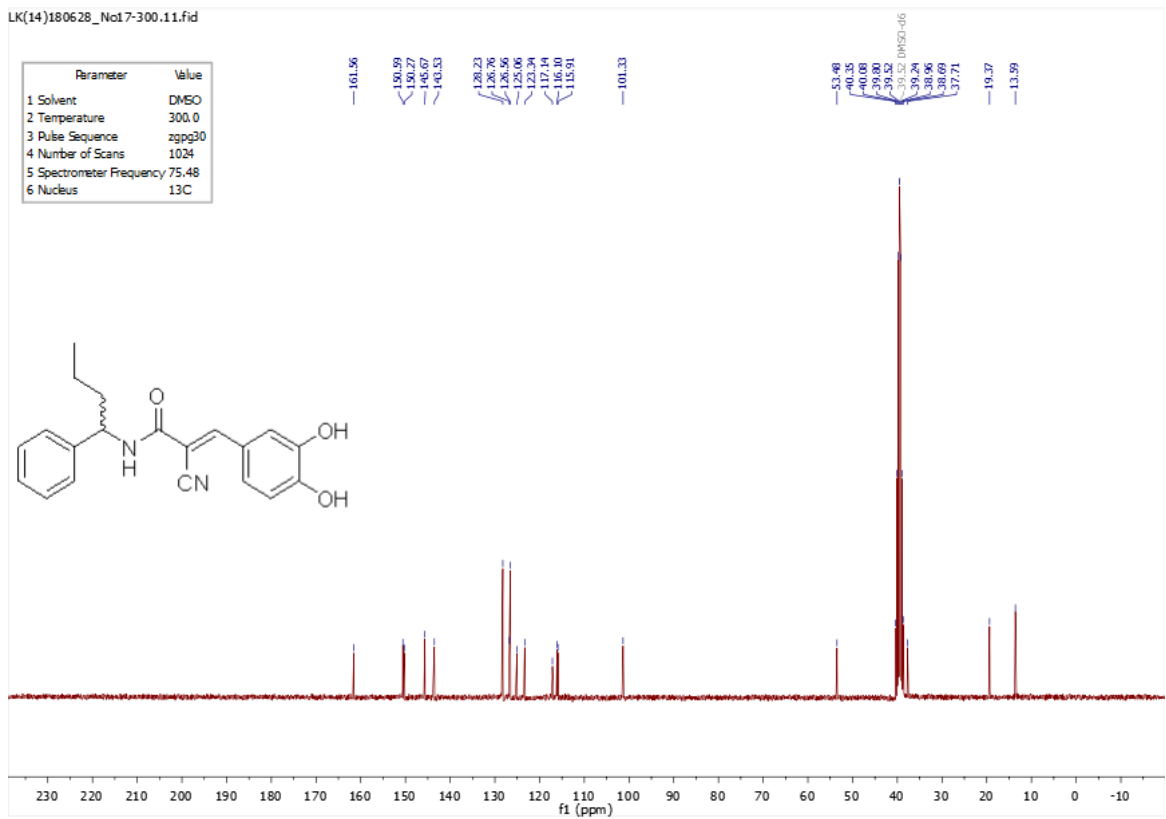
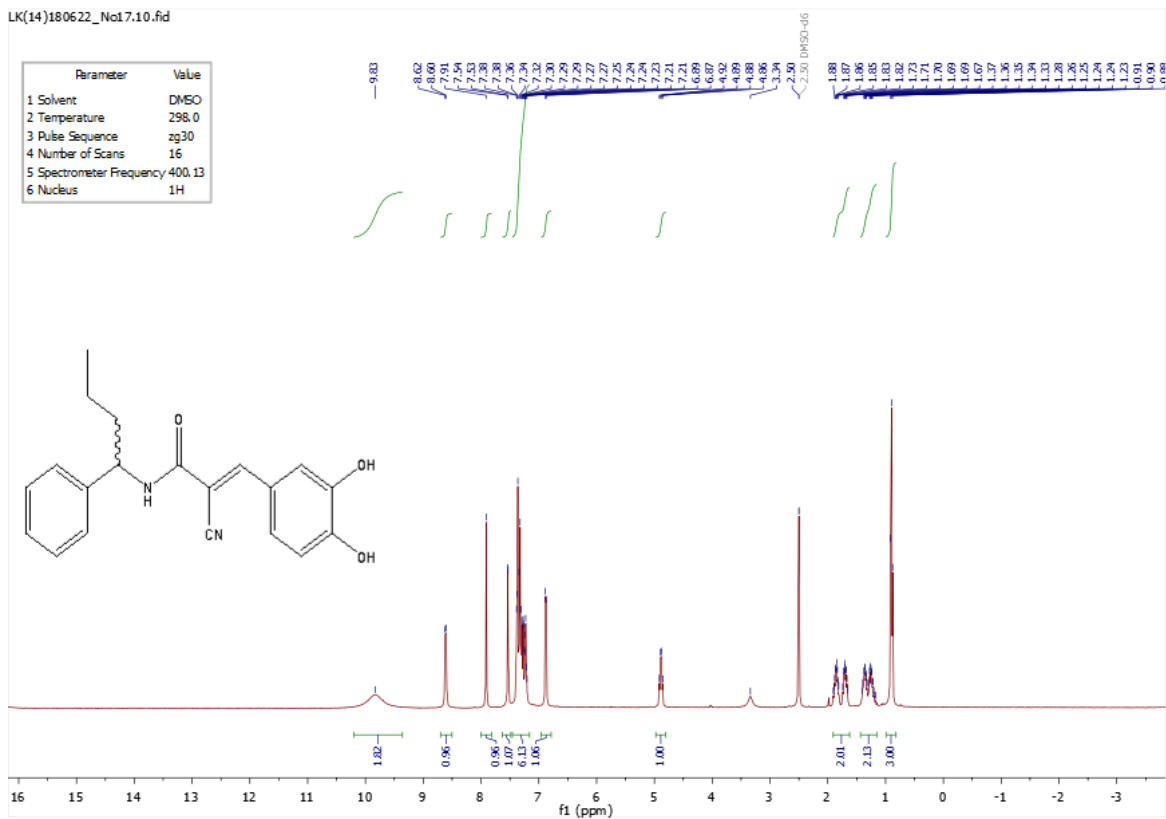
LK(14)180806_No46-300.11.fid

Parameter	Value
1 Solvent	CDCl ₃
2 Temperature	300.0
3 Pulse Sequence	zgpg30
4 Number of Scans	1024
5 Spectrometer Frequency	75.48
6 Nucleus	¹³ C

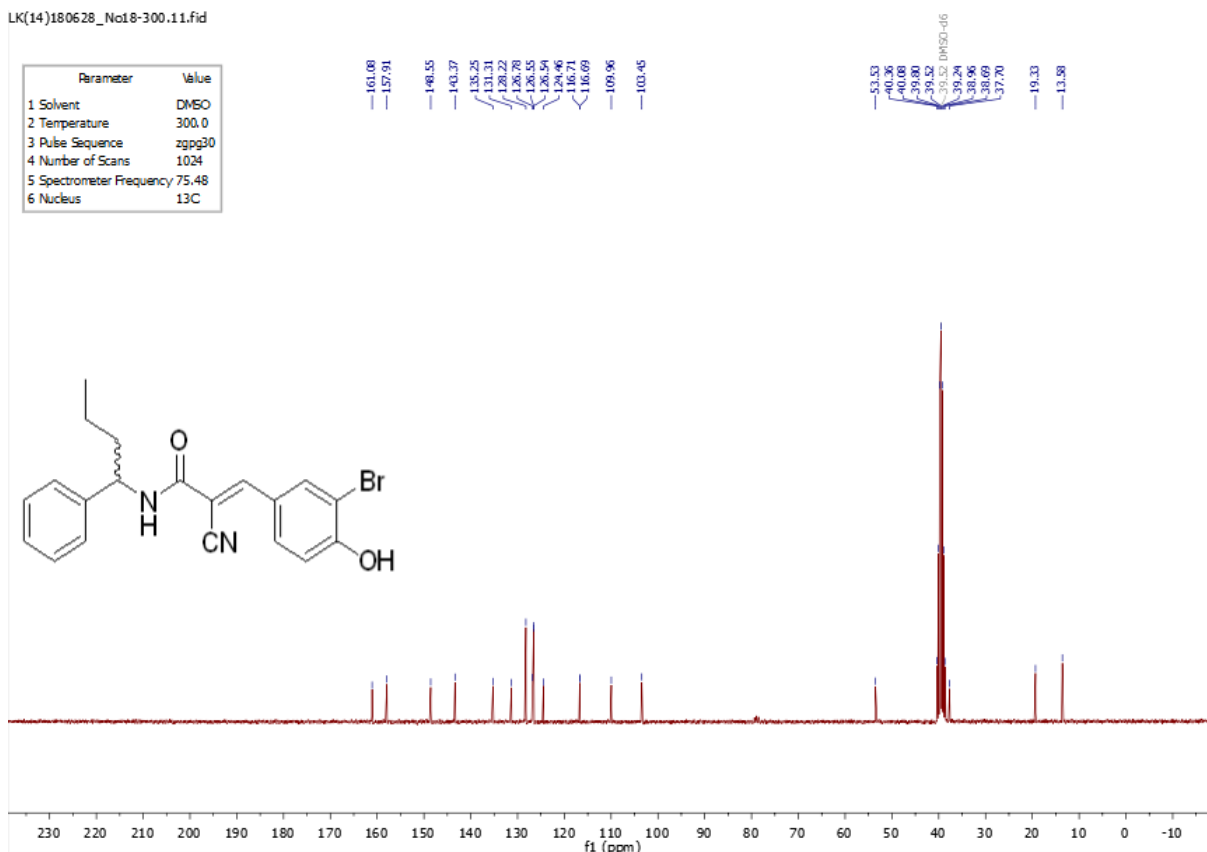
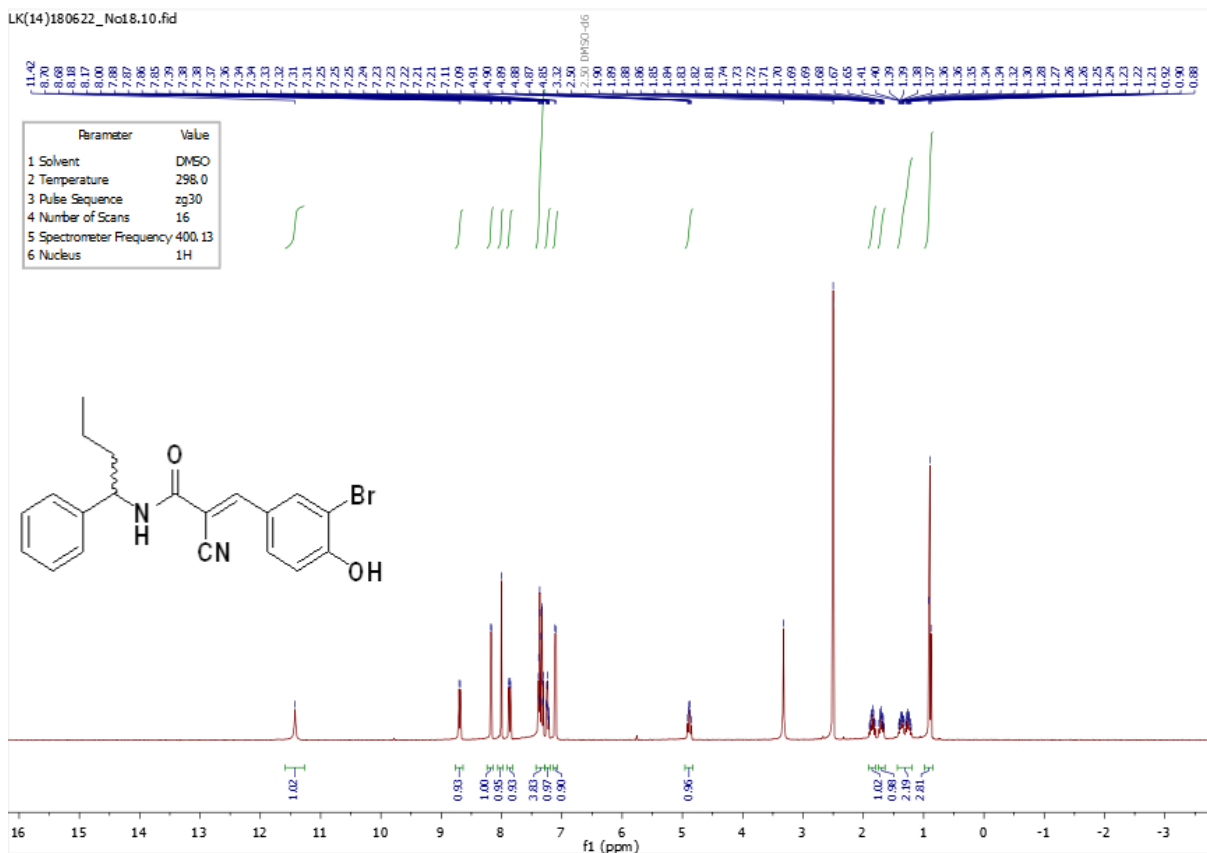
159.21, 152.04, 141.51, 138.71, 131.77, 131.26, 128.96, 127.85, 126.66, 116.91, 104.84, 100.28, 77.58, 77.16, 77.06, 76.74, 54.73, 38.30, 19.98, 13.88



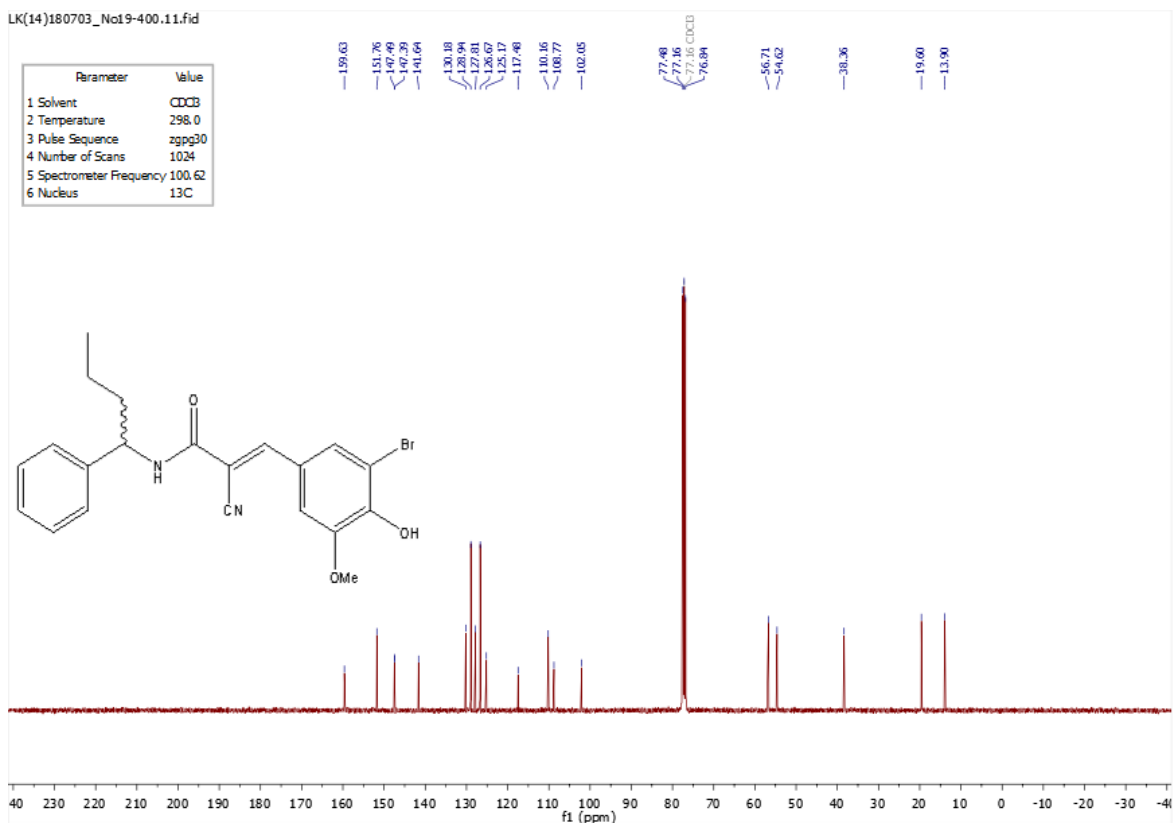
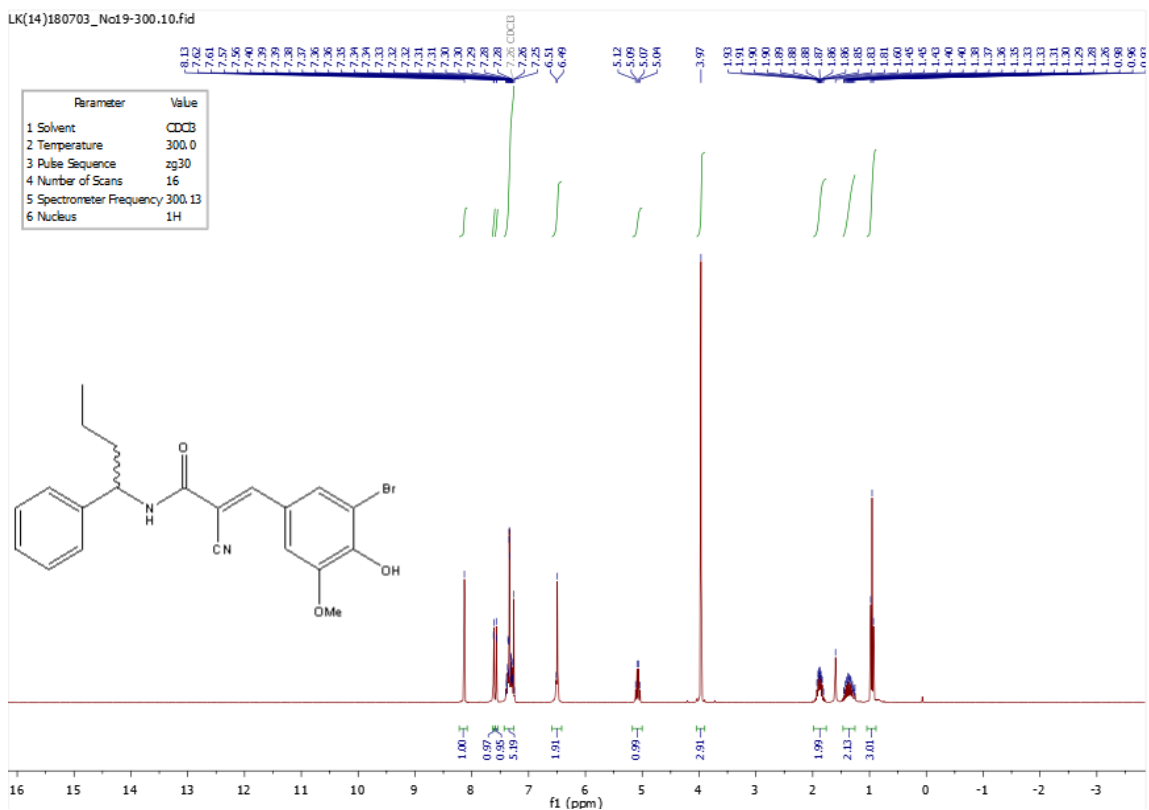
(E)-2-cyano-3-(3,4-dihydroxyphenyl)-N-(1-phenylbutyl)acrylamide (LK11)



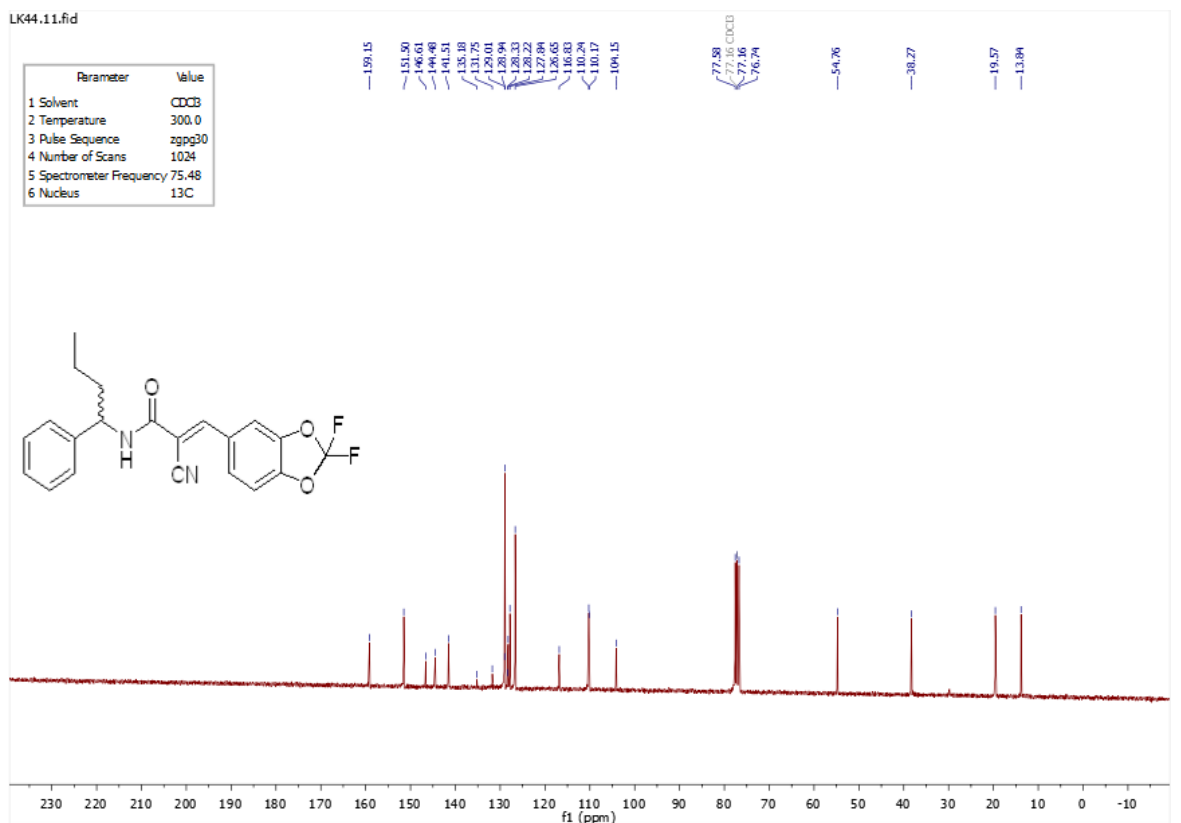
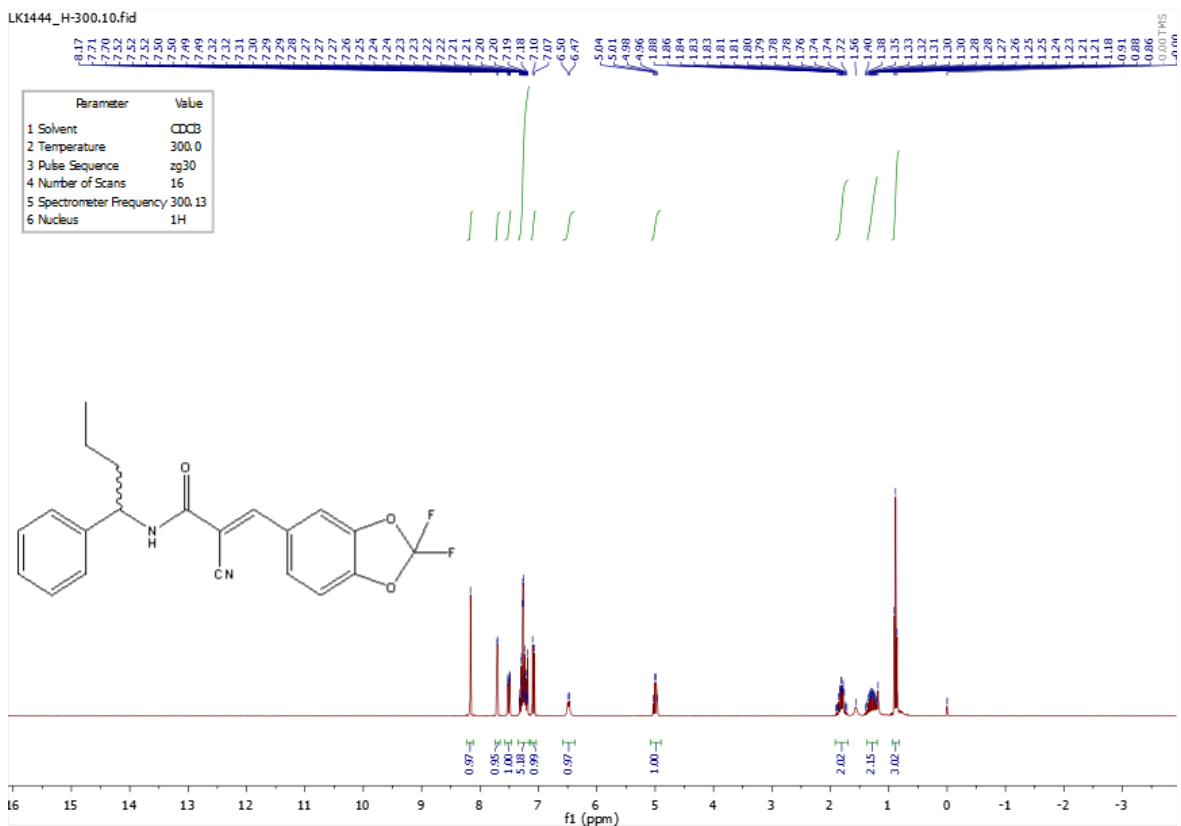
(E)-3-(3-bromo-4-hydroxyphenyl)-2-cyano-N-(1-phenylbutyl)acrylamide (LK12)



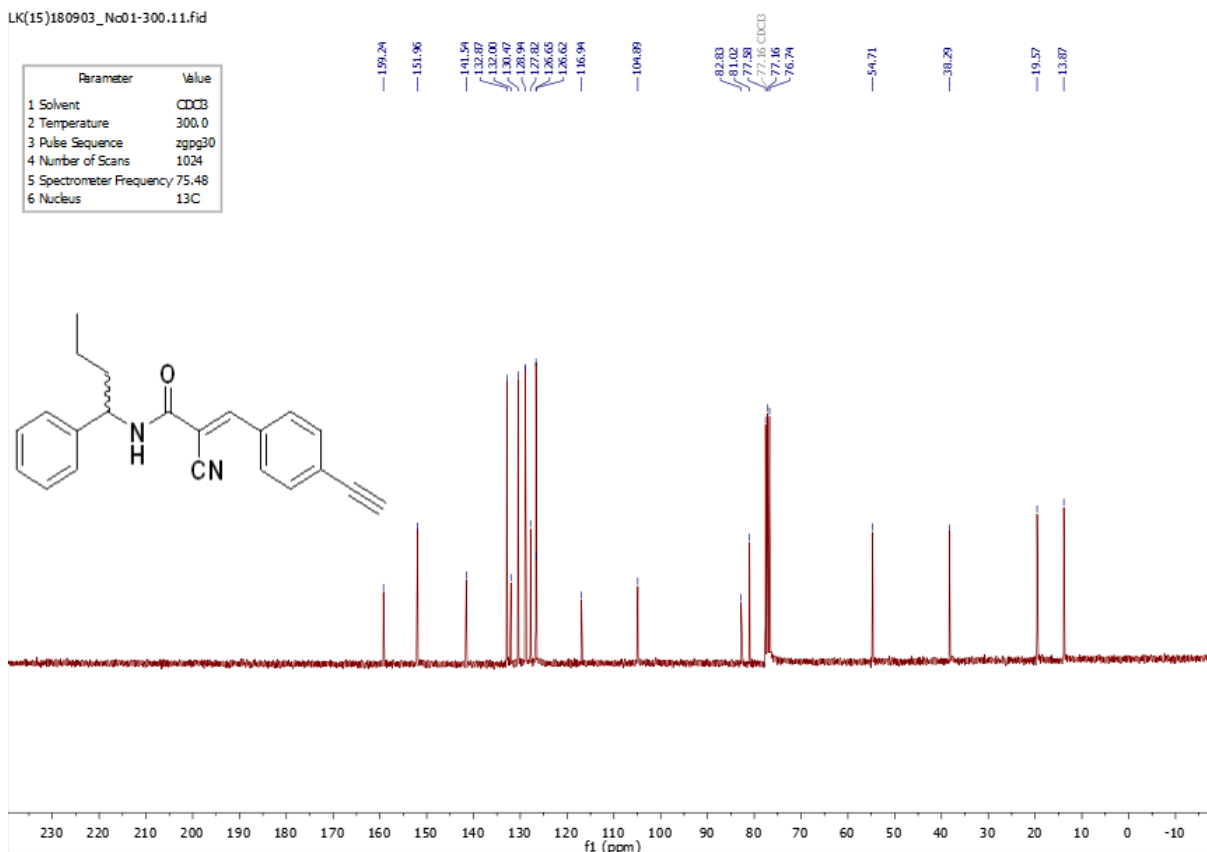
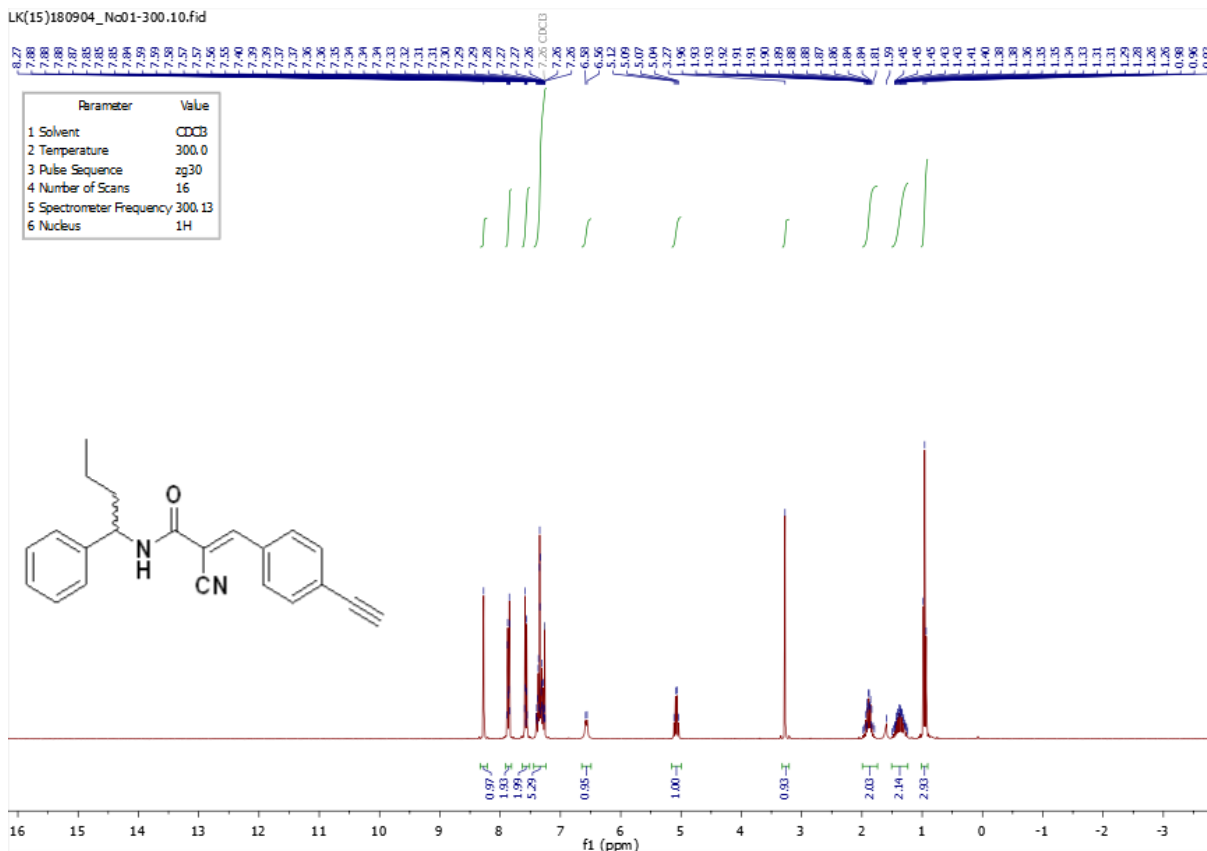
(E)-3-(3-bromo-4-hydroxy-5-methoxyphenyl)-2-cyano-N-(1-phenylbutyl)acrylamide (LK13)



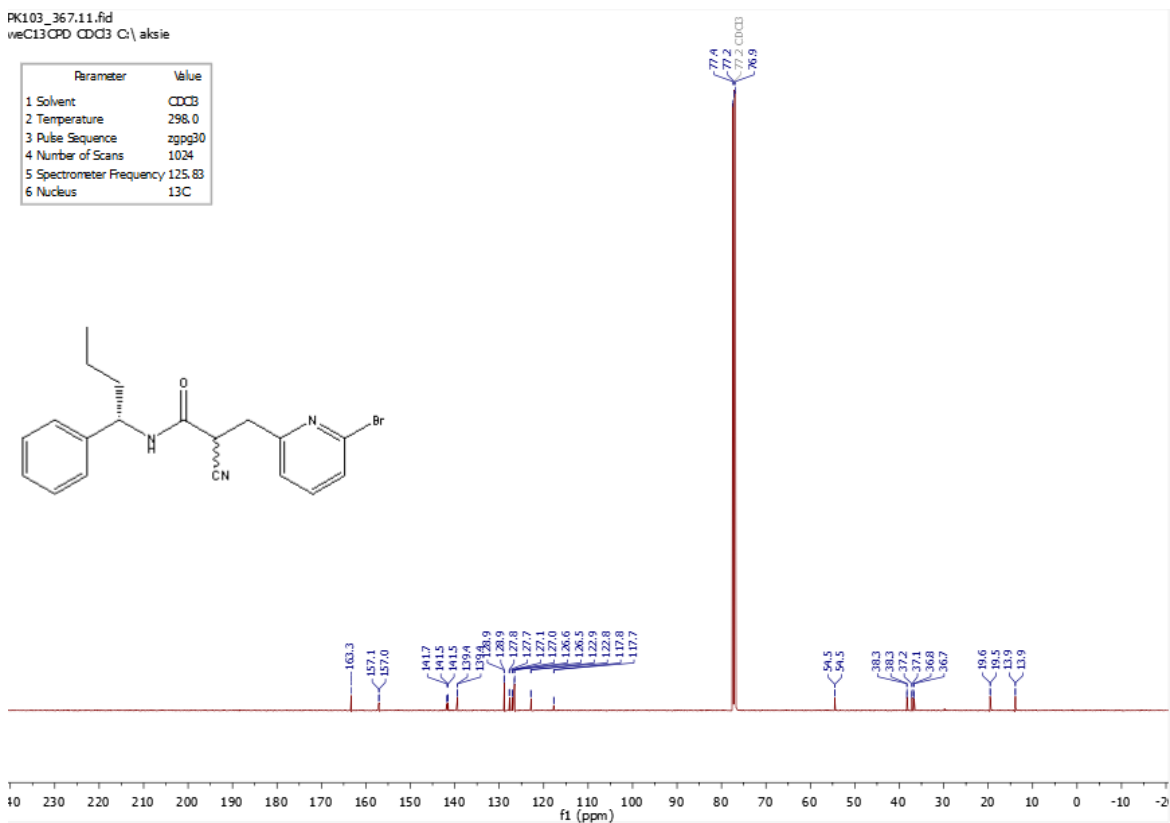
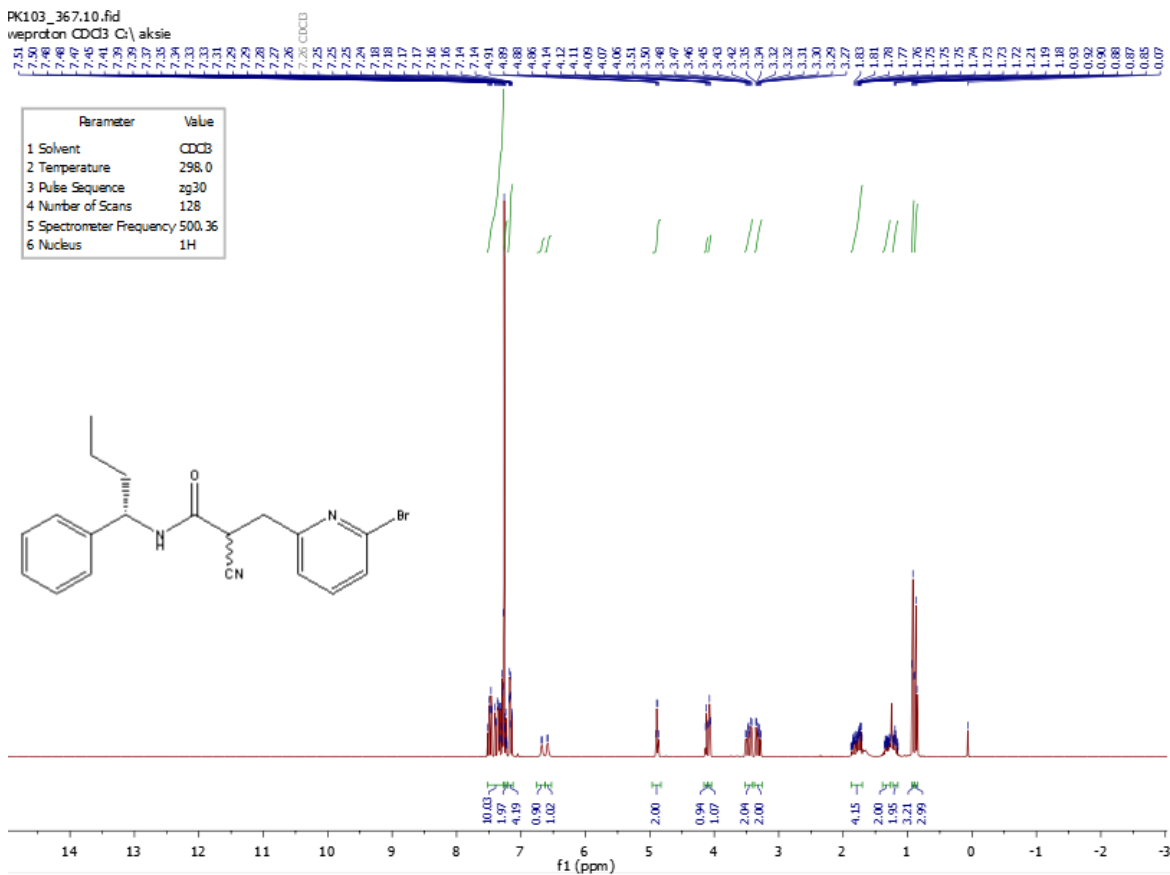
(E)-2-cyano-3-(2,2-difluorobenzo[d][1,3]dioxol-5-yl)-N-(1-phenylbutyl)acrylamide (LK14)



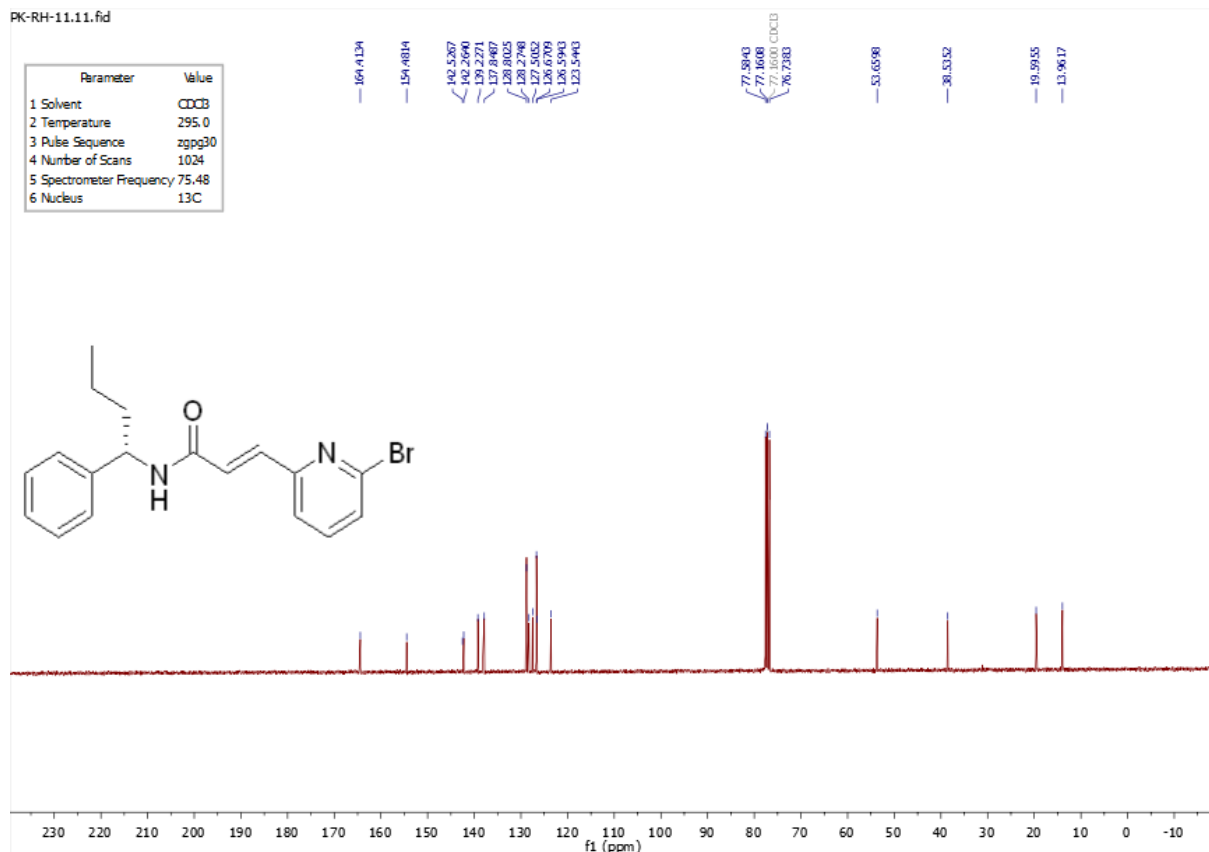
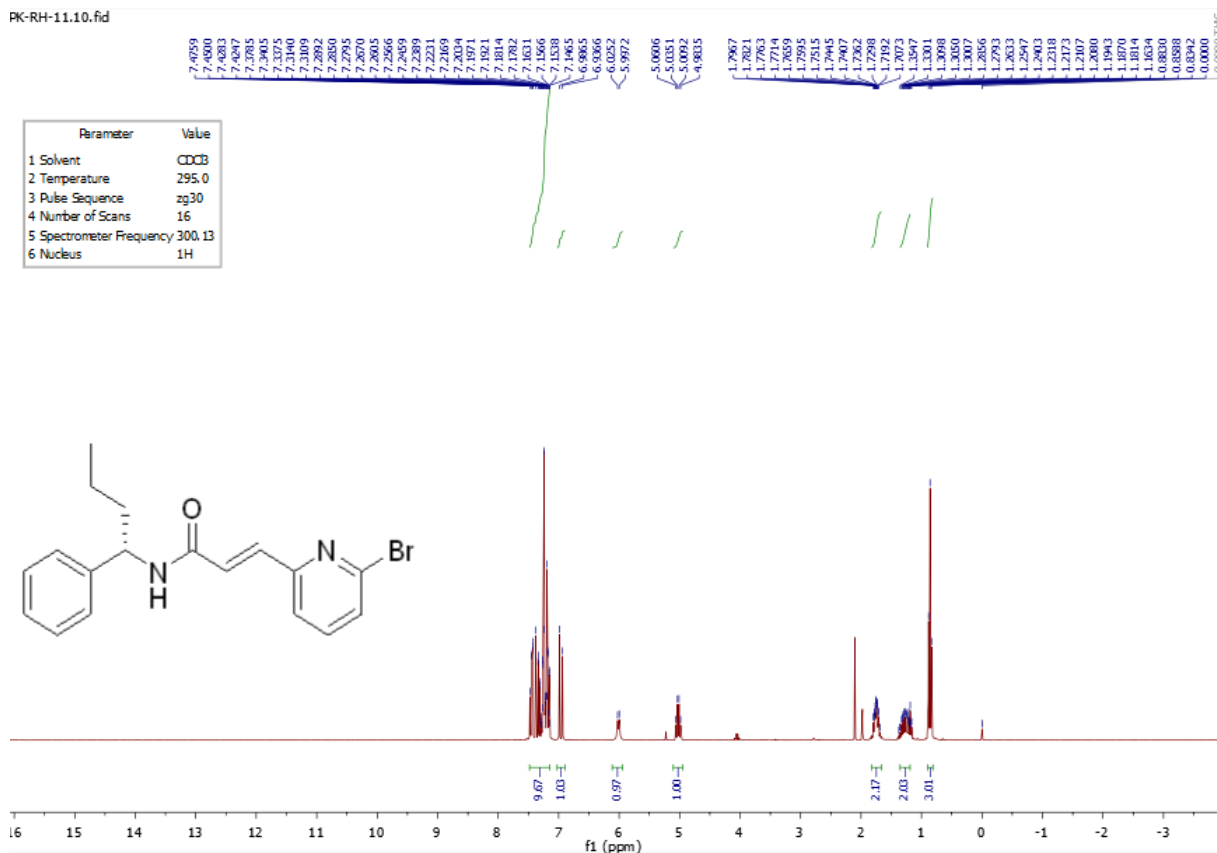
(E)-2-cyano-3-(4-ethynylphenyl)-N-(1-phenylbutyl)acrylamide (DGSp)



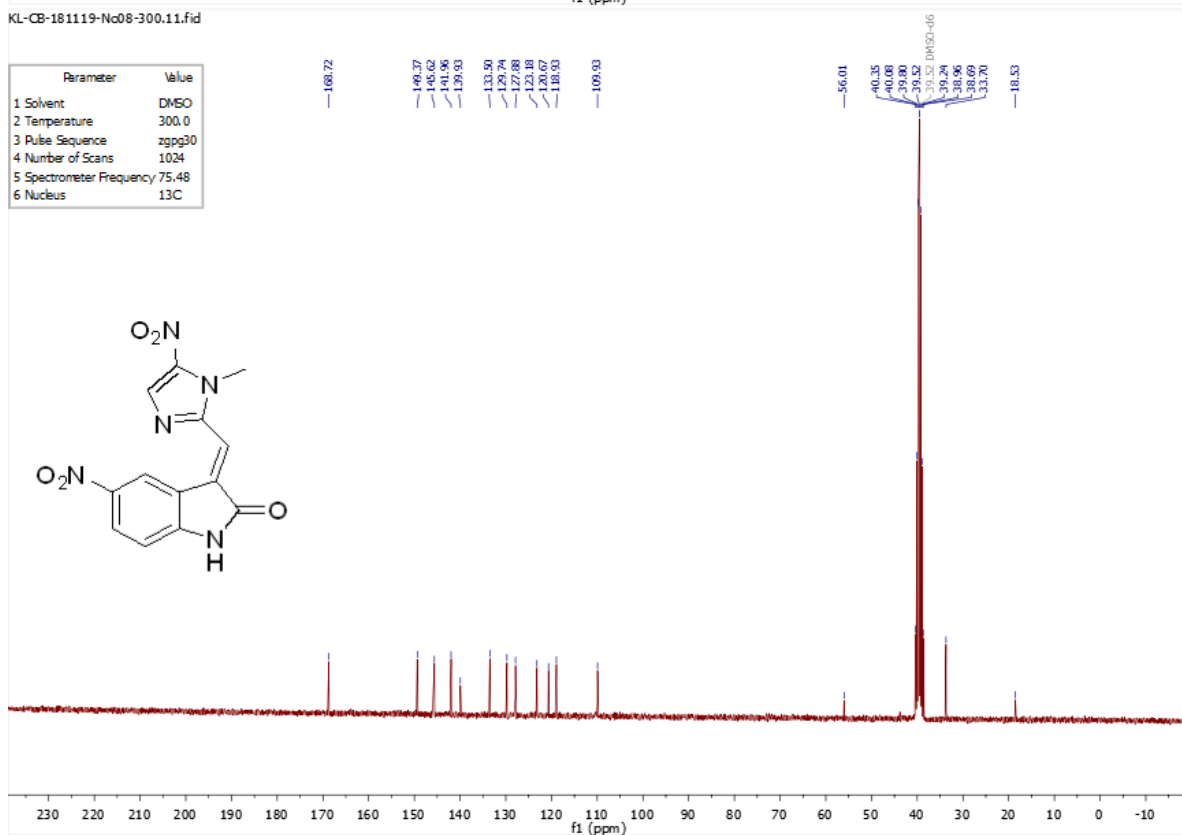
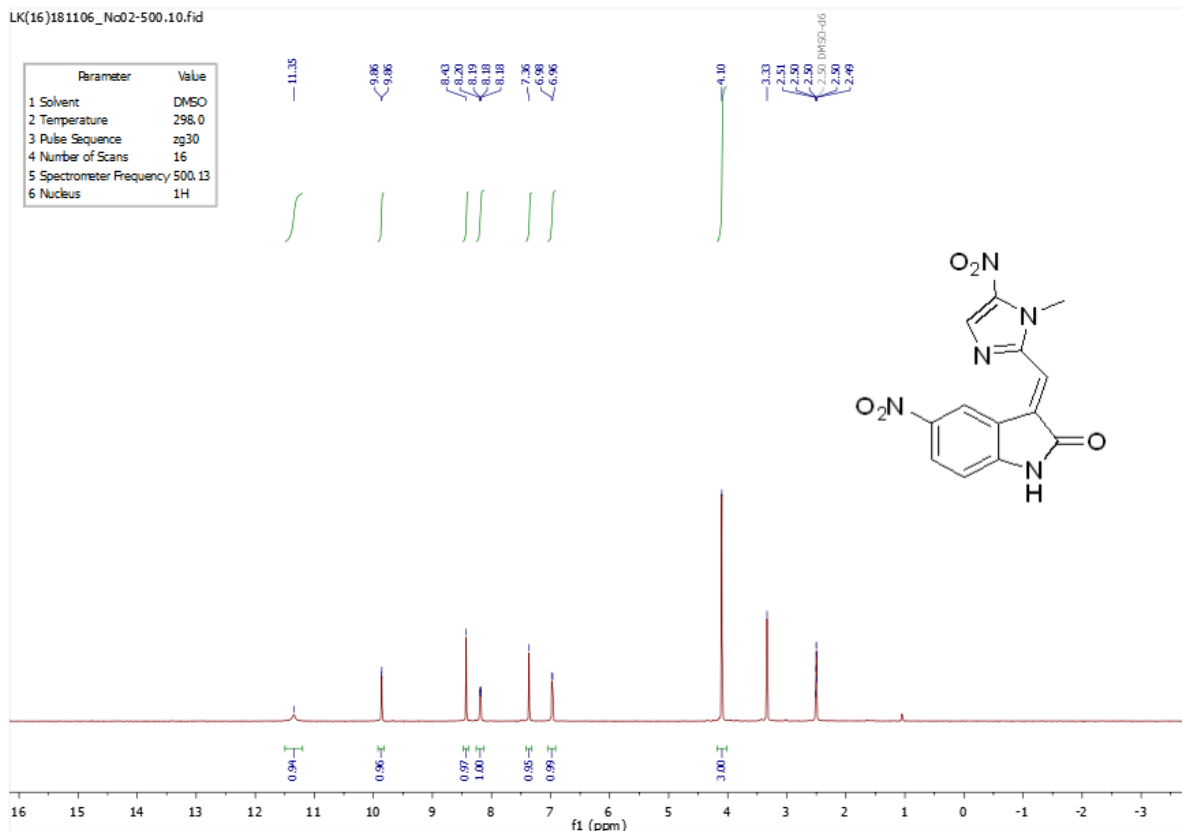
(*R,S*)-3-(6-bromopyridin-2-yl)-2-cyano-*N*-((*S*)-1-phenylbutyl)propenamide (DGS-re)



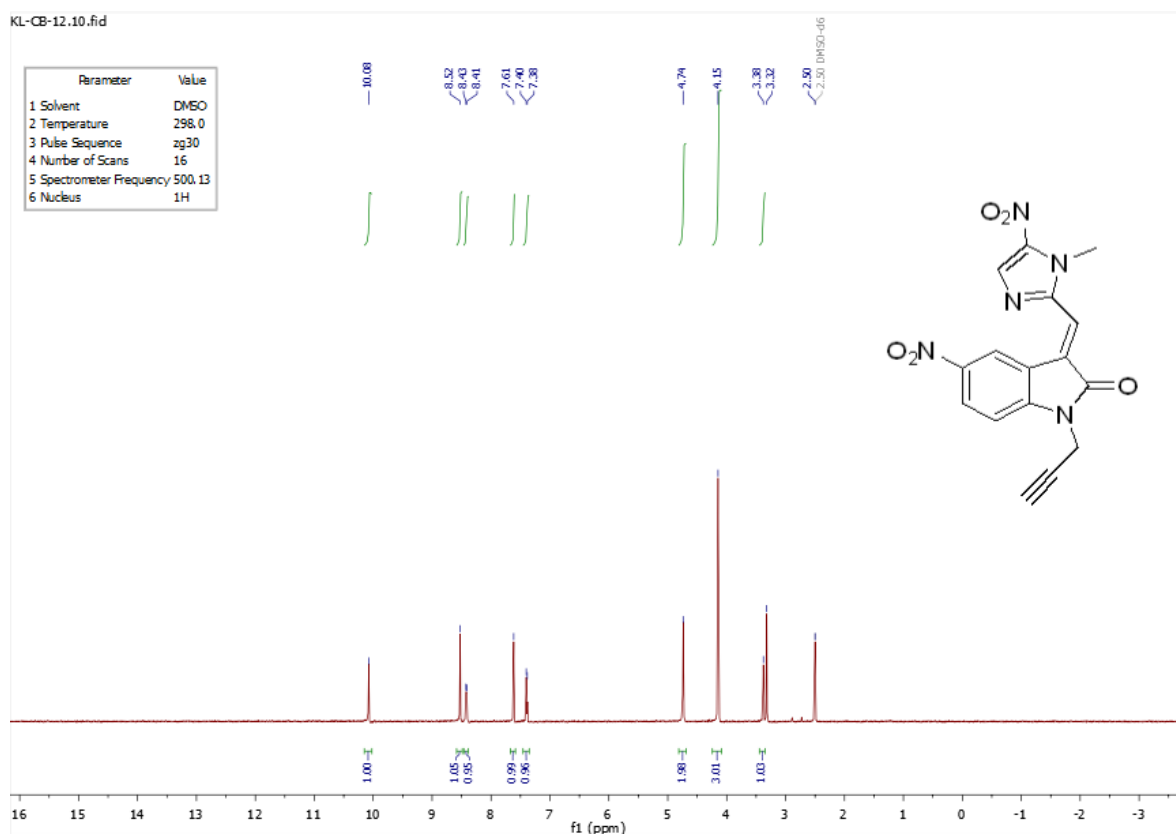
(*S,E*)-3-(6-bromopyridin-2-yl)-*N*-(1-phenylbutyl)acrylamide (DGS-CN)



(E)-3-((1-methyl-5-nitro-1H-imidazol-2-yl)methylene)-5-nitroindolin-2-one (LK1602)

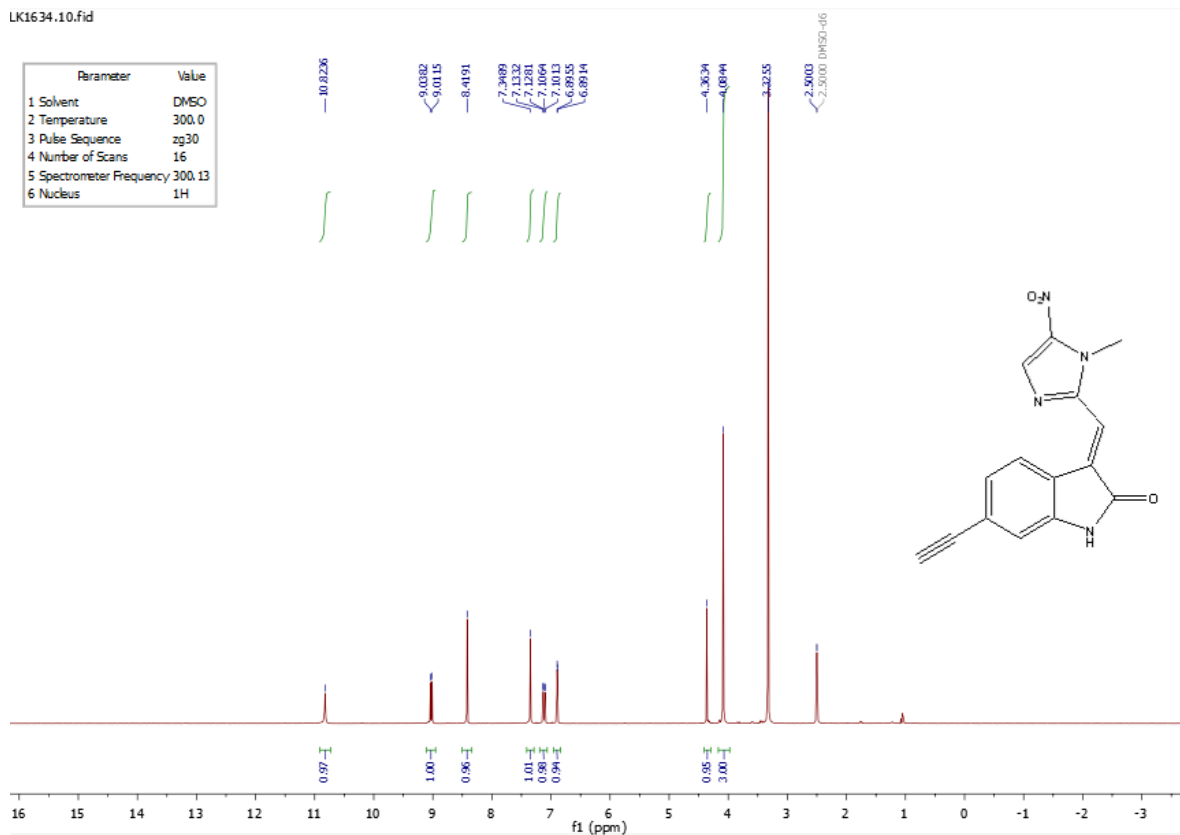


(E)-3-((1-methyl-5-nitro-1H-imidazol-2-yl)methylene)-5-nitro-1-(prop-2-yn-1-yl)indolin-2-one (101)

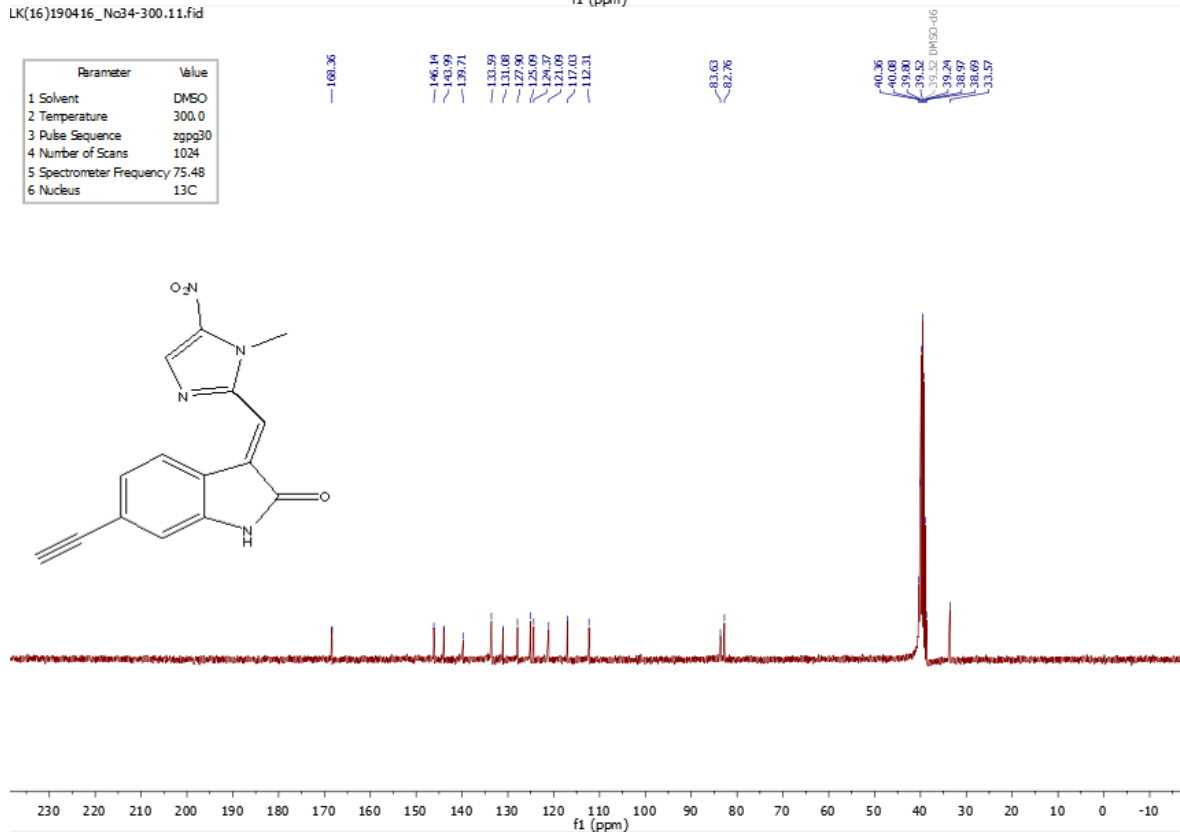


(E)-6-ethynyl-3-((1-methyl-5-nitro-1H-imidazol-2-yl)methylene)indolin-2-one (104)

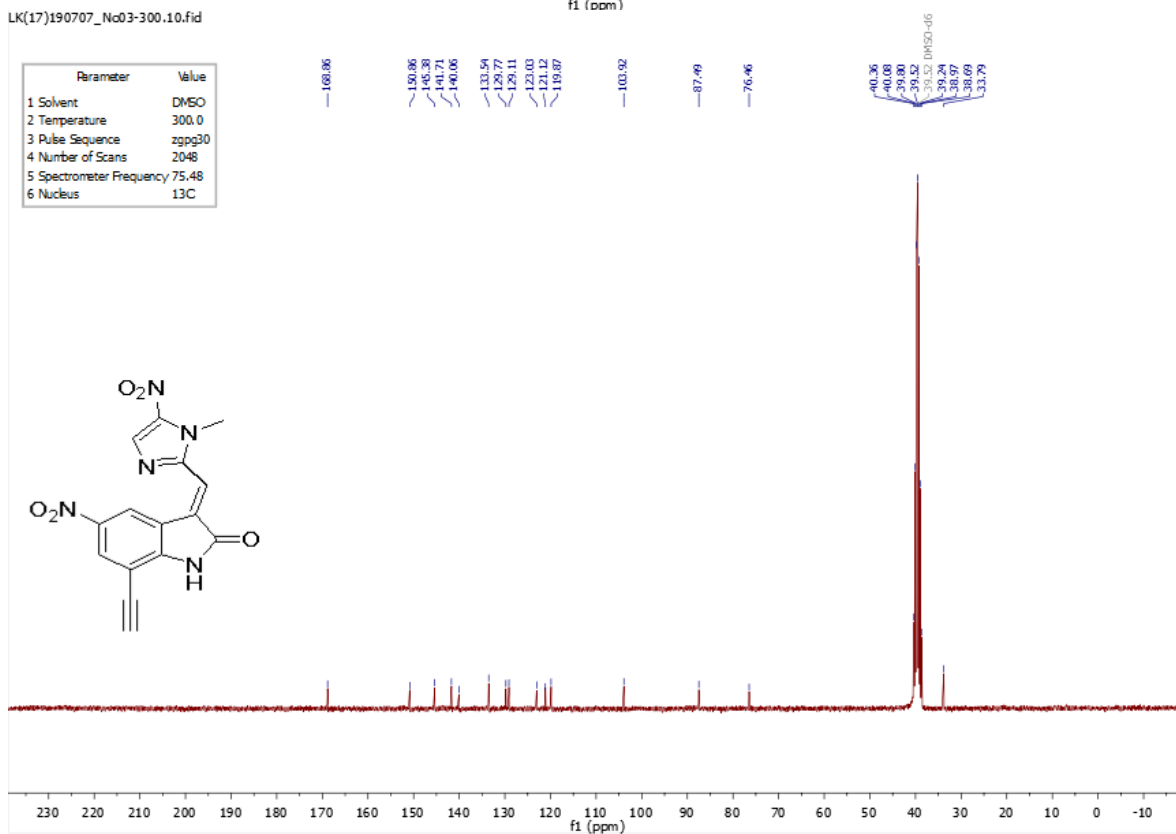
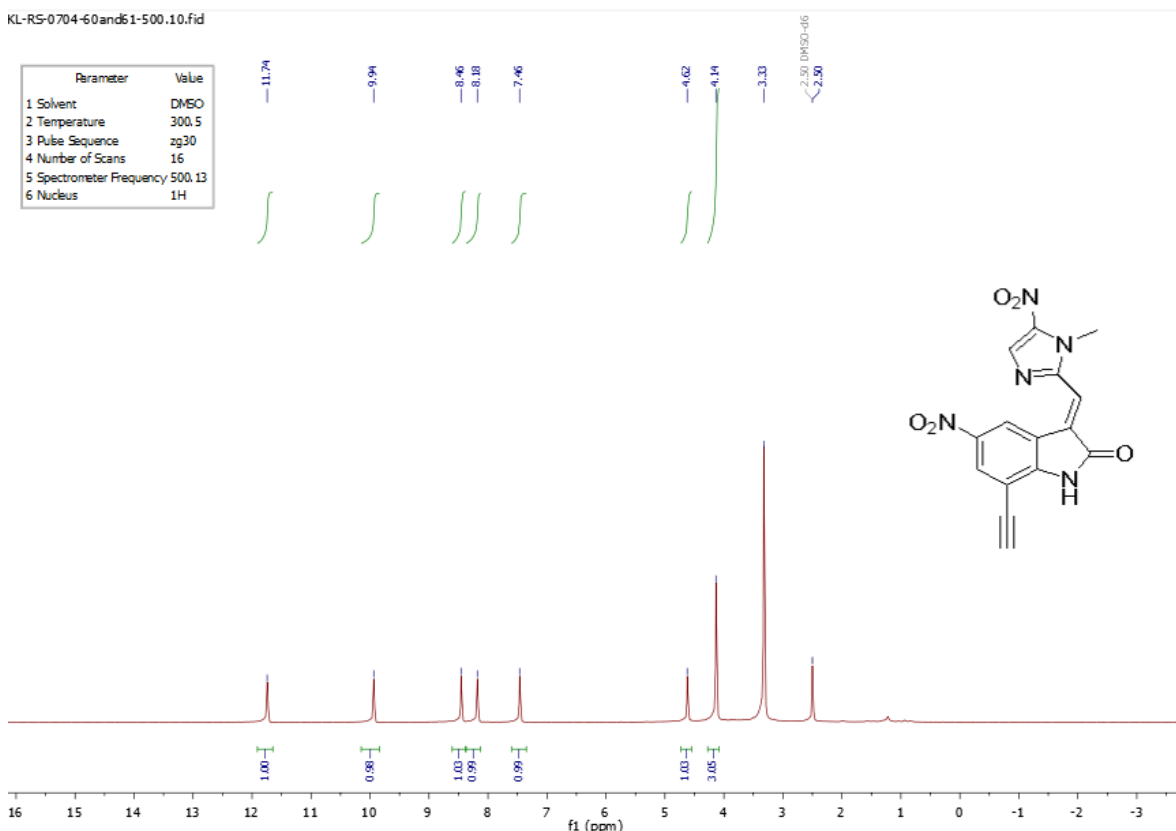
LK1634.10.fid



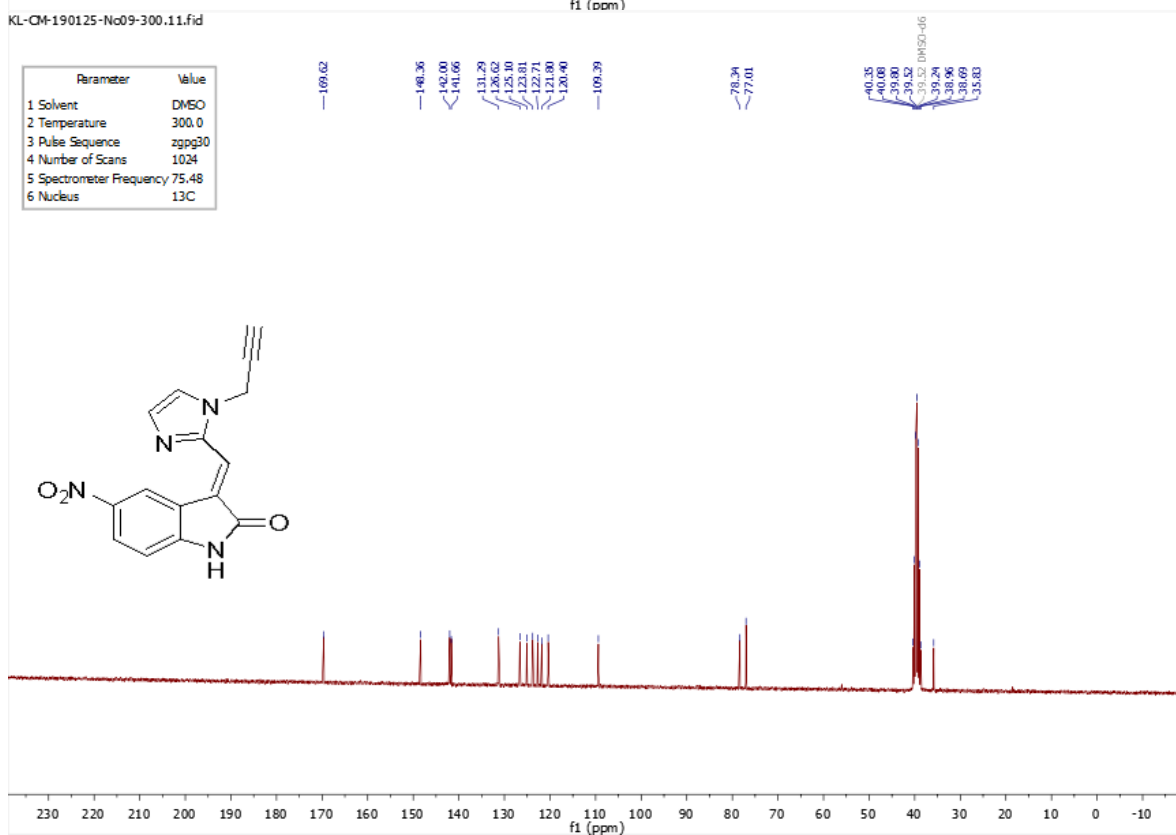
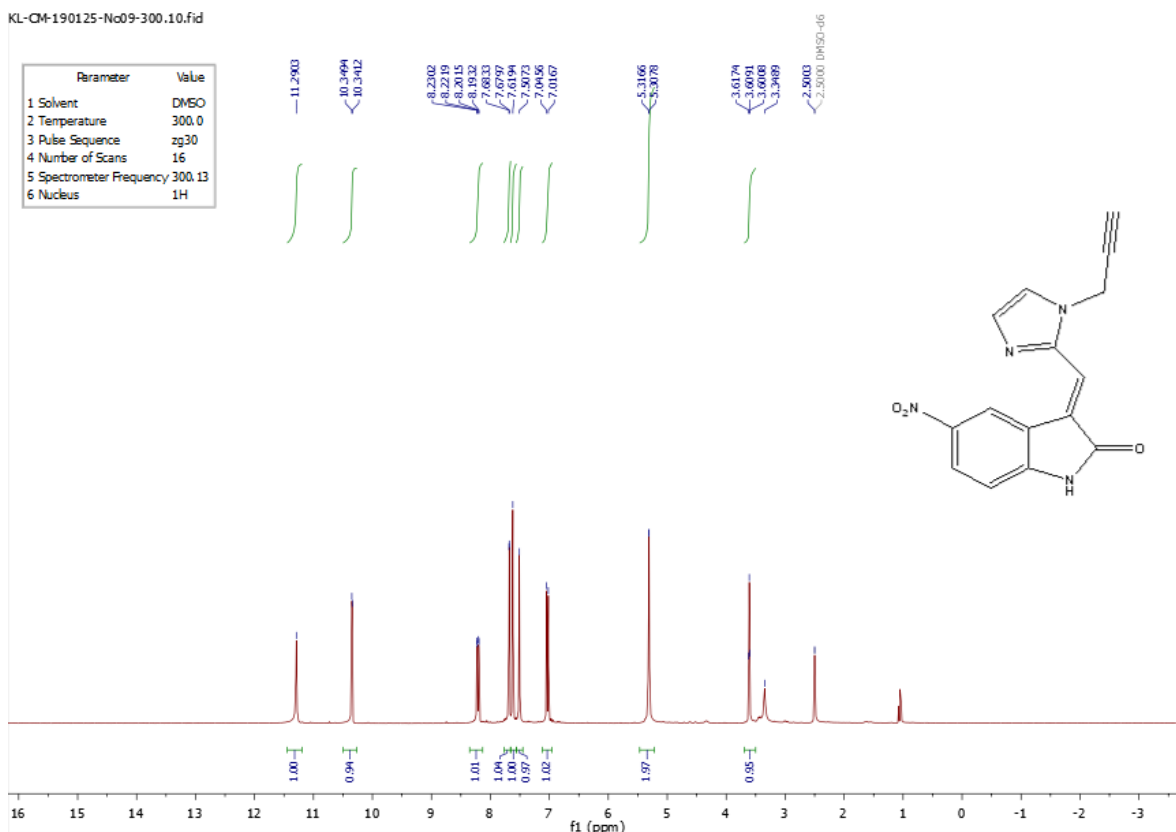
LK(16)190416_No34-300.11.fid



(E)-7-ethynyl-3-((1-methyl-5-nitro-1H-imidazol-2-yl)methylene)-5-nitroindolin-2-one
(108)



(E)-5-nitro-3-((1-(prop-2-yn-1-yl)-1H-imidazol-2-yl)methylene)indolin-2-one (110)





Bibliography

-
- ¹ N. E. Thomford, D. A. Senthebane, A. Rowe, D. Munro, P. Seele, A. Maroyi, and K. Dzobo, *Int. J. Mol. Sci.* **2018**, 19, 1578.
- ² B. Shen, *Cell* **2015**, 163, 1297-1300.
- ³ G. Molinari, *Adv. Exp. Med. Biol.* **2009**, 655, 13-27.
- ⁴ A. Fleming, *Br. J. Exp. Pathol.* **1929**, 10, 226-236.
- ⁵ D. J. Newman, and G. M. Cragg, *J. Nat. Prod.* **2016**, 79, 629-661.
- ⁶ <https://www.scripps.edu/shen/NPLI/whynaturalproducts.html>
- ⁷ <https://en.wikipedia.org/wiki/Aspirin>
- ⁸ <https://en.wikipedia.org/wiki/Hypericin>
- ⁹ V. Farina, and J. D. Brown, *Angew. Chem. Int. Ed.* **2006**, 45, 7330-7334.
- ¹⁰ R. Liu, X. Li, and K. S. Lam, *Curr. Opin. Chem. Biol.* **2017**, 38, 117-126.
- ¹¹ M. Mondala and A. K. H. Hirsch, *Chem. Soc. Rev.* **2015**, 44, 2455-2488.
- ¹² J. R. Broach, and J. Thorner, *Nature*, **1996**, 384, 14-16.
- ¹³ M. F. Lopez, K. Berggren, E. Chernokalskaya, A. Lazarev, M. Robinson, and W. F. Patton, *Electrophoresis* **2000**, 21, 3673-3683.
- ¹⁴ A. E. Speers, and B. F. Cravatt, *Chem. Bio. Chem.* **2004**, 5, 41-47.
- ¹⁵ S. P. Sygl, D. K. M. Han, A-C. Gingras, N. Sonenberg, and R. Aebersold, *Electrophoresis* **1999**, 20, 310-319.
- ¹⁶ M. F. Lopez, *J. Chromatogr. B* **1999**, 722, 191-202.
- ¹⁷ V. Santoni, M. Molloy, and T. Rabilloud, *Electrophoresis* **2000**, 21, 1054-1070.
- ¹⁸ J. L. Harry, M. R. Wilkins, B. R. Herbert, N. H. Packer, A. A. Gooley, and K. L. Williams, *Electrophoresis* **2000**, 21, 1071-1081.
- ¹⁹ B. Kobe, and B. E. Kemp, *Nature* **1999**, 402, 373-376.
- ²⁰ Y. Liu, M. P. Patricelli, and B. F. Cravatt, *Proc. Natl. Acad. Sci.* **1999**, 96, 14694-14699.
- ²¹ G. C. Adam, B. F. Cravatt, and E. J. Sorensen, *Chem. Biol.* **2001**, 8, 81-95.
- ²² N. Jessani, and B. F. Cravatt, *Curr. Opin. Chem. Biol.* **2004**, 8, 54-59.

-
- ²³ S. A. Sieber, and B. F. Cravatt, *Chem. Commun.* **2006**, 22, 2311-2319.
- ²⁴ D. Greenbaum, K. F. Medzihradzky, A. Burlingame, and M. Bogyo, *Chem. Biol.* **2000**, 7, 569-581.
- ²⁵ M. Fonovi, and M. Bogyo, *Curr. Pharm. Dess.* **2007**, 13, 253-261.
- ²⁶ M. Fonovi, and M. Bogyo, *Expert. Rev. Proteomic* **2008**, 5, 721-730.
- ²⁷ Y. Liu, M. P. Patricelli, and B. F. Cravatt, *Proc. Natl. Acad. Sci. U.S.A.* **1999**, 96, 14694-14699.
- ²⁸ M. Bogyo, S. Verhelst, V. Bellingard-Dubouchaud, S. Toba, and D. Greenbaum, *Chem. Biol.* **2000**, 7, 27-38.
- ²⁹ E. W. Chan, S. Chattopadhyaya, R. C. Panicker, X. Huang, S. Q. Yao, *J. Am. Chem. Soc.* **2004**, 126, 14435-14446.
- ³⁰ M. J. Evans, and B. F. Cravatt, *Chem. Rev.* **2006**, 106, 3279-3301.
- ³¹ H. C. Kolb, M. G. Finn, and K. B. Sharpless, *Angew. Chem. Int. Ed.* **2001**, 40, 2004-2021.
- ³² A. E. Speers, G. C. Adam, and B. F. Cravatt, *J. Am. Chem. Soc.* **2003**, 125, 4686-4687.
- ³³ A. E. Speers, and B. F. Cravatt, *Chem. Biol.* **2004**, 11, 535-546.
- ³⁴ V. Hong, N. F. Steinmetz, M. Manchester, and M. G. Finn, *Bioconjug. Chem.* **2010**, 21, 1912-1916.
- ³⁵ Kenry, and B. Liu, Trends in Chemistry, in press.
- ³⁶ A. Raulf, C. K. Spahn, P. J. M. Zessin, K. Finan, S. Bernhardt, A. Heckelc, and M. Heilemann, *RSC Adv.* **2014**, 4, 30462-30466.
- ³⁷ P. Kleiner, W. Heydenreuter, M. Stahl, V. S. Korotkov, and Stephan A. Sieber, *Angew. Chem. Int. Ed.* **2017**, 56, 1396-1401.
- ³⁸ P. P. Geurink, L. M. Prely, G. A. van der Marel, R. Bischoff, H. S. Overkleeft, *Top. Curr. Chem.* **2012**, 324, 85-113.
- ³⁹ <https://sites.google.com/site/sjnamresearchlab>.
- ⁴⁰ A. Kijjoa, and P. Sawangwong, *Mar. Drugs* **2004**, 2, 73-82.
- ⁴¹ A. M. Mayer, K. B. Glaser, C. Cuevas, R. S. Jacobs, W. Kem, R. D. Little, J. M. McIntosh, D. J. Newman, B. C. Potts, and D. E. Shuster, *Trends Pharmacol. Sci.* **2010**, 31, 255-265.
- ⁴² S. Vignesh, A. Raja, and R. A. James, *Int. J. Pharmacol.* **2011**, 7, 22-30.
- ⁴³ A. Martins, H. Vieira, H. Gaspar, and S. Santos, *Mar. Drugs* **2014**, 12, 1066-1101.

-
- ⁴⁴ H. Malve, *J. Pharm. Bioallied Sci.* **2016**, *8*, 83-91.
- ⁴⁵ G. Esposito, R. Teta, R. Miceli, L. S. Ceccarelli, G. Sala, R. Camerlingo, E. Irollo, A. Mangoni, G. Pirozzi, and V. Costantino, *Mar. Drugs* **2015**, *13*, 444-459.
- ⁴⁶ E. Owusu-Ansah, A. C. Durow, J. R. Harding, A. C. Jordan, S. J. O'Connell, and C. L. Willis, *Org. Biomol. Chem.* **2011**, *9*, 265-272.
- ⁴⁷ X. Zhang, and Z. Ma, *Mod. App. Sci.* **2011**, *5*, 217-223.
- ⁴⁸ K. N. Campbell, A. Schrage, and B. K. Campbell, *J. Org. Chem.* **1950**, *15*, 1135-1138.
- ⁴⁹ M. H. Bolli, J. Velker, C. Muller, B. Mathys, M. Birker, R. Bravo, D. Bur, R. de Kanter, P. Hess, C. Kohl, D. Lehmann, S. Meyer, O. Nayler, M. Rey, M. Scherz, and B. Steiner, *J. Med. Chem.* **2014**, *57*, 78-97.
- ⁵⁰ T. Nakamura, M. Sato, H. Kakinuma, N. Miyata, K. Taniguchi, K. Bando, A. Koda, and K. Kameo, *J. Med. Chem.* **2003**, *46*, 5416-5427.
- ⁵¹ K. Higashiyama, M. Toyama, and H. Otomasu, *Chem. Pharm. Bull.* **1986**, *34*, 7, 3015-3019.
- ⁵² D. H. R. Barton, G. Dressaire, B. J. Willis, A. G. M. Barrett, and M. Pfeffer, *J. Chem. Soc., Perkin Trans. 1* **1982**, 665-669.
- ⁵³ T. Mallegol, S. Gmouh, M. A. A. Meziane, M. Blanchard-Desce, O. Mongin, *Synthesis* **2005**, *11*, 1771-1774.
- ⁵⁴ C. C. Tsai, C. T. Chien, Y. C. Chang, H. C. Lin, and T. H. Yan, *J. Org. Chem.* **2005**, *70*, 5745-5747.
- ⁵⁵ A. Tanaka-Yanuma, S. Watanabe, K. Ogawa, S. Watanabe, and T. Usuki, *Tetrahedron Lett.* **2015**, *56*, 6777-6781.
- ⁵⁶ H. Ishibashi, T. Kobayashi, S. Nakashima, and O. Tamura, *J. Org. Chem.* **2000**, *65*, 9022-9027.
- ⁵⁷ A. Caso, A. Mangoni, G. Piccialli, V. Costantino, and V. Piccialli, *ACS Omega* **2017**, *2*, 1477-1488.
- ⁵⁸ X. Ma, Y. Chen, S. Chen, Z. Xu, and T. Ye, *Org. Biomol. Chem.* **2017**, *15*, 7196-7203.
- ⁵⁹ Y. Ikeda, and E. J. Behrman, *Synth. Commun.* **2008**, *38*, 2276-2284.
- ⁶⁰ S. Pushpakom, F. Iorio, P. A. Eyers, K. J. Escott, S. Hopper, A. Wells, A. Doig, T. Guilliams, J. Latimer, C. McNamee, A. Norris, P. Sanseau, D. Cavalla, and M. Pirmohamed, *Nat. Rev. Drug Discov.* **2019**, *18*, 41-58.
- ⁶¹ H. Xue, J. Li, H. Xie, and Y. Wang, *Int. J. Biol. Sci.* **2018**, *14*, 1232-1244.

-
- ⁶² A. Talevi, *Expert Review of Precision Medicine and Drug Development*, **2018**, 3, 49-61.
- ⁶³ M. A. Mittelman-Smith, H. Williams, S. J. Krajewski-Hall, N. T. McMullen, and N. E. Rance, *Proc. Natl Acad. Sci. USA* **2012**, 109, 19846-19851.
- ⁶⁴ L. Peyclit, S. A. Baron, and J. M. Rolain *Front. Cell. Infect. Microbiol.* **2019**, 9, 193.
- ⁶⁵ W. Zheng, W. Sun, and A. Simeonov, *Br. J. Pharmacol.* **2018**, 175, 181-191.
- ⁶⁶ W. Sun, R.A. Weingarten, M. Xu, N. Southall, S. Dai, P. Shinn, P. E. Sanderson, P. R. Williamson, K. M. Frank, and W. Zheng, *Emerg. Microbes Infect.* **2016**, 5, e116.
- ⁶⁷ V. W. Soo, B. W. Kwan, H. Quezada, I. Castillo-Juárez, B. Pérez-Eretza, S. J. García-Contreras, M. Martínez-Vázquez, T.K. Wood, and R. García-Contreras, *Curr. Top. Med. Chem.* **2017**, 7, 1157–1176.
- ⁶⁸ W. S. Yeo, R. Arya, K. K. Kim, H. Jeong, K. H. Cho, and T. Bae, *Sci. Rep.* **2018**, 8, 2521.
- ⁶⁹ L. Aguinagalde, R. Díez-Martínez, J. Yuste, I. Royo, C. Gil, Í. Lasa, M. Martín-Fontecha, N.I. Marín-Ramos, C. Ardanuy, J. Liñares, P. García, E. García, and J. M. Sánchez-Puelles, *J. Antimicrob. Chemother.* **2015**, 70, 2608-2617.
- ⁷⁰ P. K. Le, E. Kunold, R. Maccsics, K. Rox, M. C. Jennings, I. Ugur, M. Reinecke, D. Chaves-Moreno, M. W. Hackl, C. Fetzer, F. A. M. Mandl, J. Lehmann, V. S. Korotkov, S. M. Hacker, B. Kuster, I. Antes, D. H. Pieper, M. Rohde, W. M. Wuest, E. Medina, S. A. Sieber, *Nat. Chem.* **2019**, accepted.
- ⁷¹ L. F. Peterson *et al.*, *Blood* **2015**, 125, 3588-3597.
- ⁷² G. Bartholomeusz, M. Talpaz, W. Bornmann, L. Y. Kong, and N. J. Donato, *Cancer Res.*, **2007**, 67, 3912-3918.
- ⁷³ M. E. Charbonneau, M. J. Gonzalez-Hernandez, H. D. Showalter, N. J. Donato, C. E. Wobus, and M. X. O'Riordan, *PLoS One*, **2014**, 9, e104096.
- ⁷⁴ K. M. Burkholder *et al.*, *Infection and immunity* **2011**, 79, 4850-4857.
- ⁷⁵ K. D. Passalacqua *et al.*, *Antimicrob Agents Chemother* **2016**, 60, 4183-4196.
- ⁷⁶ V. Kapuria, L. F. Peterson, D. Fang, W. G. Bornmann, M. Talpaz, and N. J. Donato, *Cancer Res.* **2010**, 70, 9265-9276.
- ⁷⁷ B. Nanduri, A. E. Suvarnapuny, M. Venkatesan, and M. J. Edelmann, *Curr. Pharm. Des.* **2013**, 19, 3234-3247.
- ⁷⁸ J. Vomacka, V. S. Korotkov, B. Bauer, F. Weinandy, M. H. Kunzmann, J. Krysiak, O. Baron, T. Böttcher, K. Lorenz-Baath, and S. A. Sieber, *Chem. Eur. J.* **2016**, 22, 1622-1630.

-
- ⁷⁹ K. M. Backus et al., *Nature*, 2016, 534, 570-574.
- ⁸⁰ J. M. Bradshaw *et al.*, *Nat. Chem. Biol.*, 2015, 11, 525-531.
- ⁸¹ K. Senkane *et al.*, *Angew. Chem. Int. Ed.*, 2019, 58, 11385-11389.
- ⁸² V. V. Rostovtsev, L. G. Green, V. V. Fokin, K. B. Sharpless, *Angew. Chem. Int. Ed.* **2002**, 41, 2596-2599.
- ⁸³ K. M. Backus *et al.*, *Nature* **2016**, 534, 570-574.
- ⁸⁴ S. M. Hacker *et al.*, *Nat. Chem.* **2017**, 9, 1181-1190.
- ⁸⁵ P. R. A. Zanon, L. Lewald, S. M. Hacker, *ChemRxiv* **2019**, <https://doi.org/10.26434/chemrxiv.9853445.v1>.
- ⁸⁶ K. Senkane *et al.*, *Angew. Chem. Int. Ed.* **2019**, 58, 11385-11389.
- ⁸⁷ The UniProt Consortium, *Nucleic Acids Res.*, 2019, 47, D506-D515.
- ⁸⁸ M. Wang *et al.*, *RSC Advances*, 2017, 7, 13858-13867.
- ⁸⁹ M. S. Mulani, E. E. Kamble, S. N. Kumkar, M. S. Tawre, and K. R. Pardesi, *Front. Microbiol.* **2019**, 10, 539.
- ⁹⁰ E. W. Sewell and E. D. Brown, *J. Antibiot.*, 2014, 67, 43-51.
- ⁹¹ Y. Wang and S. Ma, *ChemMedChem*, 2013, 8, 1589-1608.
- ⁹² J. Nakonieczna, A. Wozniak, M. Pieranski, A. Rapacka-Zdonczyk, P. Ogonowska, and M. Grinholc, *Future Med. Chem.* **2019**, 11, 443-461.
- ⁹³ H. W. Boucher, G. H. Talbot, J. S. Bradley, J. E. Edwards, D. Gilbert, L. B. Rice, M. Scheld, B. Spellberg, and J. Bartlett, *Clinical Infectious Diseases* **2009**, 48, 1-12.
- ⁹⁴ N. Shanmuga Vadivoo, B. Usha. *Int. J. Microbiol.* **2018**, 7, 26-32.
- ⁹⁵ H. Nikaido, *Annu. Rev. Biochem.* **2009**, 78, 119-146.
- ⁹⁶ C. Willyard, *Nature*, **2017**, 543, 15.
- ⁹⁷ M. Rajesh Kumar, M. Alagumuthu, and V. Violet Dhayabaran, *Chem. Biol. Drug. Des.* **2018**, 91, 277-284.
- ⁹⁸ H. K. Ho, *et al. Mol Oncol.* **2014**, 8, 1266-1277.
- ⁹⁹ C. Ji, *et al. Bioorg. Med. Chem.* **2017**, 25, 5268-5277.

-
- ¹⁰⁰ R. Romagnoli, *et al. Eur. J. Med. Chem.* **2017**, 134, 258-270.
- ¹⁰¹ Y. Sun, *et al. Sci. Rep.* **2015**, 5, 13699.
- ¹⁰² G. Chen, *et al. Drug. Des. Devel. Ther.* **2014**, 8, 1869-1892.
- ¹⁰³ M. Ashraf Ali, *et al. Bioorg. Med. Chem. Lett.* **2012**, 22, 508-511.
- ¹⁰⁴ H. Akrami, *et al. Eur. J. Med. Chem.* **2014**, 84, 375-381.
- ¹⁰⁵ K. Furuta, Y. Mizuno, M. Maeda, H. Koyama, and Y. Hirata, *Chem. Pharm. Bull.* **2017**, 65, 1093-1097.
- ¹⁰⁶ K. Furuta, *et al. Bioorg. Med. Chem. Lett.* **2017**, 27, 4457-4461.
- ¹⁰⁷ N. MIDOH, *et al. Biosci. Biotechnol. Biochem.* **2010**, 74, 1794-1801.
- ¹⁰⁸ I. Ahmad, *et al. Pharm. Biol.* **2010**, 48, 716-721.
- ¹⁰⁹ P. Gholamzadeh, G. Mohammadi Ziarani, A. Badiei, A. Abolhassani Soorki, and N. Lashgari, *Res. Chem. Intermed.* **2013**, 39, 3925-3936.
- ¹¹⁰ N. Hosseinzadeh, *et al. Med. Chem. Res.* **2013**, 22, 2293-2302.
- ¹¹¹ D. H. Romero, V. E. T. Heredia, O. García-Barradas, M. E. M. López, and E. S. Pavón, *Journal of Chemistry and Biochemistry*, **2014**, 2, 25-43.
- ¹¹² D. Sharma, B. Narasimhan, P. Kumar, V. Judge, R. Narang, E. De Clercq, and J. Balzarini, *Eur. J. Med. Chem.* **2009**, 44, 2347-2353.
- ¹¹³ A. Puratchikody, and M. Doble, *Bioorg. Med. Chem.* **2007**, 15, 1083-1090.
- ¹¹⁴ J. Pandey, V. K. Tiwari, S. S. Verma, V. Chaturvedi, S. Bhatnagar, A. N. Sinha, A. N. Gaikwad, and R. P. Tripathi, *Eur. J. Med. Chem.* **2009**, 44, 3350-3355.
- ¹¹⁵ D. Zampieri, M. G. Mamolo, L. Vio, E. Banfi, G. Scialino, M. Fermeiglia, M. Ferrone, and S. Pricl, *Bioorg. Med. Chem.* **2007**, 15, 7444-7458.
- ¹¹⁶ R. Di Santo, A. Tafi, R. Costi, M. Botta, M. Artico, F. Corelli, M. Forte, F. Caporuscio, L. Angiolella, and A. T. Palamara, *J. Med. Chem.* **2005**, 48, 5140-5153.
- ¹¹⁷ M. Akkawi, A. Aljazzar, M. AbulHaj, and Q. Abu-Remeleh, *British. J. Pharmacol. Toxicol.* **2012**, 3, 65-69.
- ¹¹⁸ B. Lakshmanan, P. M. Mazumder, D. Sasmal, S. Ganguly, and S. S. Jena, *Acta Parasitologica Globalis* **2011**, 2, 01-05.

-
- ¹¹⁹ K. Bhandari, N. Srinivas, V. K. Marrapu, A. Verma, S. Srivastava, and S. Gupta, *Bioorg. Med. Chem. Lett.* **2010**, 20, 291-293.
- ¹²⁰ J. M. Kraus, H. B. Tatipaka, S. A. McGuffin, N. K. Chennamaneni, M. Karimi, J. Arif, C. L. M. J. Verlinde, F. S. Buckner, and M. H. Gelb, *J. Med Chem.* **2010**, 53, 3887-3898.
- ¹²¹ R. K. Ujjinamatada, A. Baier, P. Borowski, and R. S. Hosmane, *Bioorg. Med. Chem. Lett.* **2007**, 17, 2285-2288.
- ¹²² Y. Özkay, I. Isikdag, Z. Incesu, and G. Akalin, *Eur. J. Med. Chem.* **2010**, 45, 3320-3328.
- ¹²³ M. R. V. Finlay, D. G. Acton, D. M. Andrews, A. J. Barker, M. Dennis, E. Fisher, M. A. Graham, C. P. Green, D. W. Heaton, G. Karoutchi, S. A. Loddick, R. Morgentin, A. Roberts, J. A. Tucker, and H. M. Weir, *Bioorg. Med. Chem. Lett.* **2008**, 18, 4442-4446.
- ¹²⁴ C. D. Jones, D. M. Andrews, A. J. Barker, K. Bladesa, P. Daunt, S. East, C. Geh, M. A. Graham, K. M. Johnson, S. A. Loddick, H. M. McFarland, A. McGregor, L. Mossa, D. A. Rudge, P. B. Simpson, M. L. Swain, K. Y. Tama, J. A. Tucker, and M. Walker, *Bioorg. Med. Chem. Lett.* **2008**, 18, 6369-6373.
- ¹²⁵ F. Hadizadeh, H. Hosseinzadeh, V. S. Motamed-Shariaty, M. Seifi, and S. H. Kazemi, *Iran J. Pharm. Res.* **2008**, 7, 29-33.
- ¹²⁶ Y. Zhou, Y. Ju, Y. Yang, Z. Sang, Z. Wang, G. He, T. Yang, and Y. Luo, *J. Antibiot.* **2018**, 71, 887-897.
- ¹²⁷ N. O. Brace, *J. Org. Chem.* **1993**, 58, 7 1804-1811.
- ¹²⁸ S. Ghosh, S. Chaudhuri, and A. Bisai, *Org. Lett.* **2015**, 17, 6, 1373-1376.
- ¹²⁹ S.P. Nolan and O. Navarro, *Comprehensive Organometallic Chemistry III*, **2007**, 11, 1-37.
- ¹³⁰ W. SHI, Y. Song, Y. Bao, J. Lu, Y. Huang, and D. Weber, US2014066634A1.
- ¹³¹ J. Esteban, R. Pérez-Tanoira. C. Pérez-Jorge-Peremarch, and E. Gómez-Barrena, *Microbiology for Surgical Infections*, **2014**, 41-57.
- ¹³² W. Ried and B. Schleimer, *Angewandte Chemie* **1958**, 70, 164-164.
- ¹³³ A. Irají, O. Firuzi, M. Khoshneviszadeh, M. Tavakkoli, M. Mahdavi, H. Nadri, N. Edraki, R. Miri, *Eur. J. Med. Chem.* **2017**, 141, 690-702.
- ¹³⁴ C. V. Gómez, D. C. Cruz, R. Mose and K. A. Jørgensen, *Chem. Commun.* **2014**, 50, 6035-6038.
- ¹³⁵ J. Cox and M. Mann, *Nat. Biotechnol.*, **2008**, 26, 1367-1372.
- ¹³⁶ P. R. A. Zanon, L. Lewald and S. M. Hacker, *ChemRxiv*, **2019**, DOI:

10.26434/chemrxiv.9853445.v1, doi: 10.26434/chemrxiv.9853445.v9853441.

¹³⁷ S. Tyanova, T. Temu, P. Sinitcyn, A. Carlson, M. Y. Hein, T. Geiger, M. Mann and J. Cox, *Nat. Methods*, **2016**, 13, 731-740.

¹³⁸ R. R. Chaudhuri, A. G. Allen, P. J. Owen, G. Shalom, K. Stone, M. Harrison, T. A. Burgis, M. Lockyer, J. Garcia-Lara, S. J. Foster, S. J. Pleasance, S. E. Peters, D. J. Maskell and I. G. Charles, *BMC genomics*, **2009**, 10, 291.

¹³⁹ The_UniProt_Consortium, *Nucleic Acids Res.*, **2019**, 47, D506-D515.

¹⁴⁰ P. Gaudet, M. S. Livstone, S. E. Lewis and P. D. Thomas, *Brief. Bioinform.*, **2011**, 12, 449-462.